Institut für Veterinärphysiologie
der Vetsuisse-Fakultät der Universität Zürich

Direktor: Prof. Dr. Max Gassmann
Arbeitsgruppe: Prof. Dr. Thomas Lutz

Central neuroinflammatory pathways involved in sickness anorexia and characterization of a novel anti-anorectic ghrelin agonist

Inaugural-Dissertation

zur Erlangung der Doktorwürde der
Vetsuisse-Fakultät Universität Zürich

vorgelegt von

Laura Loi

Tierärztin
von Singen, Deutschland

genehmigt auf Antrag von

Prof. Dr. Thomas Riediger, Referent

Prof. Dr. Wolfgang Langhans, Korreferent

Zürich 2014

Institut für Veterinärphysiologie
der Vetsuisse-Fakultät der Universität Zürich

Direktor: Prof. Dr. Max Gassmann
Arbeitsgruppe: Prof. Dr. Thomas Lutz

Central neuroinflammatory pathways involved in sickness anorexia and characterization of a novel anti-anorectic ghrelin agonist

Inaugural-Dissertation

zur Erlangung der Doktorwürde der
Vetsuisse-Fakultät Universität Zürich

vorgelegt von

Laura Loi

Tierärztin
von Singen, Deutschland

genehmigt auf Antrag von

Prof. Dr. Thomas Riediger, Referent

Prof. Dr. Wolfgang Langhans, Korreferent

Zürich 2014

Table of Contents

1 Zusammenfassung

Krankheitsbedingte Anorexie trägt bei akuten und chronischen entzündlichen Krankheiten zum Anorexie-Kachexie-Syndroms (ACS) bei. Der Nucleus arcuatus (Arc) ist eine Zielstruktur für das orexigene Hormon Ghrelin. Auch die Area Postrema (AP) spielt eine wichtige Rolle bei der Kontrolle des Energiehaushalts. Der inflammatorische Neuromodulator Stickstoffmonoxid (NO) wird durch die induzierbare NO-Synthase (iNOS) gebildet und trägt zur krankheitsbedingten Anorexie bei. *Nuclear factor* (NF)-κB und STAT (*janus kinases, signal transducers and activators of transcription)* regulieren die iNOS Expression. In elektrophysiologischen in vitro Versuchen vermittelte NF-κB im Gegegnsatz zu STAT die LPS/NO-abhängige Hemmung orexigener Arc Neurone. Ausserdem aktivierte LPS in immunhistologischen Versuchen Endothelzellen in der AP. In weiteren elektrophysiologischen und Verhaltensstudien wurde die Wirkung des neuen Ghrelin-Agonisten HM01 charakterisiert. HM01 hatte eine dem Ghrelin analoge Wirkung auf die neuronale Aktivität im Arc. Darüberhinaus führte eine chronische Verabreichung in Ratten zu einer Erhöhung Futteraufnahme und des Körpergewichts. Während die funktionelle Bedeutung von NF-κB in der AP noch untersucht werden muss, scheint dieser Signaltransduktionsweg orexigenen Faktoren wie dem Ghrelin im Arc entgegen zu wirken. Zusammenfassend legen die Resultate nahe, dass eine pharmakologische NF-κB-Hemmung und eine Behandlung mit HM01 mögliche Therapieansätze gegen ACS darstellen könnten.

2 Summary

Disease-related anorexia contributes to the anorexia-cachexia syndrome (ACS) in acute and chronic inflammatory diseases. The arcuate nucleus (Arc) is a target for the orexigenic hormone ghrelin. Similar to the ARC the area postrema (AP) also plays a pivotal role in the control of energy homeostasis. The inflammatory neuromodulator nitric oxide (NO) is produced by the inducible nitric oxide synthase (iNOS) and emerged as possible mediator of sickness anorexia. *Nuclear factor* (NF)-κB and STAT (*signal transducers and activators of transcription*) regulate iNOS gene expression. Using an electrophysiological approach we demonstrated that LPS inhibits ghrelin-excited Arc neurons via NF-κB but not STAT-dependent induction of iNOS activity. LPS also induced NF-κB signaling in vascular cells of the AP as demonstrated by immunohistological studies. In electrophysiological and behavioral studies we further characterized the action of the novel ghrelin agonist HM01. HM01 mimicked the effect of ghrelin on neuronal activity in the Arc and increased food intake and body weight gain after chronic administration in rats. While the functional implications of NF-κB signaling in the AP need to be further elucidated, an activation of this pathway appears to counteract orexigenic stimuli such as ghrelin acting via the Arc. In summary, the current findings suggest that pharmacological inhibition of NF-κB and HM01 treatment might represent possible therapeutic approaches against sickness-anorexia.

3 Introduction

3.1 Energy homeostasis and control of food intake

Living organisms rely on energy intake to fulfill their biological functions. Energy balance is highly regulated accomplishing stability in body weight. Food intake causes short-term discrepancy in energy balance, but the body developed a complex system to accurately match total energy intake to energy expenditure in order to maintain body weight constant over a long period of time (Schwartz et al., 2000).

The brain plays a key role in energy homeostasis integrating signals from central and peripheral pathways (Woods, 2009). Food intake and energy expenditure are influenced by two categories of peripheral signals. One comprises several hormones produced from the GI tract and the pancreas (peptide YY, cholecystokinin, glucagone-like peptide-1, amylin, etc.) that act as satiation signals and control meal size. The second category comprises leptin from white adipose tissue and insulin from the pancreatic B cells, which are secreted in proportion to body fat and act in the brain as so-called adiposity signals. Satiation and adiposity signals interact in the hypothalamus and in other brain regions, particularly the brainstem, to control energy homeostasis (Woods and D'Alessio, 2008).

3.1.1 Role of the arcuate nucleus in the control of food intake

The arcuate nucleus (Arc) is an important brain structure for the control of food intake and energy balance (Suzuki et al., 2010). The Arc is located in the ventral hypothalamus around the basal part of the third ventricle, in close proximity to the median eminence and the pituitary gland (Chronwall, 1985). Two subpopulations of Arc neurons exert opposite effects on food intake and energy balance: in rats neurons co-expressing the orexigenic neuropeptide Y (NPY) and agouti related peptide (AgRP) (Broberger et al., 1998) are located in the ventromedial part of the Arc (ArcM). Neurons co-expressing pro-opiomelanocortin (POMC) and cocaine- and amphetamine-regulated transcript (CART) inhibit feeding and in rats they are predominantly localized in the lateral Arc (ArcL) (Broberger et al., 1997). POMC is a precursor of the neurotransmitter α-melanocyte-stimulating-hormone (αMSH), which reduces food intake acting at melanocortin 3 and melanocortin 4 receptors (MC3R and MC4R) (Fan et al., 1997). AgRP is an endogenous

antagonist of MC3R and MC4R and therefore counteracts the anorectic activity of POMC neurons (Ollmann et al., 1997). NPY stimulates ingestive behavior (Stanley et al., 1986) acting on Y receptors and inhibiting POMC neurons (Roseberry et al., 2004). Both populations of neurons project to other hypothalamic areas such as paraventricular nuclei (PVN), dorsomedial nucleus (DMN), lateral hypothalamic area (LHA), ventromedial hypothalamic nucleus (VMN) and other brain areas (Luquet and Magnan, 2009; Schwartz et al., 2000; Woods and D'Alessio, 2008). Moreover, the Arc is known to be an important target site for the hormones leptin and ghrelin.

Leptin is the product of the ob gene (Zhang et al., 1994) and it is mainly produced in white adipose tissue in proportion to total body fat (Margetic et al., 2002). Mutation of the ob gene or the leptin receptor (Ob-R) results in hyperphagia and obesity in both humans and rodents (Friedman and Halaas, 1998; Montague et al., 1997). The Ob-R is expressed in many brain areas involved in energy balance including the Arc, which is the most important target site of leptin (Elmquist et al., 1998; Schwartz et al., 1996). In the Arc, leptin inhibits NPY/AgRP neurons (Mizuno and Mobbs, 1999; Stephens et al., 1995) and it stimulates POMC neurons (Cowley et al., 2001).

Ghrelin is the only known orexigenic peptide hormone, which is secreted into the circulation by gastric endocrine cells, i.e. X/A-like cells in rodents and P/D1 cells in humans (Date et al., 2000; Inui et al., 2004; Kojima et al., 1999). It is an endogenous ligand of the G-protein coupled growth hormone secretagogue receptor (GHS-R) and stimulates the release of growth hormone (GH) from the pituitary gland (Kojima et al., 2001). Ghrelin is a potent orexigenic hormone that leads to increased body weight in animals and humans (Asakawa et al., 2001; Wren et al., 2001). Plasma ghrelin levels rise pre-prandially and fall post-prandially (Cummings et al., 2001), suggesting a possible role of ghrelin as hunger signal triggering meal initiation. The GHS-R is highly expressed in 94% of the NPY neurons in the Arc (Willesen et al., 1999). Peripheral administration of ghrelin induces Fos expression, a marker for neuronal activation, in NPY-synthesizing neurons in the Arc (Wang et al., 2002). As shown by electrophysiological studies ghrelin directly activates leptin-inhibited Arc neurons (Traebert et al., 2002), while it indirectly

(presynaptically) inhibits POMC neurons in the Arc (Cowley et al., 2003; Riediger et al., 2003).

3.1.2 The area postrema and food intake control

The area postrema (AP) is a component of the dorsal vagal complex, a major viscerosensory and autonomic center of the medulla oblongata. It is one of the three sensory circumventricular organs (sCVOs). sCVOs are specialized brain structures near the ventricular spaces in the midline of the brain. They are characterized by dense vascularization and lack of a functional blood brain barrier (BBB). Due to the fenestrated capillaries they can be reached by humoral factors including peptide hormones that cannot passively cross the BBB in other brain areas (Johnson and Gross, 1993; McKinley et al., 2003; Price et al., 2008). Due to these properties the AP represents a brain target for circulating messengers molecules. The AP was first characterized as chemoreceptor trigger zone mediating emetic responses induced by noxious chemical stimuli (Borison and Brizzee, 1951; Miller and Leslie, 1994). Subsequent studies showed its role in feeding and metabolism, fluid balance and cardiovascular control (Price et al., 2008).
The AP mediates the anorexigenic effect of the pancreatic hormone amylin, which is co-secreted with insulin during and after food intake (Butler et al., 1990; Moore and Cooper, 1991). Amylin dose-dependently reduces meal size in rats (Lutz et al., 1994; Lutz et al., 1995). The crucial role of the AP as primary target for amylin in the brain has been demonstrated in several studies. Surgical removal of the AP blocked the feeding inhibitory action of amylin (Lutz et al., 2001; Lutz et al., 1998). In immunohistochemical studies peripheral injection of amylin induced c-Fos expression in the AP (Riediger et al., 2001; Rowland et al., 1997). This neuronal activation is in line with the electrophysiological studies, which showed strong excitatory effects induced by amylin in the AP in 48% of the recorded neurons (Riediger et al., 2001).

3.2 Disease-related anorexia

Disease-related anorexia is a clinical symptom in a variety of acute and chronic inflammatory diseases such as bacterial, viral and parasitic infections, cancer, acquired

immune deficiency syndrome (AIDS), chronic obstructive pulmonary disease (COPD), inflammatory bowel disease, chronic renal failure, chronic cardiovascular diseases, rheumatoid arthritis and others (Plata-Salaman, 1996). During acute inflammatory diseases reduced food intake is considered to be part of the host's defense mechanisms (Hart, 1988). A suppressed hunger feeling eliminates the needs to search food, reducing energy expenditure. Furthermore, anorexia reduces the availability of food–derived micronutrients, impairing the growth of pathogenic microorganisms (Langhans, 2000). Despite these beneficial effects, long-term anorexia during disease delays recovery compromising host defense, reduces treatment success and decreases quality of life. Moreover, long-term anorexia during chronic diseases contributes to cachexia leading to the anorexia-cachexia syndrome (ACS).

3.2.1 The anorexia-cachexia syndrome

Cachexia is defined as a complex metabolic syndrome associated with underlying illness and characterized by loss of muscle with or without loss of fat mass. The prominent clinical feature of cachexia is weight loss in adults or growth failure in younger individuals. Anorexia and increased muscle protein breakdown are frequently associated with inflammatory chronic diseases (Evans et al., 2008). The ACS is present in a variety of diseases, including chronic infections, cancer, congestive heart failure, COPD and end-stage renal disease (Akamizu and Kangawa, 2010; Morley et al., 2006). ACS occurs approximately in up to 80% of patients with advanced cancer, particularly gastrointestinal and lung cancer. It deteriorates the clinical status leading to increased mortality and a decline in quality of life. Muscle wasting results in weakness, which leads to immobility and can cause death due to loss of respiratory functions. The ACS itself accounts for about 20% of deaths in cancer patients (Gordon et al., 2005; Tisdale, 2002).

3.3 Lipopolysaccharide: a model of inflammation-related anorexia

Lipopolysaccharides (LPS) constitute a major component of the cell membrane of gram-negative bacteria. During infections LPS is released after bacteriolysis or during rapid bacterial proliferation and represent a target molecule for the immune system (Rietschel

et al., 1998). LPS triggers a generalized host defense reaction called “acute phase response” (APR), which is characterized by alteration in immune, endocrine, metabolic and neural functions (Langhans, 2000, 2007). This pathophysiological response includes a pro-inflammatory cytokine response, leukocytosis, fever, anorexia and other behavioral responses like inactivity, somnolence and depression. LPS administration is a widespread model of inflammation and infection-related anorexia. Based on this model some generalizations with respect to other inflammatory diseases are possible, given that the pro-inflammatory cytokines triggered by LPS also play a role in the mediation of anorexia in other diseases.

3.4 Neuroinflammatory mechanisms in disease-related anorexia and ACS

Cytokines are extracellular messenger molecules that have been associated with activation of the immune system and inflammatory responses. Activation of the immune system leads to production of pro-inflammatory cytokines that trigger an APR. The peripheral immune response triggered by LPS treatment induces cytokines such as interleukin-1 (IL-1), interleukin-6 (IL-6), tumor necrosis factor-α (TNF-α) and interferon-γ (IFN-γ) (Jansky et al., 1995; Langhans, 2000).

Peripherally produced cytokines can act on the central nervous system through different mechanisms. They can reach CNS receptors crossing the blood-brain barrier (BBB) through active or passive transport or through circumventricular organs, such the AP. Moreover, they can act at the level of the brain vasculature without crossing the BBB, inducing the release of neuromodulators such as prostanoids or nitric oxide (NO) (Banks, 2001; Langhans, 2000; Licinio and Wong, 1997). In addition to the peripheral cytokine response, immune challenges such as LPS treatment have been shown to induce de novo cytokine synthesis in the brain, for example in the AP (Breder et al., 1994; Goehler et al., 2006; Konsman et al., 1999) and in the hypothalamus (Gabellec et al., 1995; Laye et al., 1994; Turrin et al., 2001).

Through their central action on the brain, cytokines are important endogenous mediators of disease-related anorexia. Several cytokines inhibit feeding after peripheral administration (Plata-Salaman, 1996). Disease-related anorexia might at least partly

results from a modulation of CNS mechanisms that are involved in the physiological control of feeding. Cytokines can directly change the activity of hypothalamic neurons involved in the control of food intake (Katafuchi et al., 1997; Langhans, 2000; Plata-Salaman and ffrench-Mullen, 1994) and several neuropeptides are presumably involved in the central mediation of anorexia during an infection. For example, LPS-treatment leads to increased POMC and CART mRNA levels in the Arc (Sergeyev et al., 2001). Similar to re-feeding and feeding-inhibitory peptides (Riediger et al., 2004), peripheral LPS application inhibits fasting-induced neuronal activation in the Arc suggesting an interaction between LPS and hunger signals (Becskei et al., 2008).

Due to the lack of the BBB peripherally circulating substances can directly act on the AP (Broadwell and Sofroniew, 1993). Neuronal activation has been shown in the AP after immunological challenge with LPS and IL-1 (Brady et al., 1994; Sagar et al., 1995). Different studies showed an involvement of the AP in sickness-related anorexia. In fact, AP lesions attenuated TNF-α-induced anorexia (Bernstein et al., 1991), and tumor-induced anorexia and body weight loss (Bernstein et al., 1985). Although lesion of the AP did not attenuate acute LPS-induced anorexia (Weingarten et al., 1993), AP-lesioned rats did not show social withdrawal (Marvel et al., 2004), indicating that the AP seems to be implicated in the modulation of sickness-related behavior.

3.5 Nitric oxide

There is emerging evidence that the inflammatory neuromodulator NO contributes to sickness anorexia. Nitric oxide has been first recognized as a messenger molecule by Garthwaite and colleagues (Garthwaite et al., 1988). NO is implicated in a wide range of physiological processes acting as intracellular and intercellular messenger molecule. It mediates blood vessel relaxation, plays a role in immune function and serves as neuromodulator in the central and peripheral nervous system. NO is synthesized from the amino acid L-arginine by NO synthase (NOS) (Palmer et al., 1988).

There are three isoforms of NOS: neuronal NOS (nNOS), endothelial NOS (eNOS) and inducible NOS (iNOS). nNOS is expressed in the peripheral and central nervous system (Bredt et al., 1990) and it is involved in neurotransmission and in memory and learning (Prast and Philippu, 2001). eNOS was first identified in endothelial cells (Pollock et al.,

1991) but its expression has also been found in other cell types (Forstermann et al., 1998). It is involved in smooth muscle relaxation and vascular tone. Both nNOS and eNOS are constitutively expressed (Schmidt et al., 1993) and produce NO in a calcium dependent manner. iNOS has been first purified from murine macrophages (Hevel et al., 1991) but it is also expressed in several other cell types, such as lymphocytes, neutrophils, fibroblasts, hepatocytes, vascular smooth muscle and others (Moncada et al., 1991). In the brain iNOS is expressed in endothelial cells, neurons, glia and microglial cells (Kuo and Schroeder, 1995; Moncada et al., 1991). In contrast to the other two isoform, iNOS is not constitutively expressed but its synthesis is induced by inflammatory cytokines, bacterial products or infection in different cell types (Aktan, 2004). After induction it remains active up to 24 hours and synthesizes 100 times higher amounts of NO than the constitutive NOS (Kuo and Schroeder, 1995).

NO acts as a paracrine messenger with a short half-life of a few seconds. As a lipophilic gas it diffuses across membranes and activates the cytoplasmatic enzyme soluble guanylate cyclase (sGC). Once activated sGC catalyzes the synthesis of the intracellular second messenger cyclic guanosine monophosphate (cGMP), which in turn regulates protein phosphorylation, ion channel conductivity and phosphodiesterase activity (Schmidt et al., 1993). These mediators regulate several functions in the cells. In neuronal tissues cGMP modulates neuronal activity acting on cGMP-dependent protein kinases (cGKs), cyclic nucleotide hydrolyzing phosphodiesterases and cyclic nucleotide-gated (CNG) cation channels (Feil and Kleppisch, 2008).

3.5.1 Central iNOS signaling in disease-related anorexia

NO seems to be involved in the inflammatory signaling cascade triggered by LPS and might play a pivotal role in the modulation of neuronal activity transducing cytokine action. Previous studies have shown a high induction of iNOS messenger RNA in vascular, glial and neuronal structures of the rat brain after peripheral LPS administration. iNOS expression occurs in the meninges, choroid plexus, median eminence and subfornical organ. Interestingly, the Arc and PVN showed a strikingly high induction of iNOS (Wong et al., 1996). iNOS expression has also been observed in the PVN and LHA of tumor bearing mice (Wang et al., 2005). Unfortunately the Arc has not been analyzed

in this study. In electrophysiological in vitro studies NO produced by the artificial NO-donor sodium nitroprusside (SNP) strongly inhibited Arc neurons that were exited by ghrelin (Riediger et al., 2006). These inhibitory effects were mediated by cGMP since they were prevented by the specific sGC inhibitor ODQ and mimicked by a membrane permeating cGMP analogue. In accordance, immunohistological studies showed a cGMP formation induced by SNP, which could also be blocked by ODQ (Riediger et al., 2006). These results suggest that pro-inflammatory stimuli with NO as possible mediator antagonize orexigenic stimuli that activate Arc neurons. The anorectic role of iNOS-dependent NO formation in sickness anorexia is supported by the finding that the specific and long acting iNOS inhibitor 1400W (Garvey et al., 1997) attenuates the reduction of food intake after LPS stimulation (Borner et al., 2012; Riediger et al., 2010). Direct evidence for a NO-dependent inhibition of Arc neurons by LPS came from electrophysiological studies demonstrating that iNOS blockade by 1400W disinhibits ghrelin responsive Arc neurons after in vitro and in vivo stimulation with LPS (Borner et al., 2012). Interestingly, third ventricular administration of 1400W almost completely blocked LPS-induced anorexia underlining the importance of central NO signaling in LPS-dependent suppression of food intake (Borner et al., 2012).

3.5.1.1 iNOS signaling in the AP under inflammatory conditions

There is evidence for a role of NO signaling in the AP under inflammatory conditions. In fact, AP neurons kept in primary cell cultures showed NO responsiveness in calcium imaging studies (Wuchert et al., 2009). Moreover, systemic LPS treatment induces iNOS mRNA in the AP (Konsman et al., 1999). Pre-treatment with the iNOS inhibitor aminoguanidine reduced c-Fos expression in the AP during sepsis induced by cecal ligation and puncture suggesting an activation of AP neurons through iNOS-derived NO during sepsis (Bruhn et al., 2009).

3.5.2 Transcriptional regulation of iNOS gene expression

The regulation of iNOS transcription is the main regulatory step to control iNOS activity (Kleinert et al., 2003). The promoter regions of the iNOS gene have been studied in

humans, mice, rats and birds and several binding sequences for transcription factors have been identified (Rao, 2000). Activation of the transcription factors nuclear factor (NF)-κB and the janus kinase, signal transducers and activators of transcription pathway (JAK/STAT) seem to be essential in the regulation of iNOS expression in most cells (Kleinert et al., 2003; Pautz et al., 2010).

3.5.2.1 Nuclear factor κB (NF-*k*B)

NF-κB is an important inducible transcription factor activated by different stimuli, amongst others, by pro-inflammatory cytokines and LPS (Hayden and Ghosh, 2004; Perkins, 2007). It is involved in a variety of biological processes like innate and adaptive immunity, inflammation, cellular stress responses, cell adhesion, apoptosis and proliferation. NF-κB is a member of the rel family of proteins (Ghosh et al., 1998; Verma et al., 1995). It is present in the cytosol of unstimulated cells as homo- or heterodimers of the subunits p50 and p65, bound to inhibitory κB (IκB) proteins. The binding to IκB protein maintains NF-κB in an inactivate state preventing its translocation to the nucleus. IκBα plays a pivotal role in the regulation of NF-κB activity. LPS, IFNγ and TNFα activate the inhibitor kappa B kinase (IKK) that phosphorylates the IκB-NF-κB complex. Phosphorylated IκB proteins are then ubiquinated and degraded, and the liberated NF-κB dimers can translocate into the nucleus to regulate target gene expression (Ghosh et al., 1998; Hayden and Ghosh, 2004).

NF-κB fulfills a pivotal role in early events of innate immune response through Toll-like receptor (TLR) signaling pathways. TLRs recognize specific patterns of microbial components and TLR4 has been shown to recognize LPS (Takeda et al., 2003). TLR4 is thus responsible for triggering NF-κB pathway activation in response to immune challenge with LPS (Nguyen et al., 2002). TLR4 has been shown to be constitutively expressed in CVOs, for example in the AP, and other brain areas such as in the arcuate nucleus. In the AP TLR4 expression is even up-regulated after LPS stimulation. (Laflamme and Rivest, 2001).

LPS treatment in mice led to NF-κB activation in the Arc, whereas in the AP nuclear translocation of NF-κB was observed after immune challenge with IL-1β (Jang et al., 2010; Nadjar et al., 2003). ICV administration of the NF-κB inhibitor Bay 11-7085

significantly blocked the feeding inhibitory effect of systemic LPS treatment (Jang et al., 2010). Moreover, inactivation of the central NF-κB signaling with ICV injection of a NF-κB inhibitor significantly blocked the behavioral effects of IL-1β treatment, such as decreased food intake, locomotor activity and social interaction (Nadjar et al., 2005).
These data support a role of NF-κB signaling in the transmission of immune signals from the periphery to the brain and suggest an involvement of NF-κB in the Arc and AP during illness-anorexia and other related symptoms. However, the specific involvement of NF-κB in LPS/NO-dependent effects on neuronal function in the Arc and have not yet been investigated. Moreover it is not known if NF-κB signaling mediates inflammatory signals acting via the AP.

3.5.2.2 Janus kinase, signal transducers and activators of transcription pathway (JAK-STAT)

Several studies have underlined the involvement of STAT signaling in the regulation of iNOS expression (Dell'Albani et al., 2001; Doi et al., 2002; Kim et al., 2002). The JAK-STAT pathway is an intracellular signaling cascade that transduces signals from transmembrane receptors to the nucleus to activate gene expression. In mammals there are seven STAT genes. In absence of stimulation, STAT proteins are inactive and localize in the cytoplasm. STATs are activated by various cytokines as well as by growth factors and hormones (Bromberg, 2001; Schindler, 2002). Receptor-ligand coupling leads to conformational change of the receptor-associated tyrosine kinase known as Janus kinases (JAKs) recruiting STATs to the intracellular domain of the receptor. Subsequent phosphorylation of STATs leads to STAT homo- and heterodimerisation (pSTAT). STAT dimers rapidly translocate to the nucleus where they can bind to the DNA binding motifs (Aaronson and Horvath, 2002; Lim and Cao, 2006).
Several studies showed an LPS induced activation of STAT1 and STAT3 in the Arc, suggesting an involvement of these pathways in iNOS expression under inflammatory condition. In fact, LPS triggers a time-dependent nuclear STAT3 translocation in the Arc and other brain areas in guinea pigs (Rummel et al., 2005) and rats (Gautron et al., 2002; Rummel et al., 2005). The LPS-induced nuclear translocation of STAT3 peaked after 4 hours in the hypothalamus (Gautron et al., 2002). Moreover, a time dependent STAT3

phosphorylation occurs in the Arc of rats after LPS treatment 4 hours after injection (Riediger et al., 2010).

Similar to what has been demonstrated for pSTAT3, peripheral LPS treatment induces pSTAT1 formation in the Arc of mice (Borner et al., 2012). In astroglial cell cultures JAK2/STAT1 is involved in iNOS expression (Dell'Albani et al., 2001). Furthermore, IFN-γ, IFN-γ receptor and STAT1 knockout mice are defective for the induction of NO synthesis by LPS and/or cytokines (Dalton et al., 1993; Kamijo et al., 1993; Meraz et al., 1996). In mouse macrophages LPS triggers iNOS expression through JAK2/STAT1 signaling (Tsoyi et al., 2008). Inhibition of JAK2/STAT-signaling by AG490, a JAK2 inhibitor, reduced sickness behavior such as reduced locomotor activity and decreased water intake in LPS treated rats. These findings suggest a role of the JAK/STAT signaling in LPS induced sickness behavior (Damm et al., 2013).

Together, these data suggest an involvement of JAK/STAT signaling the Arc after immune challenge with LPS. However, its specific involvement in LPS/NO-dependent effects on neuronal function in the Arc has not yet been investigated.

3.6 Therapeutic approaches in disease related anorexia and ACS

The management of chronic sickness anorexia and ACS represents a great challenge. No therapy has proven to be sufficiently effective in the treatment of the metabolic derangement caused by the ACS. The successful management of this accompanying catabolic disorder would further increase the therapy success and ameliorate the quality of life of the patients during their treatment. In the past two decades different therapeutic approaches and substances have been tested, e.g. anti-inflammatory agents, corticosteroids, progestagens. The exact mechanism of action of these compounds in treatment of anorexia is largely unknown. Moreover, most of them show severe side effects (Kumar et al., 2010).

Among other treatment strategies, agonists of the growth hormone secretagogue receptor (GHS-R), like ghrelin and its mimetics, appear promising for the treatment of illness-associated anorexia.

Several studies with different anorexia and/or cachexia animal models evaluated the effectiveness of ghrelin treatment. In most of these studies ghrelin or ghrelin agonists

showed beneficial effect on food intake, body weight and body composition (DeBoer et al., 2007; Hanada et al., 2003; Hataya et al., 2003; Wang et al., 2006).

However, there is some evidence for a decreased responsiveness to ghrelin treatment under tumor conditions. In fact, central ghrelin administration in tumor-bearing animals failed to increase food intake if compared to non-tumor-bearing controls and increased endogenous serum ghrelin levels accompanied this reduced effectiveness (Wisse et al., 2001). These findings might suggest a state of ghrelin resistance or at least reduced ghrelin responsiveness under tumor conditions.

Ghrelin or GHS-R agonists have been studied in few human studies. Most of them included cancer patients. (Burney B, 2012; Garcia and Polvino, 2007; Levinson and Gertner, 2012; Lundholm et al., 2010; Nagaya et al., 2005; Nass et al., 2008; Neary et al., 2004; Strasser et al., 2008). Some of these studies indicate positive effects of treatment with ghrelin or its agonists on energy intake and body weight of the patients. Others did not report any beneficial effects of ghrelin treatment. However, due to the heterogeneity of the study design, negative findings should be interpreted with caution.

Due to the short half-life of ghrelin (Akamizu et al., 2004) its therapeutic use in human is limited because of these the insufficient pharmacokinetic properties of the native peptidergic hormone. Synthetic ghrelin mimetics have longer half-life allowing a daily single administration (Blum R, 2006; Nass et al., 2008) and oral route of administration.

4 Questions

1. Are JAK2/STAT- and NF-*κ*B-signaling involved in the LPS-induced iNOS/NO-mediated inhibition of orexigenic Arc neurons?

Using electrophysiological single cell recording techniques we tested whether STAT and NF-κB pathway blockers inhibit LPS/NO-mediated inhibition of electrical activity of Arc neurons under in vitro conditions. If our assumptions were correct, we would expect a decreased number of ARC neurons showing disinhibitory responses to iNOS blockade after LPS stimulation (Figure 1). To inhibit the JAK2/STAT pathway, we used WP1066, which inhibits JAK2 activation preventing STAT1 and STAT3 phosphorylation (Ferrajoli et al., 2007; Heimberger and Priebe, 2008; Horiguchi et al., 2010). To inhibit NF-κB activation we used the compound Bay 11-7085, which inhibits IκB phosphorylation preventing an activation and nuclear translocation of NF-κB (Koedel et al., 2000; Pierce et al., 1997).

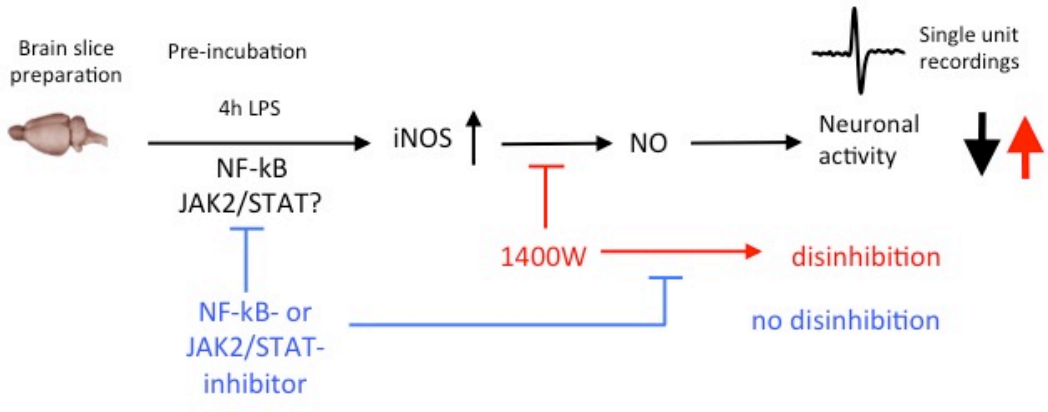

Figure 1: Experimental approach for the electrophysiological studies. Co-incubation of Arc slice preparations in LPS with the NF-κB or JAK2/STAT inhibitor should prevent the disinhibition caused by the iNOS inhibitor 1400W.

2. Is LPS sufficient to activate the STAT1 and STAT3 pathways in the Arc after in vitro stimulation?

Since LPS-induced systemic inflammation in rats induces an activation of the STAT1 and STAT 3 pathway in the Arc, we wanted to study if a similar response occurs under in vitro conditions independently of a systemic immune response. For this purpose we used

immunohistochemical methods to examine if a pSTAT1 and pSTAT3 formation occurs after in vitro LPS stimulation of Arc slices as well.

3. Does LPS treatment induce NF-*κ*B-signaling in the Arc and the AP and which cell type is affected?

We performed an immunohistological detection of NF-κB signaling in the Arc after LPS treatment in vivo as well as in vitro LPS stimulation. We further immunohistologically investigated whether NF-κB is activated in the AP after LPS treatment.

4. Does HM01 mimic the effects of ghrelin on neuronal activity of Arc neurons?

Using extracellular electrophysiological recordings we characterized the effect of the novel ghrelin analog HM01 (Helsinn Healthcare SA, Pambio-Noranco, Switzerland) on Arc neurons. As a specific ghrelin receptor agonist, HM01 is expected to mimic ghrelin-induced responses as reflected by a high degree of co-sensitivity of Arc neurons to HM01 and ghrelin.

5. Does chronic administration of HM01 increase food intake and body weight in healthy rats?

In these experiments the effect of chronic HM01 administration (subcutaneously implanted osmotic minipumps) on food intake and body weight development was investigated. According to ghrelin's positive effects on energy balance, HM01 was expected to increase food intake and body weight gain.

5 Material und Methods

5.1 Preface

Most of the basic techniques used in the studies of this project were the same as reported in the master thesis "*Intracellular pathways mediating nitric oxide dependent inhibition of orexigenic hypothalamic neurons by anorectic lipopolysaccharide"* (Loi, 2012). Extensions or modifications were added for all additional experimental procedures of the current work.

5.2 Animals and housing conditions

For all experiments adult male Wistar rats (Elevage Janvier, Le-Genest-St. Isle, France) weighing between 200-380 g were used. Animals were kept in a temperature-controlled room (21 ± 1°C) on a 12:12 h light/dark cycle with ad libitum access to feed (standard chow, 890 25 W16, Provimi Kliba, Switzerland) and tap water. For the electrophysiological and immunohistochemical studies they were housed in groups of five animals in standard macrolon cages. For the in vivo testing of the ghrelin agonist HM01 10 animals were single housed in hanging wire-mash cages. Before the experiments, rats were handled daily and kept in the cages for an adaptation period of at least one week. All the experiments were conducted in accordance with the regulations of the Veterinary Office of the Canton Zurich, Switzerland.

5.3 Preparation of the arcuate nucleus (Arc) for electrophysiological and in vitro immunohistological studies

Artificial cerebrospinal fluid (aCSF)

aCSF was used for the preparation and incubation of the brain slices as well as for the perfusion of the recording chamber during the electrophysiological recordings. Table 1 shows the composition of the stock solutions and the final concentration of all the components. The stock solutions were stored at 4°C and the aCSF was prepared daily for each experiment in order to prevent bacterial growth. The final solution was oxygenated

and equilibrated with oxycarbon (95% O_2, 5% CO_2) for at least one hour before and during the entire duration of the experiments.

Table 1 Composition of stock solution and final aCSF concentration

Solution	Substance	Concentration (g/L)	aCSF final concentration (mM)
I	NaCl	72.46	124
	KCl	3.73	5
	$NaH_2PO_4 \cdot H_2O$	1.65	1.2
	$MgSO_4 \cdot 7H_2O$	3.2	1.3
II	$NaHCO_3$	21.84	26
III	$CaCl_2 \cdot 2H_2O$	1.76	1.2
IV	Glucose H_2O	19.82	10

Preparation of arcuate nucleus slices

The animals were decapitated using a guillotine. The skull was opened from the caudal side using a surgical rongeur and superfused with ice-cold aCSF. The olfactory bulb and the optic nerves were cut and the brain was transferred into a preparation dish containing ice-cold aCSF. The brainstem and the cerebellum were dissected with a cut at the level between cerebrum and cerebellum. The meninges were removed from the cerebrum using curved tweezers under a dissecting microscope. To prepare the arcuate nucleus the cerebrum was fixed with instant glue in vertical position and stabilized with an agar block in a vibratom chamber filled with ice-cold aCSF. A custom made vibratom (Leica VT 1000S, Leica microsystems) was used to obtain 700 μm thick coronal brain slices containing the Arc, starting with the first section caudal to the end of the optic chiasm. The obtained slices where then manually trimmed to 3x3 mm sections containing the Arc (Figure 2) and finally transferred in the temperature controlled (37°C) incubation chamber containing 240 ml of continuously oxygenated aCSF.

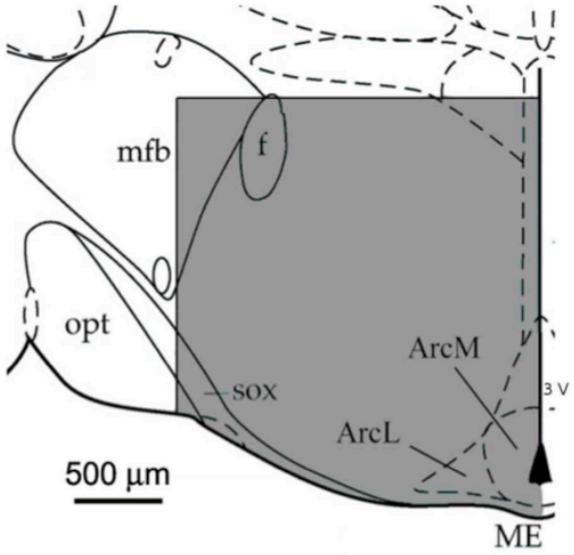

Figure 2: Schematic half-section of the hypothalamus region close to the Arc. The grey area indicates the surface that has been removed and prepared for the following experiments. ArcM: medial arcuate nucleus, ArcL: lateral arcuate nucleus, ME: median eminence, 3V: third ventricle, sox: supraoptic decussation, mfb: medial forebrain bundle, opt: optic tract, f: fornix (modified from Paxinos and Watson, 1998).

5.4 Electrophysiological studies

5.4.1 Electrophysiological setup

Recording chamber

The recording chamber consisted of solid brass and was gold-plated. When perfused it contained a volume of 0.7 ml aCSF, which was constantly replaced at a rate of 1.6 ml/min by a peristaltic pump (Minipuls 2, Gilson, ABIMED, Germany). The slice preparations were transferred to the recording chamber and fixed on the bottom with a small metal weight.

Temperature control

A thermocouple in the recording chamber transmitted the effective temperature of the aCSF to a Peltier-controller (PTC-10, npi electronics, Germany). A Peltier element fixed with heat conducting paste under the recording chamber kept the temperature of the aCSF at 37 ± 0.2°C. The superfused aCSF was prewarmed before entering the chamber. The monitored temperature signals were stored on a PC through an analog-digital converter (CED1410, Science Park, England). The temperature was checked and if necessary adjusted before the recordings.

Electrodes

Extracellular recordings of single cell action potentials were obtained from Arc neurons using self-made glass-coated platinum-iridium electrodes. After sharpening the electrodes (platinum/iridium 70/30, 0.1 mm diameter, Chempur, Germany) electrolytically in a NaCN-solution (30% NaCN, 30% NaOH) up to a tip diameter of about 2 µm, they were glass coated with a vitrification device for electrical isolation. To allow electrical conductance the glass was removed from the tip of the electrode by melting. The electrodes were connected to a 3-axis hydraulic micromanipulator (MHW-103, Narishige, Japan). The electrode was carefully inserted into the tissue under optical guidance until an action potential was detected. According to the neuroanatomical brain map of Paxinos and Watson (Paxinos and Watson, 2007) the recordings were conducted in the medial Arc, where NPY neurons are located that are activated by the orexigenic hormone ghrelin.

Signal processing

The extracellularly recorded action potentials were first amplified 1000-fold by a differential amplifier (DAM50, WPI, USA) and after passing a high- and low-pass filters they were amplified 10-fold and recorded by a DAT-recorder (DTR-1205, Bio-Logic, Science Instruments, France). A window discriminator (SL-04, BM&T, Heidelberg, Germany) allowed a discrimination of action potential signals from background noise. When the voltage of the action potential passed an adjustable threshold level the window discriminator generated a TTL-signal (Transitor-Transitor-Logic). At the same time, the signals were passed to an analogue oscilloscope (COS5020, Kikusui electronics, Japan) and to a digital storage oscilloscope (DRO1602, Gould, UK), which was externally triggered by the TTL signals generated by the windows discriminator. The TTL-signals were converted by a CED 1401 interface (Cambridge Electronic Design UK) and recorded as ratemeter histograms with an interval of 5 seconds. An audiomonitor (AM8, Grass Medical Instruments, Quincy Massachusetts) facilitated the search for active cells (Figure 3).

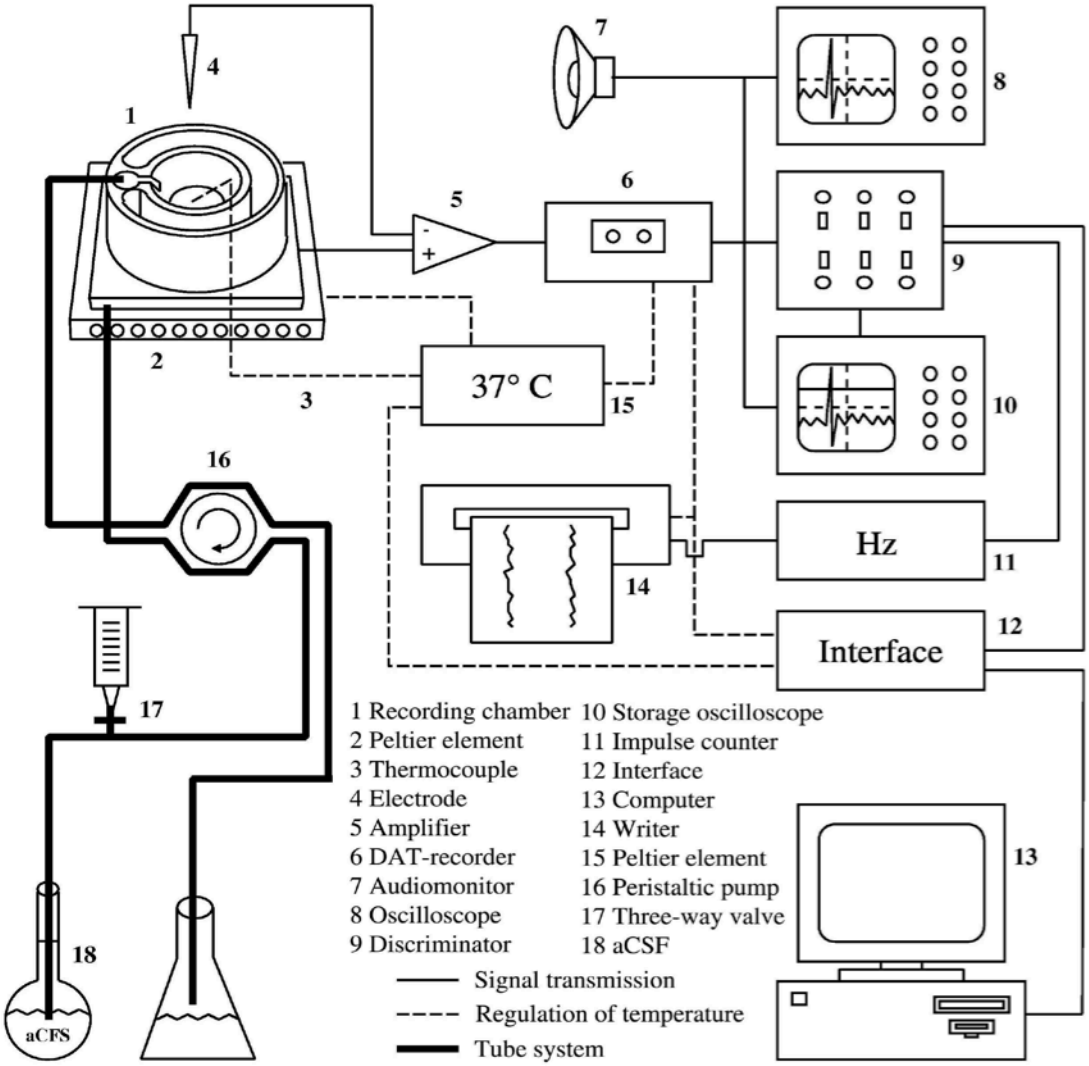

Figure 3: Electrophysiological setup stand (from T. Riediger)

5.4.2 In vitro stimulation

In order to test whether the activation of NF-κB and JAK2-dependent STAT phosphorylation are involved in the LPS induced iNOS-dependent NO formation, Arc slices were incubated for 4 hours with LPS (100 ng/ml) in combination with Bay 11-7085 (10^{-6} M) or WP 1066 (10^{-5} M). Bay 11-7085 and WP 1066 were dissolved in DMSO and stored in frozen aliquots. LPS was freshly prepared before each experiment. To control for the vehicle used for Bay 11-7085 and WP1066 250 µl of DMSO were added to the aCSF (Table 2).

Table 2: Substances used for the incubation and their molecular weight (MW), stock solution, final concentration and source of supply.

Substance	MW (g/mol)	Stock solution	Final concentration	Source of supply
LPS *E.coli*, serotype 0111:B4	-	Daily prepared; 4°C	100 ng/ml	Sigma-Aldrich
Bay 11-7085	249.3	$2.4 \cdot 10^{-3}$ M (in 250 µl DMSO)	10^{-6} M	Sigma-Aldrich
WP 1066	356.22	$2.4 \cdot 10^{-2}$ M (in 250 µl DMSO)	10^{-5} M	Calbiochem

5.4.3 Substance application

For the superfusion of the tested substances a three-way valve was connected to the superfusion tubing system. The substances were added to a 10 ml syringe filled with aCSF and due to the small diameter of the tubing system they reached the recording chamber 60 s after the onset of the stimulus. Ghrelin, 1400W, Bay 11-7085, WP 1066, GLP-1 and HM01 were stored in frozen aliquots at -20°C. SNP was prepared before each experiment. The final concentrations are shown in (Table 3). Bay 11-7085 and WP1066 were superfused to test whether the compounds have short-term effects on neuronal activity of the recorded neurons. To test NO responsiveness SNP was superfused; further, ghrelin was used as functional reference stimulus. The ghrelin-agonist HM01 was superfused after ghrelin stimulation to look for co-sensitivity of the neurons for these two substances. When a recording of a single cell action potential was established, the neuronal activity was recorded for at least 600 s. If a stable baseline was observed during this period of time, the stimulus was set. At the beginning and the end of the stimuli a marker was set in the continuous ratemeter recordings via keyboard inputs. For data analysis, a duration of 60 s was taken into account to correct for the lag time caused by the substance passage through the tubing system.

Table 3: Substances used for the superfusion and their molecular weight (MW), stock solution, final concentration and source of supply

Substance	MW (g/mol)	Stock solution	Final concentration	Source of supply
Bay 11-7085	249.3	$2 \cdot 10^{-4}$ M in DMSO aliquot	10^{-6} M	Sigma-Aldrich
WP 1066	356.22	$2 \cdot 10^{-3}$ M in DMSO aliquot	10^{-5} M	Calbiochem
1400 W	250.2	10^{-2} M in H_2O aliquot	10^{-4} M	Calbiochem
SNP	298	0,4-1 mg aliquote; room temperature; freshly prepared	10^{-5} M	Calbiochem
Ghrelin (rat recombinant)	3315	10^{-5} M in H_2O aliquot;	10^{-8} M	Bachem
HM01	437.86	10^{-3} M in H_2O aliquot;	$10^{-6}/10^{-7}$ M	Helsinn
GLP-1 (7-36) amide	3297.68	10^{-4} M in H_2O aliquot	10^{-7}	Bachem

5.4.4 Data evaluation and statistics

The program Spike2 (CED, England) was used to record the firing rate, the temperature and the keyboard markers. The obtained histogram showed the recorded impulses in an interval of 5 seconds. The average discharge rate of the neuron was determined for 60 seconds preceding the stimulus. This "mean spontaneous activity" was subtracted from the changes in firing rate resulting in the absolute mean response (Hz) that was then used to calculate the percentage of change in firing rate (%). Additionally the following parameters were evaluated: the latency (period of time between the begin of the stimulus in the chamber and the onset of the response), the duration (period of time between the beginning and the end of the response), the absolute (Hz) and relative (%) peak response (30 s interval of the maximum or minimum firing rate during the response). A neuron was considered sensitive to the applied substance if the averaged change of firing rate during the response was larger than ± 20% and ± 0.5 Hz. The parameters were averaged and expressed as mean ± standard error. The percentage of disinhibited neurons after 1400W superfusion was compared between the LPS incubation and the co-incubation

with LPS and the inhibitors using the Fisher's exact test. The effect parameters were analyzed using the Student's *t*-test, one-way ANOVA or the Kruskal-Wallis Test if not normally distributed. The Newmann-Keuls Multiple Comparison Test served as post hoc test.

5.5 Immunohistological studies

5.5.1 In vitro LPS stimulation

Rats were decapitated and 700 µm thick coronal brain slices containing the Arc were prepared as described before and transferred to the incubation chamber. The Arc slices of one half of the animals were stimulated with LPS (100 ng/ml) for 1 or 4 h. The slices of the remaining animals served as control and were kept 1, or 4h in aCSF. The obtained sections were processed for pSTAT or NF-κB immunostaining.

5.5.1.1 STAT phosphorylation

Fixation and slicing

After the incubation the Arc preparations were transferred to a 12 well-plate filled with 2 ml of oxygenated aCSF. 2 ml of ice-cold 4% Fix were added in each well (final conc. 2% Fix) and the plates were stored at 4° C for 1 h. The fixative was replaced with 2 ml of 20% sucrose in 0.02 M KPBS (potassium phosphate buffered saline, Table 5) for 3 h at 4°C. The slices were mounted on parafilm covered glass slides and residual sucrose was removed with filter paper. The preparations were covered with tissue freezing medium (Leica Microsystems, Nussloch, Germany) and frozen at -20°C in a cryostat (Leica CM3050S, Nussloch, Germany). Two series of 20 µm thick sections were obtained using the cryostat and mounted on adhesive glass slides (Menzel-Gläser, Superfrost® Plus, Thermo scientific, Braunschweig, Germany). The sections were processed for pSTAT1 and pSTAT3 immunoreactivity.

Staining

The slices were air dried for 1 hour and rehydrated in 0.02 M KPBS (Table 5). Antigen retrieval was achieved by 20 min incubation at room temperature in 0.02 M KPBS 0.3% NaOH and 0.3% H_2O_2. Sections were incubated first in 0.02 M KPBS 0.3% glycine for

10 min followed by 10 min incubation in 0.02 M KPBS 0.03% sodium dodecyl sulfate (SDS). Unspecific binding was blocked by incubation in 4% donkey normal serum (DNS), 0.4% Triton® X-100, 1 bovine serum albumin (BSA) in KPBS at room temperature for 20 min. The two primary antibodies (rabbit anti-pSTAT1, 1:50, Santa Cruz Biotechnology and rabbit anti-pSTAT3, 1:500, Cell signaling Technology) were applied for 48h at 4° C in KPBS containing 1% DNS, 0.4% Triton® X-100, 1% BSA. The secondary antibody (donkey anti-rabbit Alexa 555, 1:100, Invitrogen) was applied in KPBS containing 1% DNS, 0.3% Triton® X-100 for 2h at room temperature. Finally the sections were coverslipped with citifluor (Citifluor Ltd, London).

5.5.1.2 NF-*κ*B activation

After an incubation of 1 hour the Arc and AP preparations were processed like for the pSTAT staining. In this case, the final concentration of fixative was 4% and PBS (Table 4) was used instead of KPBS.

Staining

The staining protocol was the same as used for the tissue of the in vivo LPS stimulation (see point 5.5.2).

5.5.2 NF-κB activation after in vivo LPS stimulation

LPS injection and perfusion

Rats were randomly assigned to one of the experimental groups. At dark onset the animals were intraperitoneally (i.p.) injected either with LPS (from *E. coli*, serotype 0111:B4, Sigma-Aldrich, Buchs, Switzerland) or with saline. LPS was dissolved in sterile 0.9% NaCl and injected at doses of 100 or 300 µg/kg BW. The animals were deeply anesthetized 2 or 4 hours later by an i.p. injection of pentobarbital (80 mg/kg ip). The thorax was opened and the rats were transcardially perfused for 1.5 minutes with ice cold PB 0.1 M (phosphate buffer) pH 7.2 followed by ice cold paraformaldehyde solution (4% PFA in 0.1 M PB) for 2 minutes. The brains were postfixed in 4% PFA for 2 hours at 4°C and then transferred to 20% sucrose in PB for 2 days at 4°C for cryoprotection. Brains were snap-frozen at -20°C in hexane. 20 µm Arc and AP sections were cut using a cryomicrotome and mounted on adhesive glass slides.

Tissue processing and staining

Sections were air dried for 1 hour and then rehydrated in PBS (Table 4). Unspecific binding was blocked by incubation in 5% DNS in PBST 0.3% (phosphate buffer saline, 0.3 % Triton® X-100) for 1 hour at room temperature. The primary antibodies (Table 6, Table 7) were applied in 0.3% PBST for 3 days at 4°C. The secondary antibodies (Table 6, Table 7) were applied in PBST 0.3% for 2 hours at room temperature. After washing in PBS, DAPI staining was performed. 300 nM DAPI (DAPI dihydrochloride, Life Technologies, NY, USA) in PBS was applied at room temperature for 5 minutes. After final washing the section were coverslipped with Citifluor.

5.5.3 Evaluation and statistics of immunohistochemical studies

A fluorescence microscope equipped with a digital camera system (AxioImager, Carl Zeiss AG) was used to analyze the slices.

To quantify the number of pSTAT1 and pSTAT3 immunoreactive cells, five corresponding Arc sections from each animal were analyzed in blind fashion and the number of immunoreactive cells was averaged for each animal.

To evaluate the activation of NF-κB the co-localization of NF-κB and DAPI fluorescence was analyzed. Five corresponding Arc or AP sections from each animal were analyzed manually in blind fashion and the number of cells with nuclear NF-κB was averaged for each animal.

From these averaged values the means ± SEM were determined for each group. Statistical evaluation between groups was performed using Student´s *t*-test or one-way ANOVA. Dunn's Multiple Comparison Test served as post hoc test.

Table 4: PBS buffer

Substance	Weight (g)	
NaCl	8	Dissolved in 1 l of dd H_2O
KCl	0.2	
Na_2HPO_4	1.8	
KH_2PO_4	0.2	

Table 5: KPBS buffer

Substance	Weight (g)	
KH_2PO_4	9.7	Dissolved in 20.58 l dd H_2O to final concentration of 0.02 M
K_2HPO_4	56.6	
NaCl	178.2	

Table 6: Antibodies used for NF-κB immunostainings in the arcuate nucleus

Primary antibody			Secondary antibody		
Antibody	**Supplier**	**Concentration**	**Antibody**	**Supplier**	**Concentration**
Rabbit anti-NF-κB p65 subunit (C 20)	sc-372, Santa Cruz Bio-technology Inc,	1:500	Donkey anti-rabbit Alexa-555	Invitrogen, Life Technologies,	1:100
Sheep anti-rat von Willebrand Factor	SARTW-IG Stago BNL,	1:3'000	Dpnkey anti-sheep Alexa-488	Invitrogen, Life Technologies,	1.200

Table 7: Antibodies used for NF-κB immunostainings in the area postrema

Primary antibody			Secondary antibody		
Antibody	**Supplier**	**Concentration**	**Antibody**	**Supplier**	**Concentration**
Rabbit anti-NF-κB p65 subunit (C 20)	sc-372, Santa Cruz Biotechnology Inc,	1:500	Donkey anti-rabbit Alexa-555	Invitrogen, Life Technologies,	1:300
Mouse anti-RECA-1	MCA970R AbD Serotec,	1:2'000	Donkey anti-mouse Alexa-488	Invitrogen, Life Technologies,	1:200

5.6 Implantation of the osmotic minipumps

After an adaptation period of one week 10 animals were randomly assigned to one of the two experimental groups (n = 5). An osmotic minipump (ALZET® osmotic pumps, DURECT corporation, Cupertino, CA 95015-0530) was implanted subcutaneously in one flank at the lower level of the abdomen between the chest and the hind limbs. Half of the minipumps were filled with saline (controls), whereas the remaining minipumps were filled with HM01 (10 µg/µl). The total volume of the minipumps was 2 ml. One hour prior to anesthesia the animals were treated with Norocarp® (10 mg/kg s.c., ufamed AG, Sursee, Switzerland). Anesthesia was induced in a Plexiglas chamber with 5% isoflurane in oxygen (1 l/min). After an adequate depth of anesthesia was achieved, rats were sheared with an electric razor and disinfected with betadine scrub. Rats were then placed in prone position on a heating pad and the head was positioned in a nose cone. For the maintenance of anesthesia 2–4% isoflurane in oxygen, was supplied for the duration of surgery. A 2 cm skin incision was made in the caudal part of the lateral torso. The subcutaneous tissue was spread by opening and closing the jaws of a Metzenbaum scissor. This procedure created a pocket for the minipump. The filled minipumps were inserted into the pocket and the incision was closed with an intracutaneous suture. The pumps delivered the compound into the subcutaneous space. The minipump released a constant amount of HM01 (50 µg/h with a pump rate of 5 µl/h). The capacity of the minipump allowed a constant compound release of 14 days. Body weight and food intake were measured daily. Thirteen days after minipump implantation the animals were deeply anesthetized and transcardially perfused as described before. All data are expressed as mean ± SEM. Food intake and body weight were compared at each time point using a parametric unpaired student's *t*-test.

6 Results

6.1 Intracellular pathways involved in the iNOS mediated NO production in the Arc

During this first part of the electrophysiological studies 48 ArcM neurons were recorded. The mean amplitude of the action potentials was 120 µV, which allowed an accurate discrimination from background noises.

1400W sensitivity after incubation with LPS (100 ng/ml)

After 4 h incubation with LPS 8 neurons were superfused with 1400W and their electrical activity was recorded and analyzed. 63% of the recorded neurons (5/8) showed an increase in their firing rate in response to 1400W (Figure 4), while the remaining neurons were 1400W-insensitive. SNP sensitivity was tested in 5 recordings, 4 (80%) of the cells were reversibly inhibited, while one neuron was insensitive. 80% (4/5) of the neurons that were tested for ghrelin sensitivity showed an excitatory response while 1 neuron was insensitive.

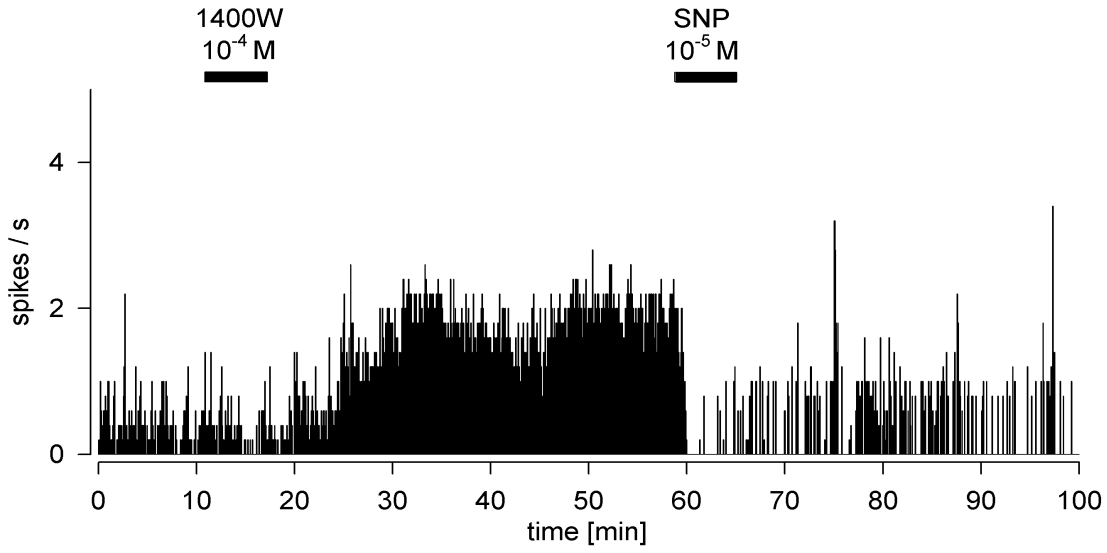

Figure 4: Representative recording of ArcM neuron, which increased the firing rate after 1400W superfusion (10^{-4} M) after 4 h incubation with LPS (100 ng/ml). The neuron was inhibited by SNP (10^{-5} M).

The excitatory responses to 1400W started after a mean latency of 700 ± 149 s and displayed a mean response duration of 762 ± 136 s. During the stimulatory response, the mean absolute increase of the firing rate was 1.5 ± 0.5 Hz with a mean spontaneous activity of 0.9 ± 0.6 Hz before the superfusion of 1400W (Table 8).

Table 8: Effect parameters of the excitatory responses induced by 1400W (10^{-4}M) after LPS in vitro stimulation (n = 5).

Parameters	**M ± SEM**
Mean spontaneous activity (Hz)	0.9 ± 0.6
Mean latency (s)	700 ± 149
Absolute response (Hz)	1.5 ± 0.5
Absolute peak response (Hz)	2.4 ± 0.8
Mean response duration (s)	762 ± 136

To test the co-sensitivity for 1400W and ghrelin we compared the response of the recorded neurons (n = 5) to both substances. 60% (3/5) of the tested neurons showed an excitatory response to both substances (Table 9).

Table 9: Co-sensitivity between 1400W (10^{-4} M) and ghrelin (10^{-8} M) tested after in vitro LPS stimulation (n = 5).

		1400 W			
		Excited	Inhibited	Insensitive	**Total**
Ghrelin	Excited	3 (60%)	0 (0%)	1 (20%)	**4 (80%)**
	Inhibited	0 (0%)	0 (0%)	0 (0%)	**0 (0%)**
	Insensitive	1 (20%)	0 (0%)	0 (0%)	**1 (20%)**
	Total	**4 (80%)**	**0 (0%)**	**1 (20%)**	

Involvement of NF-κB signaling in the iNOS mediated NO production in the Arc

To test possible immediate effects on neuronal activity of the compound Bay 11-7085, 10 Arc neurons were superfused with Bay 11-7085. None of the neurons showed a

significant response to the NF-κB inhibitor. Figure 5 shows a SNP-inhibited/ghrelin-excited Arc neuron that was insensitive to Bay 11-7085.

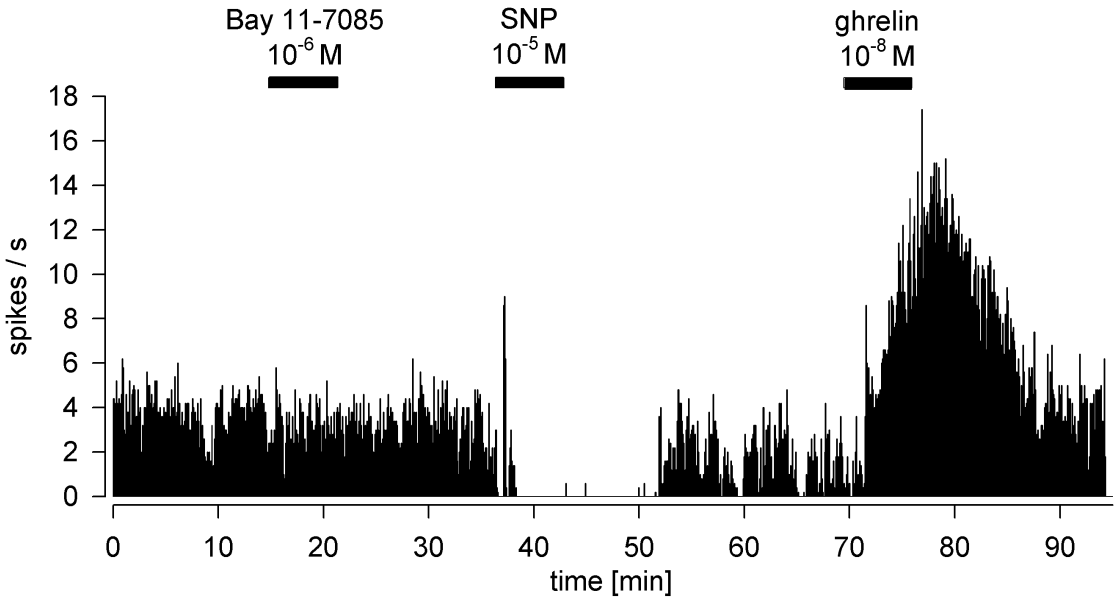

Figure 5: Representative recording of an ArcM neuron showing that superfusion of Bay 11-7085 (10^{-6} M) did not alter neuronal activity. This neuron was inhibited by SNP (10^{-5} M) and excited by ghrelin (10^{-8} M).

To test the involvement of NF-κB in LPS-mediated iNOS-dependent NO signaling in the Arc, we incubated Arc slices with LPS and the NF-κB inhibitor Bay 11-7085. After the incubation the sensitivity of ArcM neurons for 1400W was tested. 90% (9/10) of the tested neurons were 1400W-insensitive (Figure 6). Only one neuron (10%) showed a significant increase in the baseline activity after 1400W superfusion (Figure 7). 50% of the neurons were insensitive to ghrelin administration, 30% (3/10) were excited and 20% (2/10) showed a decrease in their baseline activity. SNP was tested on 9 neurons and it reversibly inhibited 8 of them (89%), while 1 neuron was insensitive (11%).

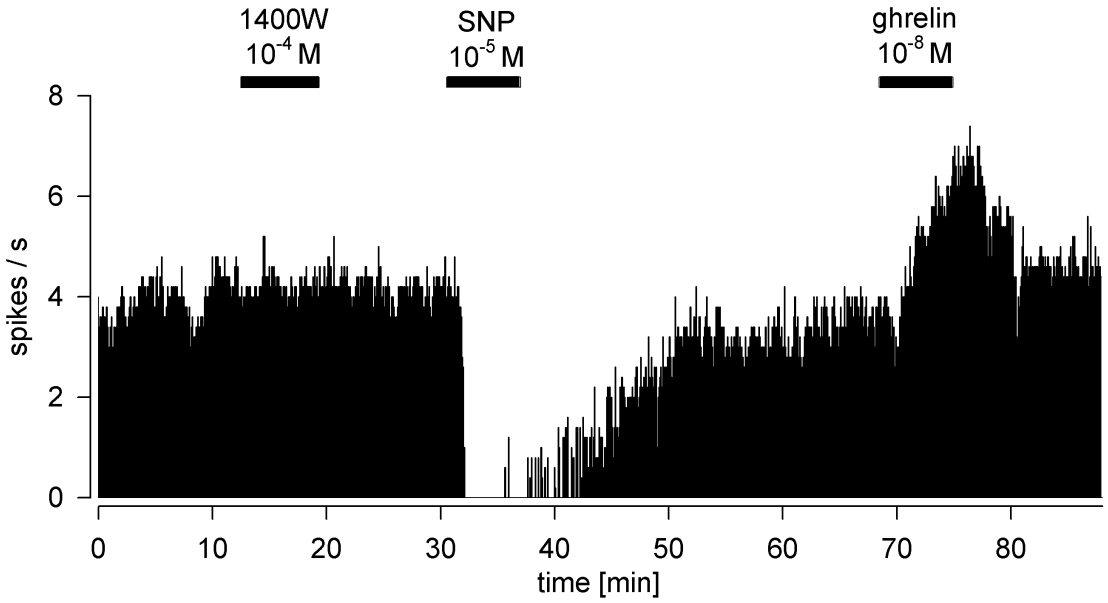

Figure 6: Recording of a representative ArcM neuron insensitive to 1400W (10^{-4} M), SNP (10^{-5} M) inhibited and ghrelin (10^{-8} M) excited after 4 h incubation with LPS (100 ng/ml) and Bay 11-7085(10^{-6} M).

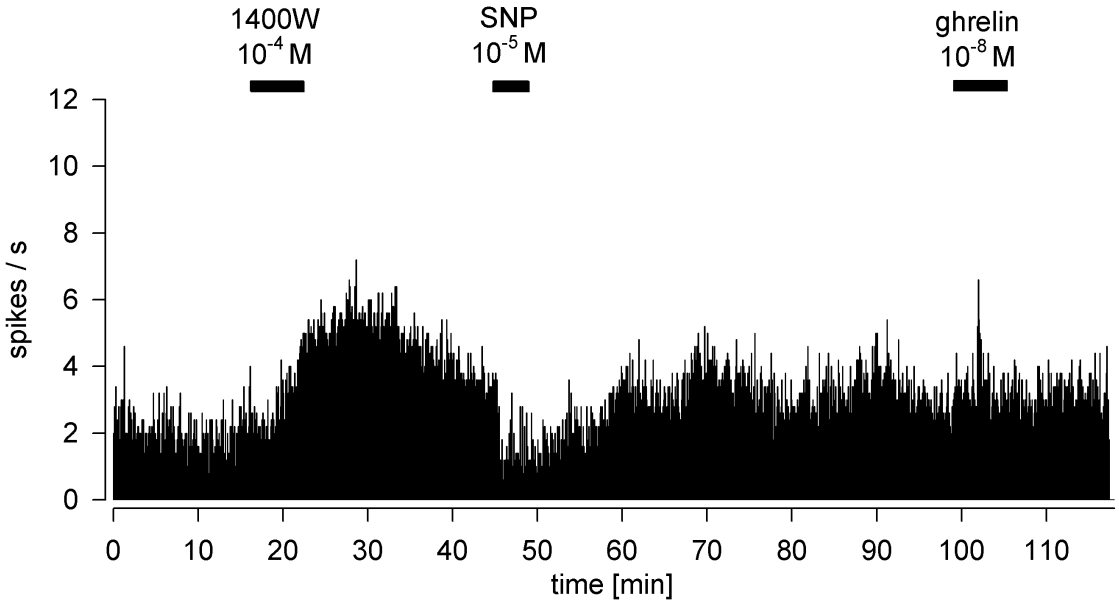

Figure 7: Recording of the only ArcM neuron that showed an increase in baseline activity after 1400W administration after 4 h incubation with LPS (100 ng/ml) and Bay 11-7085 (10^{-6} M). The cell was inhibited by the NO donor SNP (10^{-5} M) but was insensitive to ghrelin (10^{-8} M).

Involvement of STAT signaling in the iNOS mediated NO production in the Arc

To investigate a possible short-term effect on the electrical activity of the Arc neurons, we tested the compound WP1066 on 10 neurons. 6 neurons (60%) did not show any change in their baseline activity (Figure 8). 40 % of the recorded neurons were affected by WP1066 superfusion: 2 (20%) of them where inhibited (Figure 9), while other 2 neurons showed an increase in their firing rate (Figure 10).

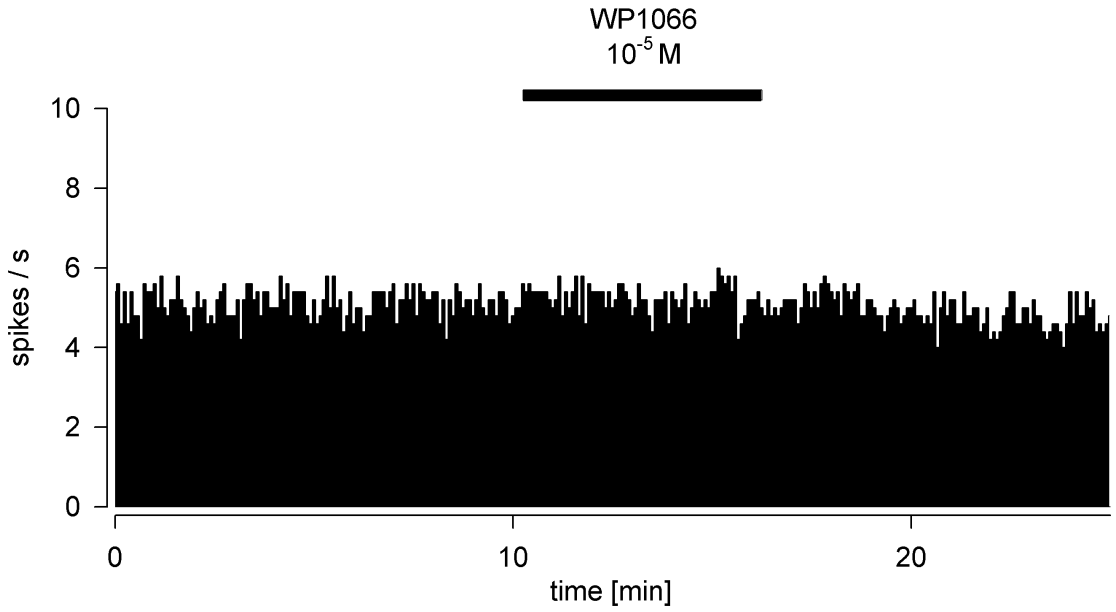

Figure 8: Representative recording of an ArcM neuron without change in the baseline activity after superfusion with WP1066 (10^{-5} M).

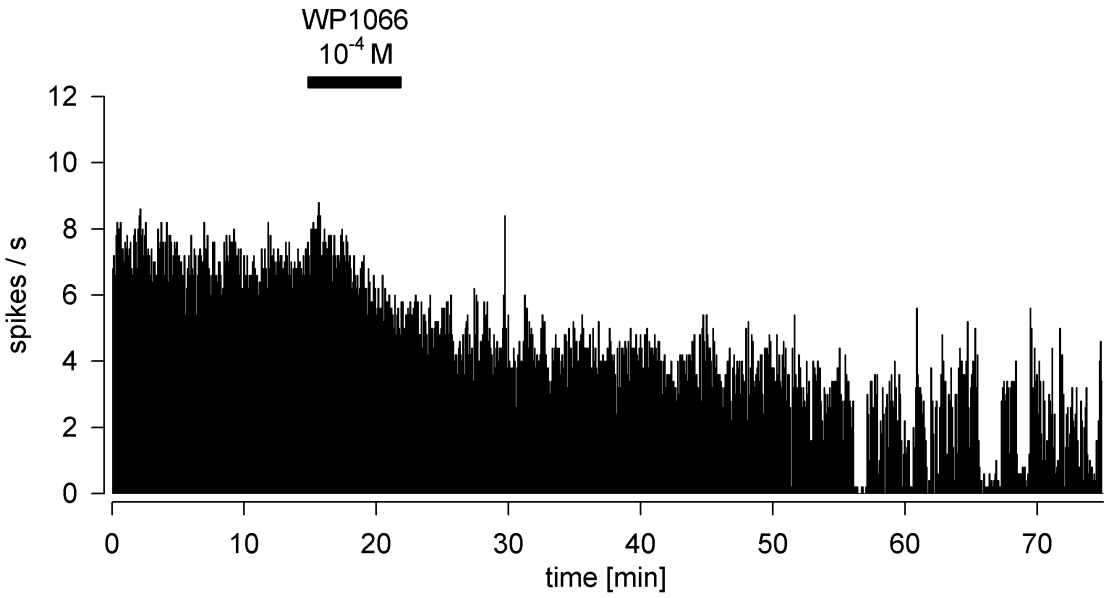

Figure 9: Representative recording of an ArcM neuron, which was inhibited after superfusion of WP1066 (10^{-5} M).

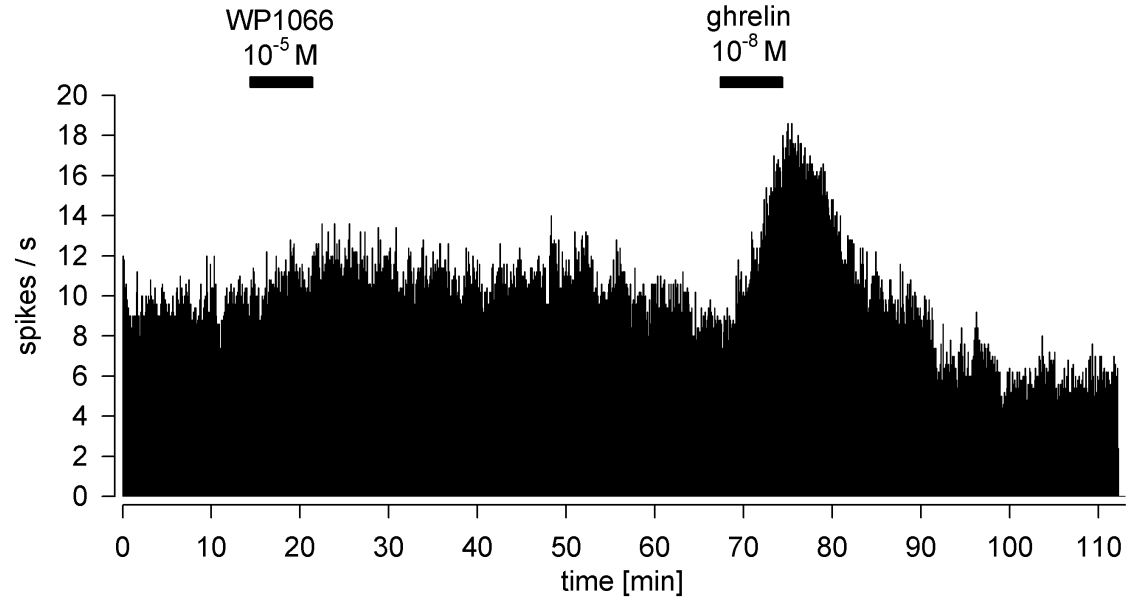

Figure 10: Representative recording of an ArcM neuron, which was excited after superfusion of WP1066 (10^{-5} M) and excited by ghrelin (10^{-8} M).

In order to investigate the involvement of STAT signaling in the LPS triggered iNOS-dependent NO production, the Arc sections were incubated in LPS and the JAK2/STAT inhibitor WP1066. 67% (8/12) of the recorded neurons were 1400W insensitive (Figure 11). 25% (3/12) of the neurons showed a significant increase in their firing rate after 1400W superfusion (Figure 12), while 1 neuron (8%) showed a decrease in the firing rate. 100% of the neurons tested for SNP sensitivity (9/9) showed a strong and reversible inhibition. Ghrelin lead to excitatory effect in 33 % (4/12) of the recorded neurons. 58% (7/12) were insensitive and 1 neuron (8%) showed a decrease in the firing rate.

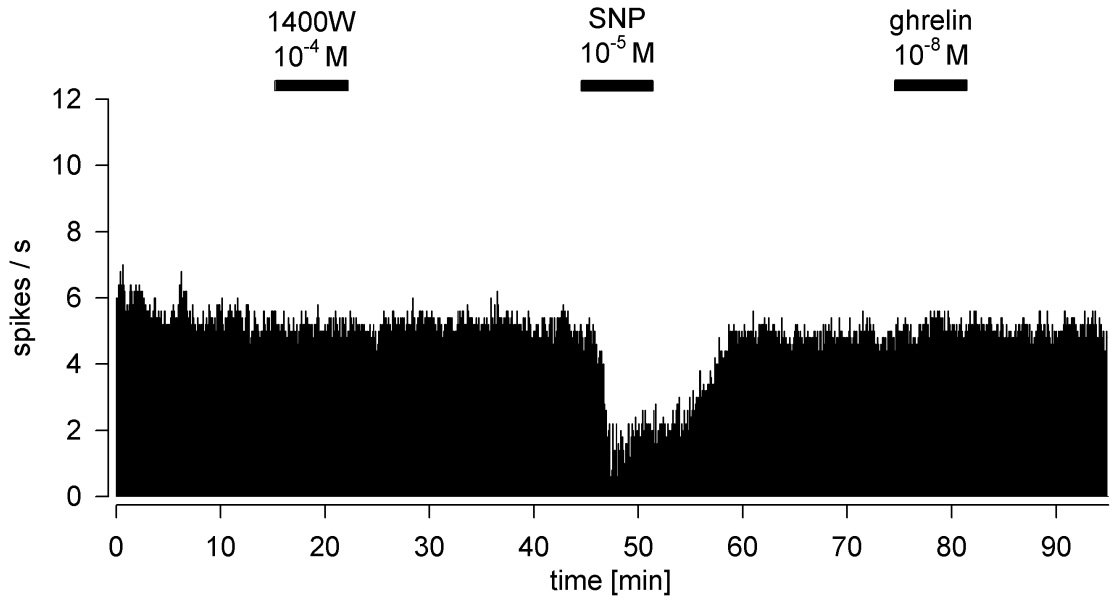

Figure 11: Recording of an ArcM neuron after co-incubation with LPS and WP1066 (10^{-5} M) insensitive to 1400W (10^{-4} M), inhibited by SNP (10^{-5} M) and insensitive to ghrelin (10^{-8} M).

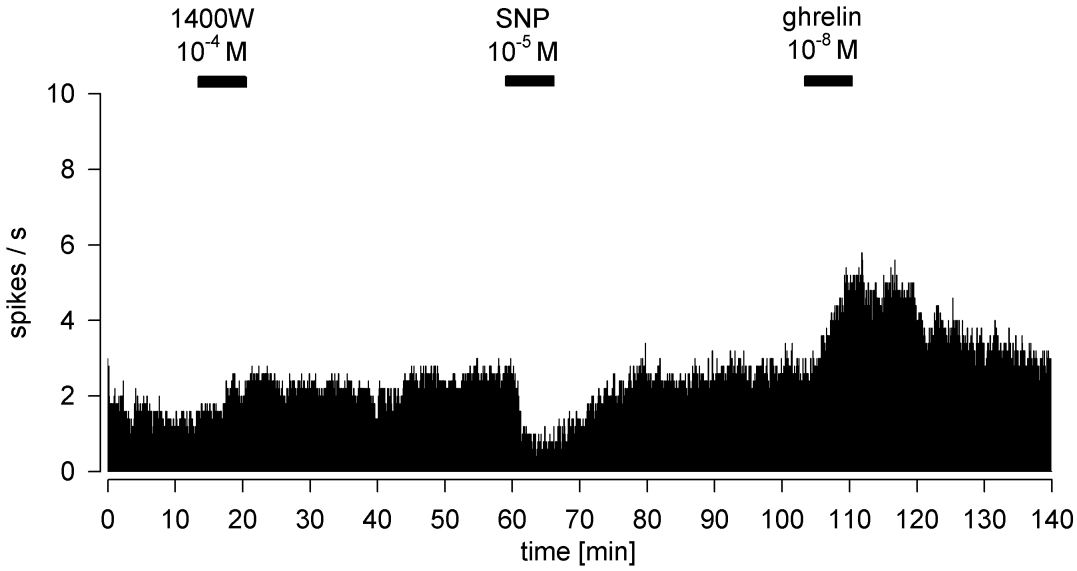

Figure 12: Representative ArcM neuron after 4 h incubation with LPS (100 ng/ml) and WP1066 (10^{-5}M), which showed an increase in baseline activity after 1400W (10^{-4} M) administration. The neuron was inhibited by SNP (10^{-5} M) and excited by ghrelin (10^{-8} M).

The excitatory effect of 1400W started with a mean latency of 376 ± 70 s after the substance reached the recording chamber and displayed a mean response duration of 1436 ± 58 s. During the stimulatory response, the mean absolute increase of the firing rate was 0.8 ± 0.2 Hz with a mean spontaneous activity of 2.7 ± 1.1 Hz before the superfusion of 1400W (Table 10).

Table 10: Effect parameters of the excitatory responses induced by 1400W (10^{-4} M) after incubation with LPS (100 ng/ml) and WP1066 (10^{-5} M) (n = 3).

Parameters	**M ± SEM**
Mean spontaneous activity (Hz)	2.7 ± 1.1
Mean latency (s)	376 ± 70
Absolute response (Hz)	0.8 ± 0.2
Absolute peak response (Hz)	1.4 ± 0.3
Mean response duration (s)	1436 ± 58

Percentage of 1400W sensitive cells

Figure 13 shows the percentage of 1400W sensitive cells after incubation with LPS and co-incubation with LPS and Bay 11-7085 or WP1066. After LPS incubation 63% of the recorded neurons showed an increase in their firing rate after 1400W superfusion. After co-incubation with LPS and Bay 11-7085 only 10% of the tested neurons were 1400W sensitive. After co-incubation with LPS and WP1066 25% of the neurons were exited after 1400W application and 8% showed an inhibition. Using the Fisher's exact test we found a significant difference in proportion of 1400W sensitive cells between the LPS incubated group and the LPS/Bay 11-7085 co-incubated group ($p = 0.043$). On the other hand no significant difference was found between the LPS incubated group and the LPS/WP1066 co-incubated group ($p = 0.18$).

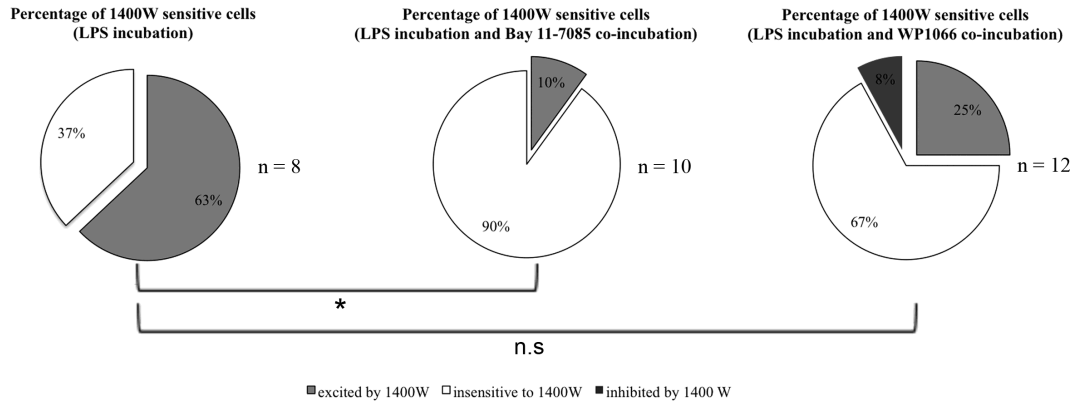

Figure 13: Percentage of 1400W sensitive cells. (Analysis conducted using the Fischer's exact test; * = $p < 0.05$; n.s. = $p > 0.05$)

6.2 NF-κB activation after in vivo LPS stimulation

The aim of these experiments was to investigate whether nuclear translocation of NF-κB occurs after in vivo LPS stimulation. We analyzed nuclear translocation of NF-κB at 2 and 4 hours after LPS injection.

6.2.1 NF-κB activation 4 hours after LPS injection

The animals were randomly assigned to one of the two groups. Half of the animals were injected intraperitoneally with 100 µg/kg LPS. The rest of the animals served as saline-treated controls. Activation of the NF-κB pathway was detected by a doublestaining for NF-κB and DAPI, which binds to dsDNA resulting in a nuclear staining.

4 h after LPS injection NF-κB immunoreactivity in the Arc was present in both groups (Figure 14). The Arc displayed a high immunoreactivity in blood vessels (Figure 15 and Figure 16) and NF-κB-positive cells were present in the brain parenchyma. At this time point immunoreactivity was confined to the cytoplasm indicating the absence of nuclear translocation of NF-κB in both treatment groups (Figure 17 and Figure 18). Similarly there was no obvious difference in the density or intensity of NF-κB immunoreactivity between the LPS and the saline treated group (Figure 14).

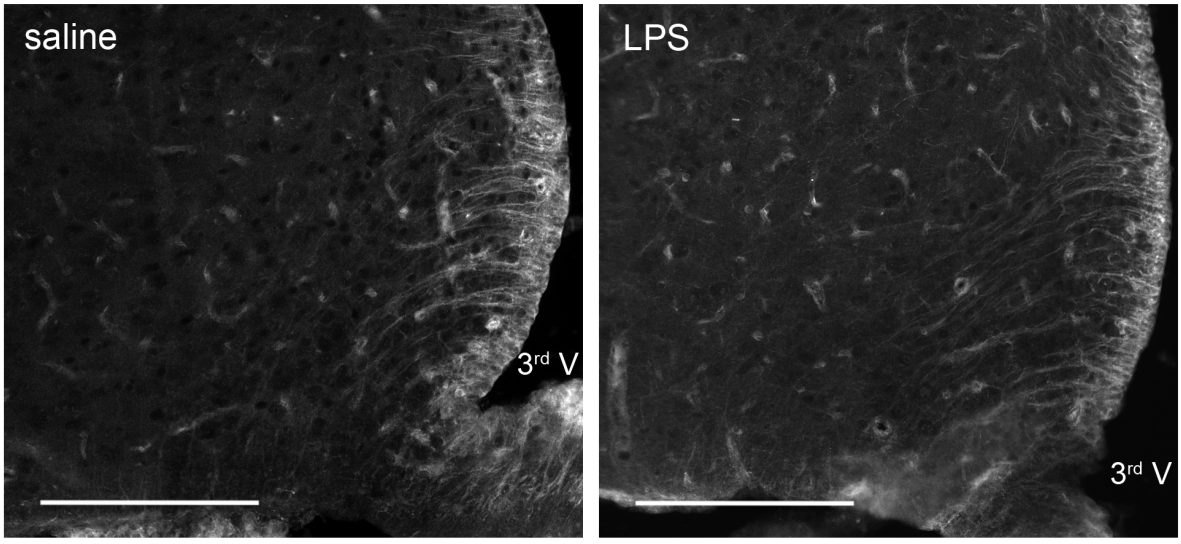

Figure 14: NF-κB immunostaining of the Arc 4 hours after saline or LPS injection. (3rdV = third ventricle, scale bar = 100 µm)

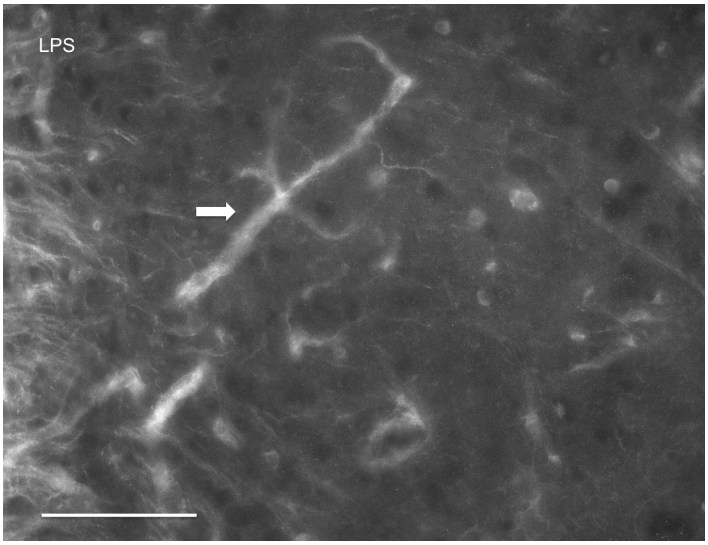

Figure 15: NF-κB immunostaining in the Arc 4 hours after LPS injection showing an immunoreactive blood vessel (arrow). (Scale bar 50 μm)

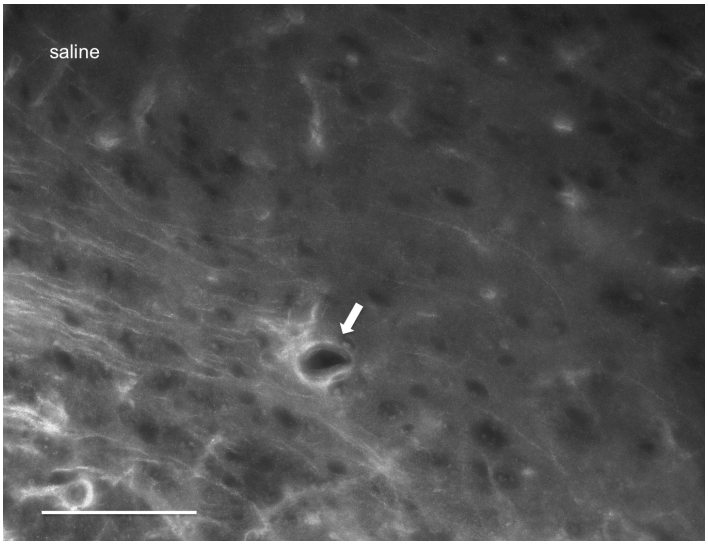

Figure 16: NF-κB immunostaining of the Arc after saline treatment showing c NF-κB immunoreactivity in a blood vessel (arrow). (Scale bar = 50 μm)

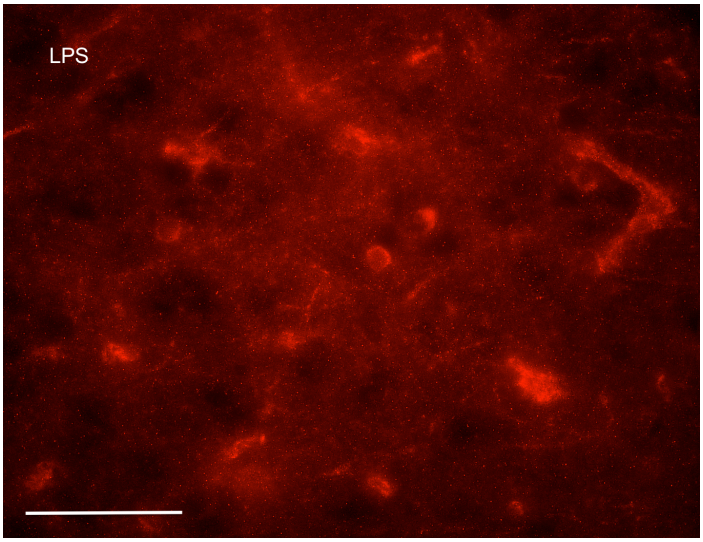

Figure 17: NF-κB immunostaining in the Arc 4 hours after LPS injection (Scale bar = 50 µm).

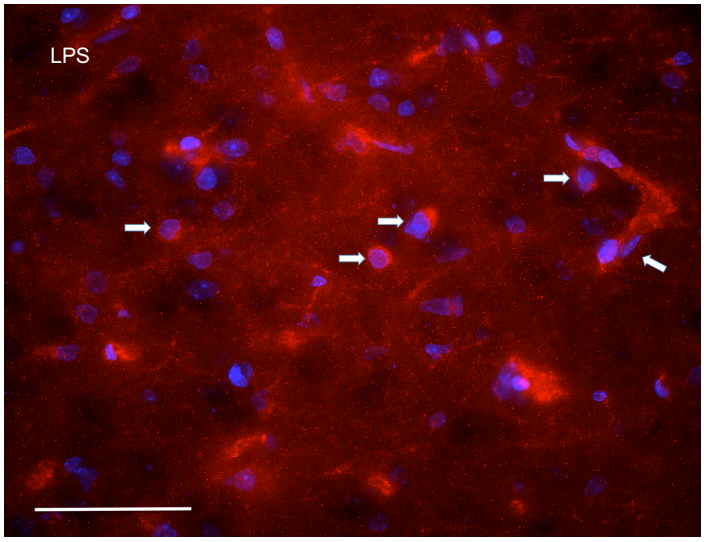

Figure 18: NF-κB/DAPI double-staining (red and blue, respectively) in the Arc of an LPS-treated rat showing cytoplasmatic localization of NF-κB immunoreactivity (arrows). The blue staining represents DAPI positive cell nuclei. (Scale bar = 50 µm)

6.2.2 NF-κB activation 2 hours after LPS stimulation

Proceeding from the negative outcome of the study conducted at the 4h time point, we analyzed the effect of LPS on NF-κB activation 2h after treatment at the standard dose of 100 µg/kg and a higher dose of 300 µg/kg LPS (hLPS). The area postrema was included in these studies. The NF-κB/DAPI staining was combined with the immohistochemical detection of the vascular markers von Willebrand factor or RECA-1. The latter staining

was used for the AP because we did not detected vW immunoreactivity in the AP (data not shown).

Arcuate nucleus

NF-κB immunoreactivity in the Arc was seen in each of the treatment groups (Figure 20) without obvious differences. Although the highest numbers of NF-κB/DAPI positive cells were detected in animals belonging to the LPS treatment groups, the absolute cell counts were very low and characterized by considerable individual variability. For these reasons, we were unable to detect a significant effect of LPS treatment on nuclear translocation of NF-κB as measured by the co-localization of NF-κB immunoreactivity and DAPI fluorescence (Figure 19).

All cells showing a NF-κB/DAPI co-localization were identified as endothelial cells, while in non-vascular cells of the brain paremchyma NF-κB immunoreactivity was confined to the cytoplasm (Figure 21).

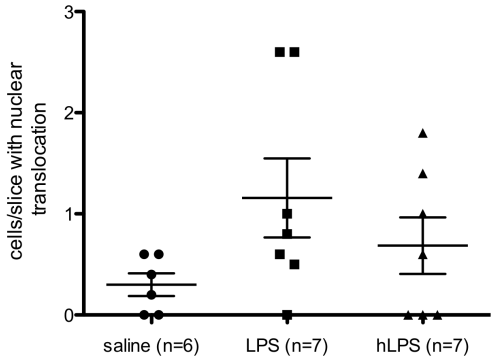

Figure 19: Numbers of cells with nuclear localization of NF-κB 2 hours after injection of LPS (one-way ANOVA, $p > 0.05$). (LPS = 100 µg/kg, hLPS = 300 µg/kg).

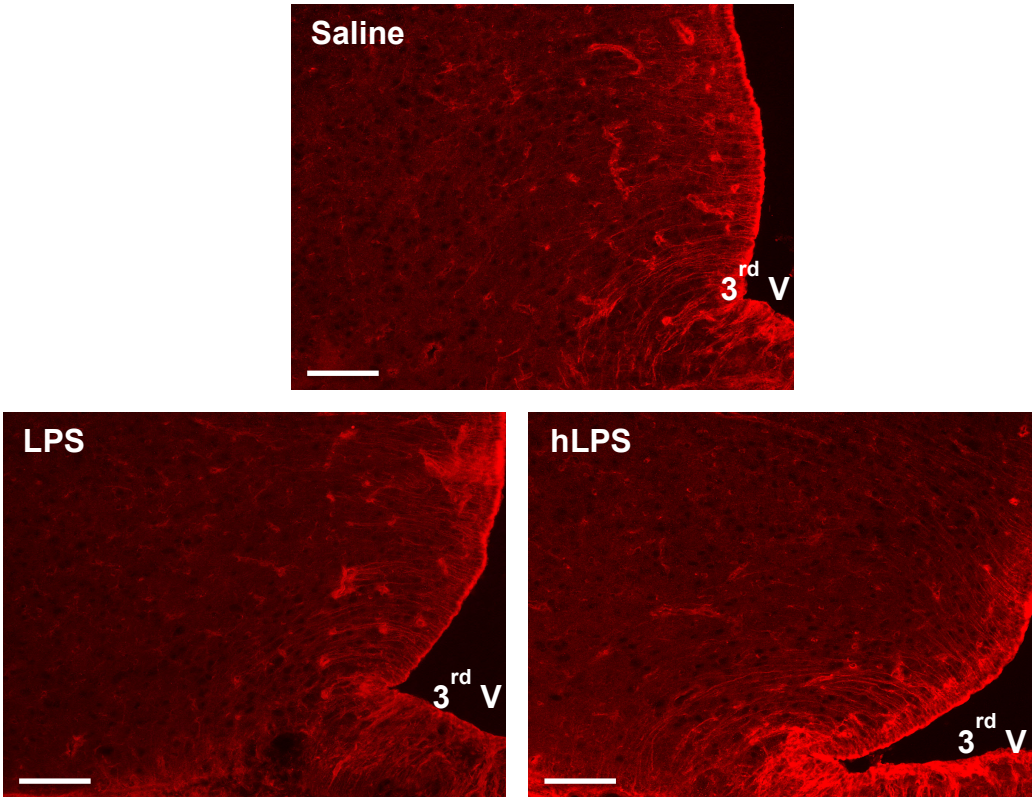

Figure 20: NF-κB immunostaining in the Arc 2 hours after injection with saline, LPS (100 µg/kg) and hLPS (300 µg/kg). (Scale bar = 100 µm)

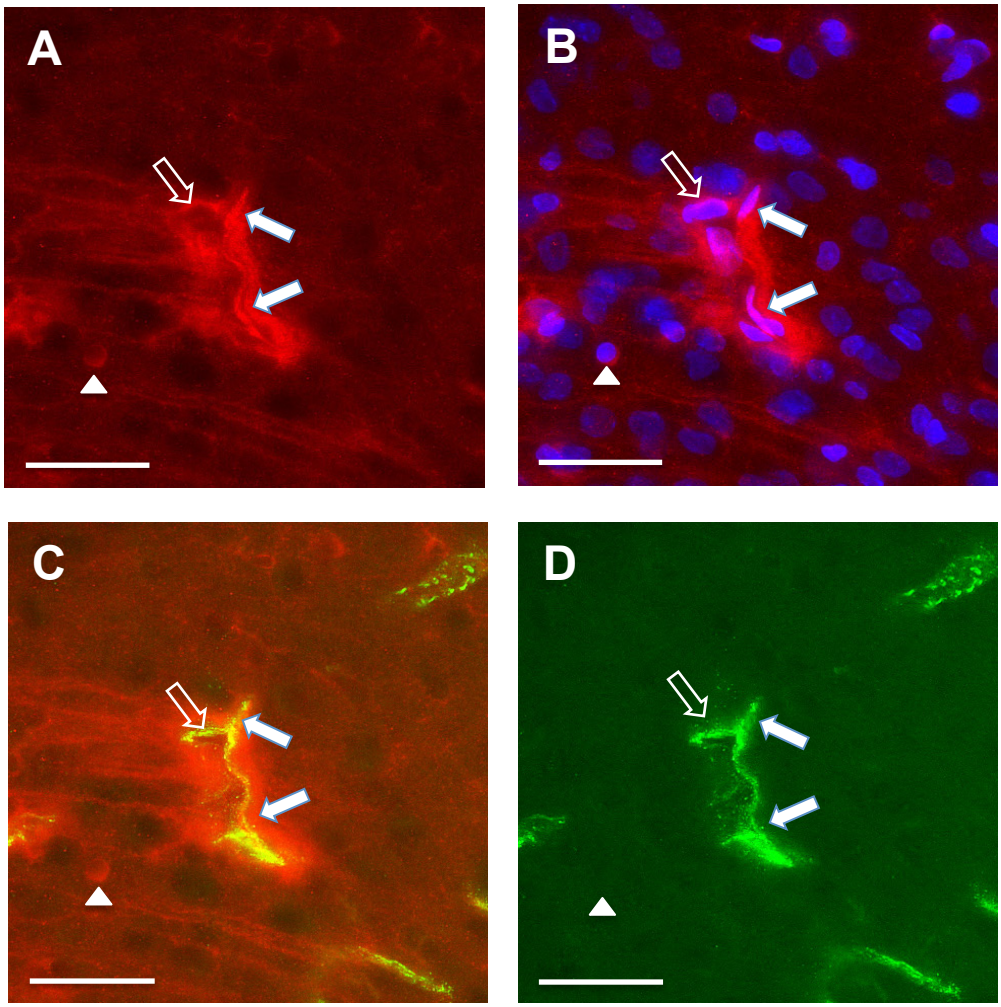

Figure 21: Nuclear translocation (close arrows) of NF-kB in endothelial cells of the Arc 2 hours after LPS injection (100 µg/kg). Open arrow: endothelial cell without nuclear NF-κB staining. Arrowhead: non-vascular cell in the brain parenchyma without nuclear translocation of NF-κB. (A) NF-κB (red), (B) NF-κB + DAPI (blue), (C) NF-κB + vW (green), (D) vW (scale bar = 20 µm).

Area postrema

2 hours after injection of LPS NF-κB immunoreactivity was seen in the AP in all groups (Figure 23). Nuclear translocation of NF-κB was detected in some cells. To phenotype these cells an antibody against the rat endothelial cell antigen-1 (RECA-1) was used to mark endothelial cells of the AP. The cells that showed NF-κB activation were identified as endothelial cells or were in close vicinity to vascular structures (Figure 24 and Figure 25). The sections of animals treated with LPS or hLPS showed a significantly increased number of cells with nuclear translocation of NF-κB (Figure 22).

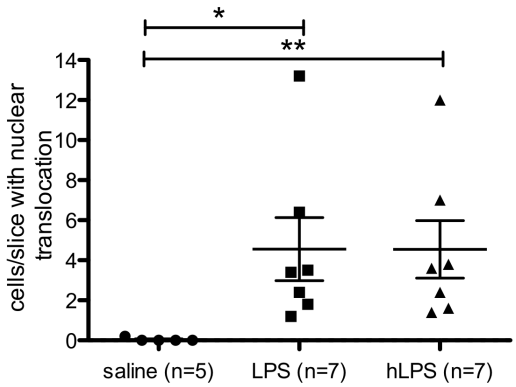

Figure 22: Number of cells with nuclear staining of NF-κB. 2 hours after injection of LPS (Kruskal-Wallis test *p = 0.0049*; Dunn's Multiple Comparison Test served as post hoc test).

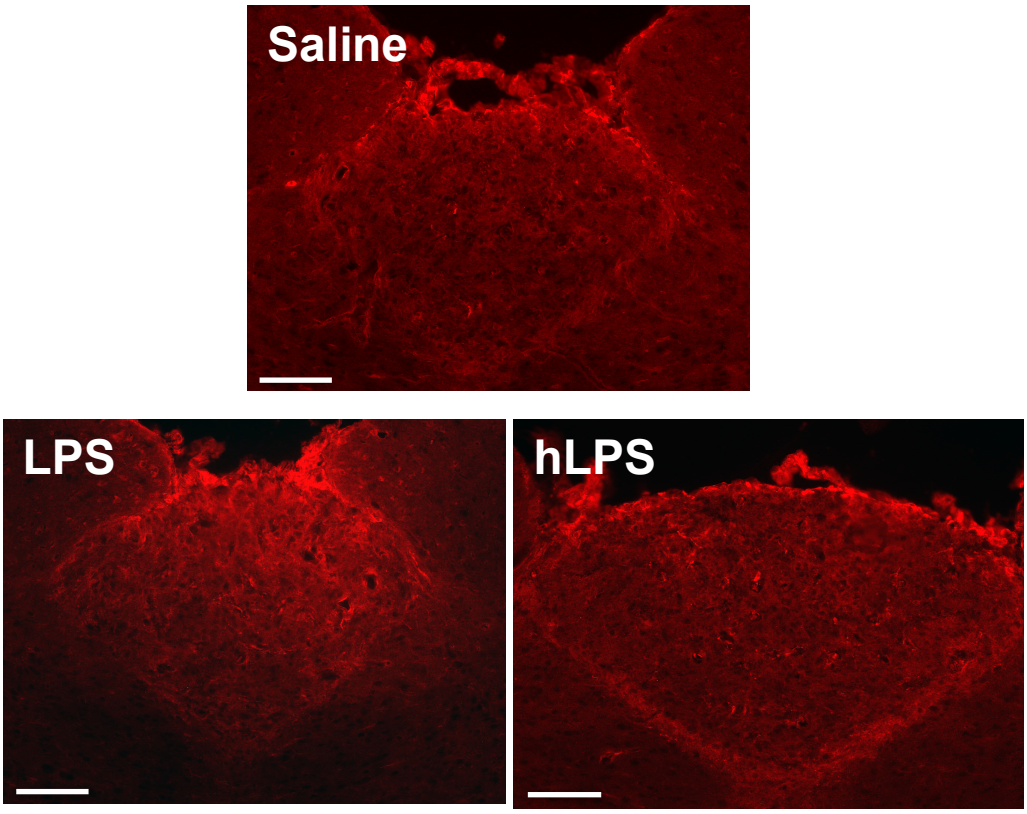

Figure 23: NF-κB immunoreactivity in the AP 2 h after injection. LPS = 100 µg/kg, hLPS = 300 µg/kg. (Scale bar = 100 µm).

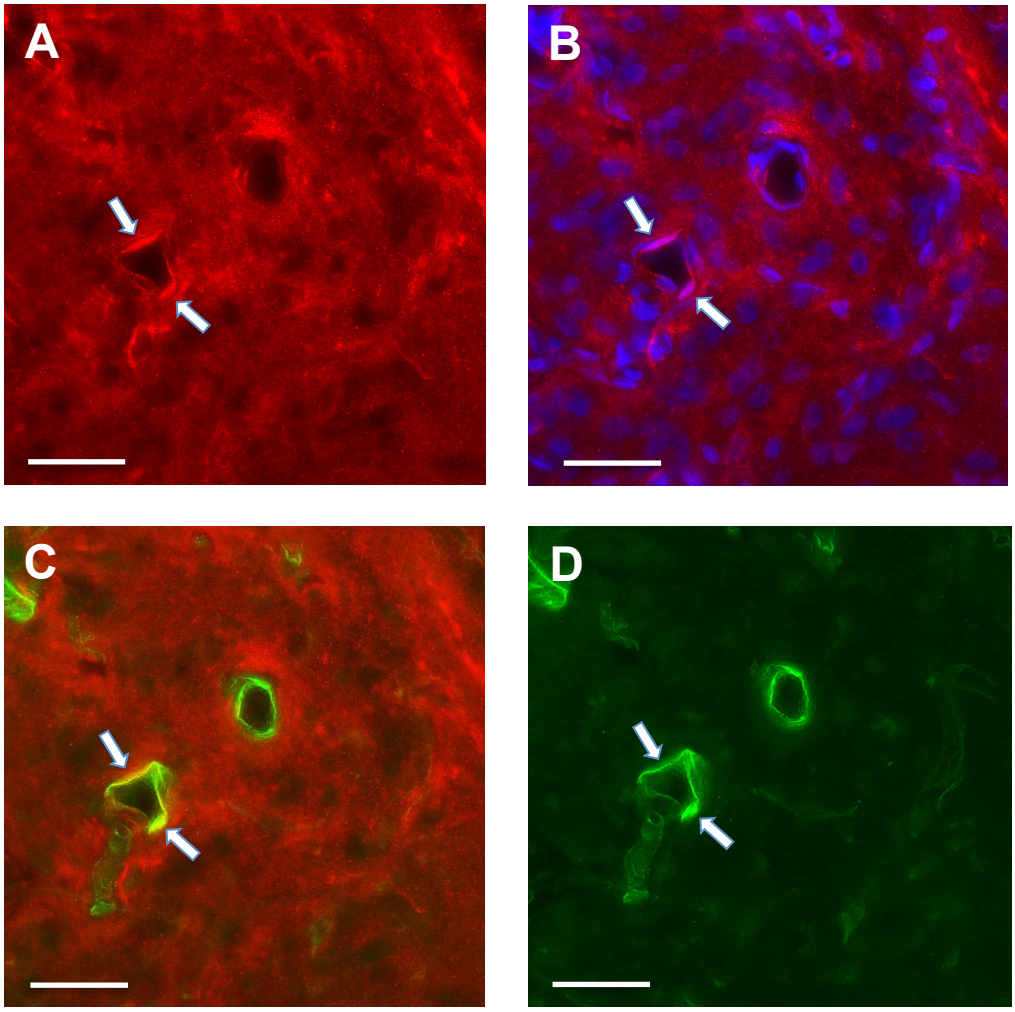

Figure 24: Nuclear translocation of NF-kB in endothelial cells of the AP (arrow) 2 hours after LPS injection (100 µg/kg). (A) NF-κB, (B) NF-κB + DAPI, (C) NF-κB + RECA-1, (D) RECA-1. (scale bar = 20 µm).

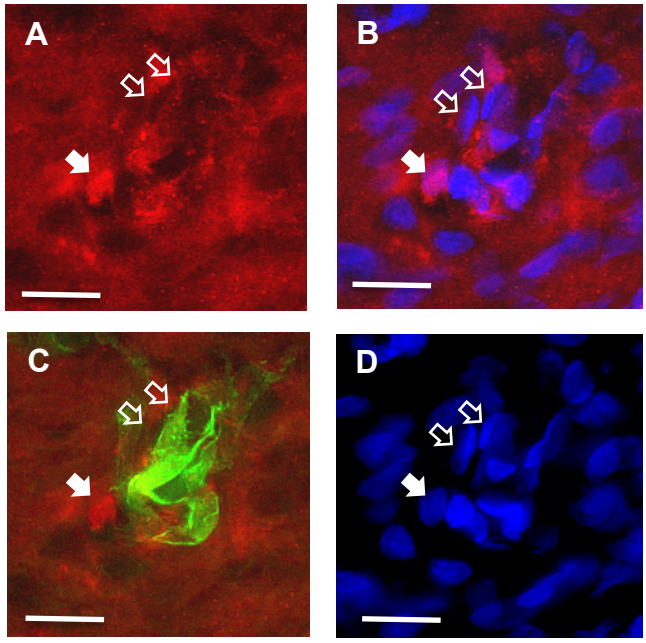

Figure 25: Immunostaining of the AP 2 hours after LPS injection (300 µg/kg). Closed arrow: nuclear translocation of NF-kB in a cell in close vicinity to a blood vessel Open arrows: two endothelial cells without nuclear localization of NF-κB (A) NF-κB (red), (B) NF-κB + DAPI, (C) NF-κB + RECA-1 (green), (D) DAPI (blue). (Scale bar = 10 µm)

6.3 NF-*κ*B activation after in vitro stimulation of Arc sections

To investigate whether in vitro incubation with LPS leads to activation of NF-κB, Arc sections were incubated for 1 h and a NF-κB triple staining with DAPI and vW was performed. After 1 h in vitro incubation, NF-κB immunoreactivity was seen in both groups. A high number of cells with nuclear staining of NF-κB was present in the LPS incubated sections, but also in the controls (Figure 27). There was no difference in the number of cells with nuclear NF-κB staining between the controls and the LPS stimulated sections (Figure 26). Most of these cells were located in a 100-200 µm wide margin at the outer area of the tissue slices (Figure 27).

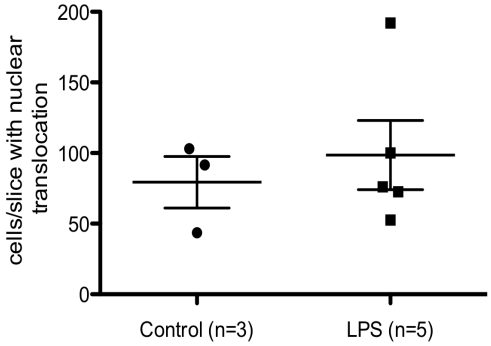

Figure 26: NF-κB immunostaining in the Arc after 1 h incubation in aCSF (control) or LPS (100 ng/ml). No difference was seen between the two groups (Mann-withney test).

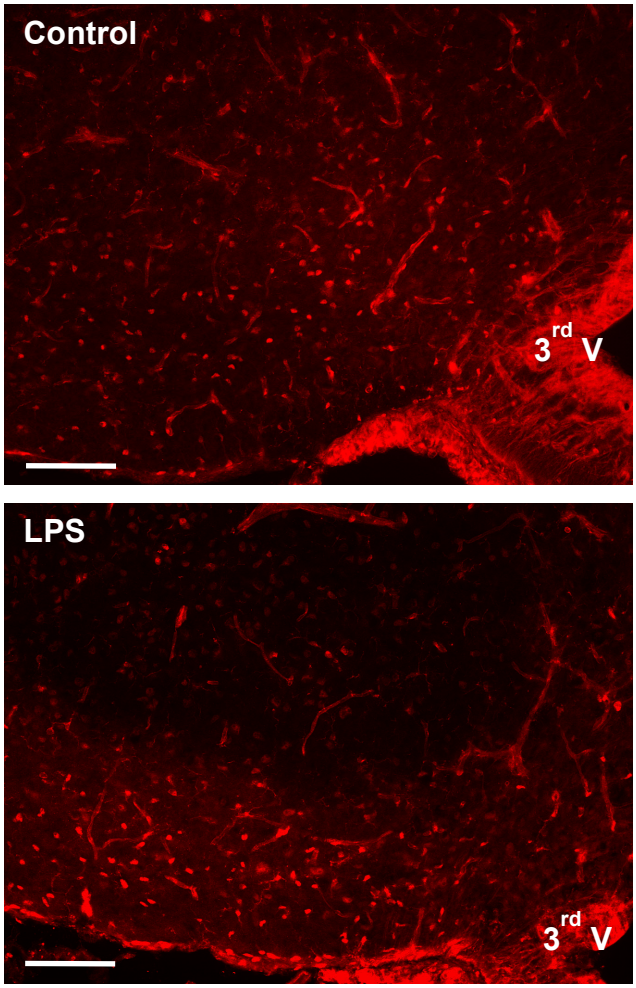

Figure 27: NF-kB immunoreactivity in the Arc after 1 h in vitro incubation in aCSF (control) or LPS (100 ng/ml). (3^{rd}V = third ventricle, scale bar = 100 µm)

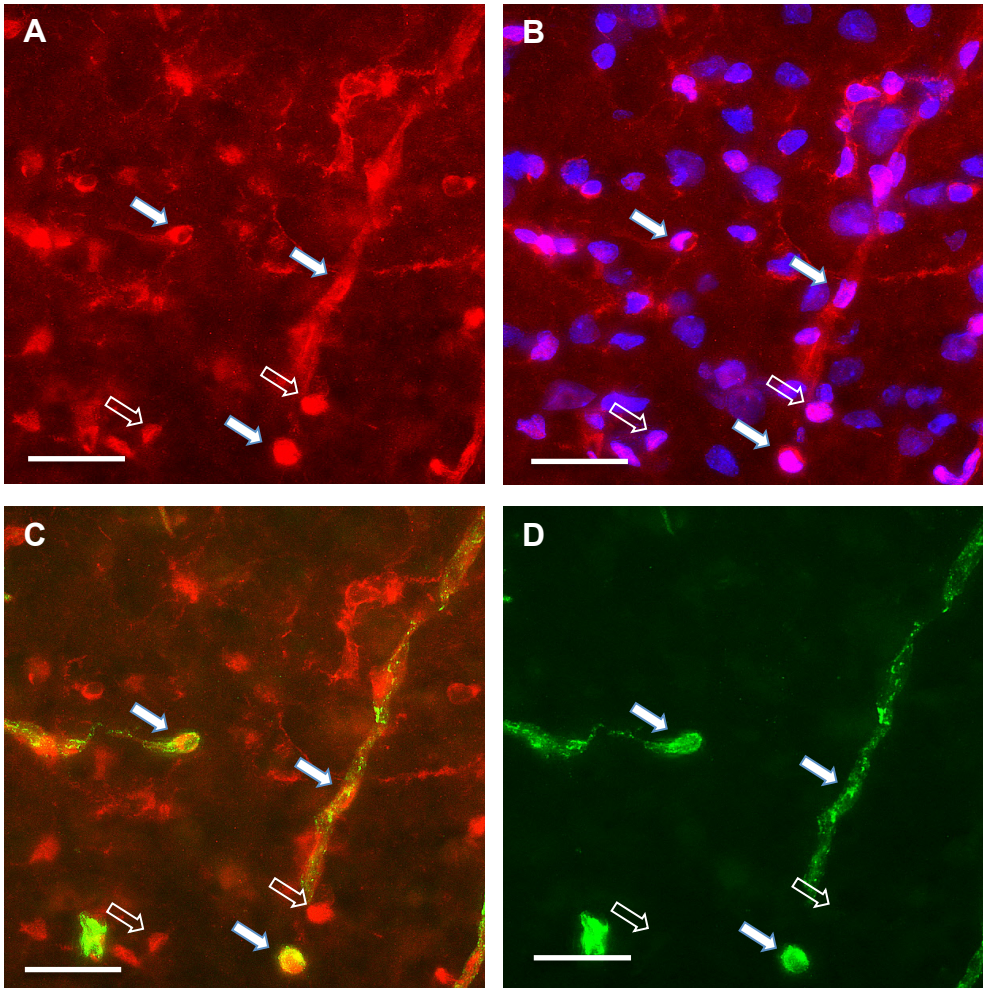

Figure 28: NF-κB immunoreactivity in the Arc after 1h incubation in aCSF (control). Close arrows: nuclear translocation of NF-κB in endothelial cells; open arrow: NF-κB translocation in non-vascular cells spread through the parenchyma (A) NF-κB (red), (B) NF-κB + DAPI (blue), (C) NF-κB + vW (green), (D) vW (scale bar = 20 μm).

6.4 STAT1 and STAT3 phosphorylation in the Arc after in vitro LPS stimulation

It has been shown in previous studies that in vivo LPS treatment induces phosphorylation of both STAT1 and STAT3 in the Arc 4 h after injection. To investigate whether in vitro incubation with LPS triggers a phosphorylation of STAT1 and STAT3, Arc sections were incubated in LPS for 4 h and a staining for pSTAT1 and pSTAT3 was performed.

In vitro incubation of Arc slices for 4 h in LPS triggered a STAT3 phosphorylation in the Arc of rats. LPS stimulated sections showed a significantly increased number of pSTAT3 positive cells (Figure 29).

No significant difference in STAT1 phosphorylation was noticed between the in vitro LPS stimulated group and the control group (Figure 30).

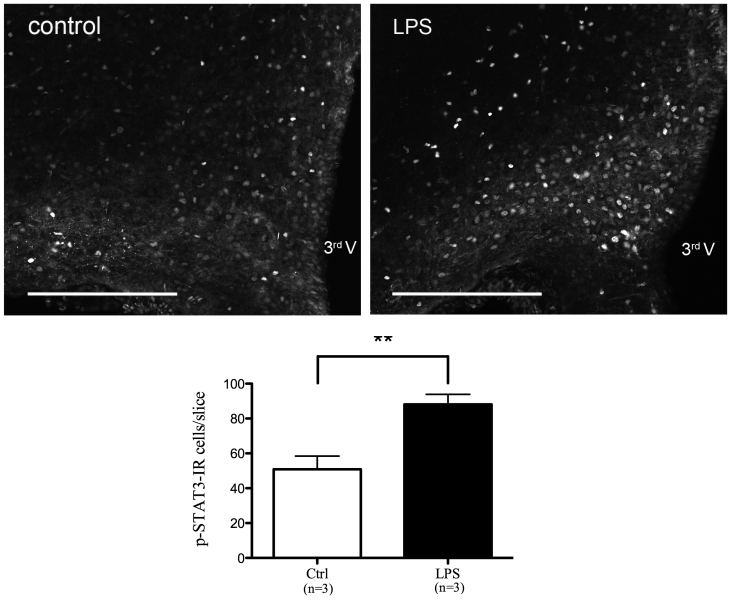

Figure 29: pSTAT3 immunostaining in the Arc after 4 h incubation in aCSF (control) or LPS. (3^{rd}V = third ventricle, scale bar = 50 µm). 4h LPS incubation lead to a significantly increased number of pSTAT3 immunoreactive cells (Student't test, $p < 0.005$)

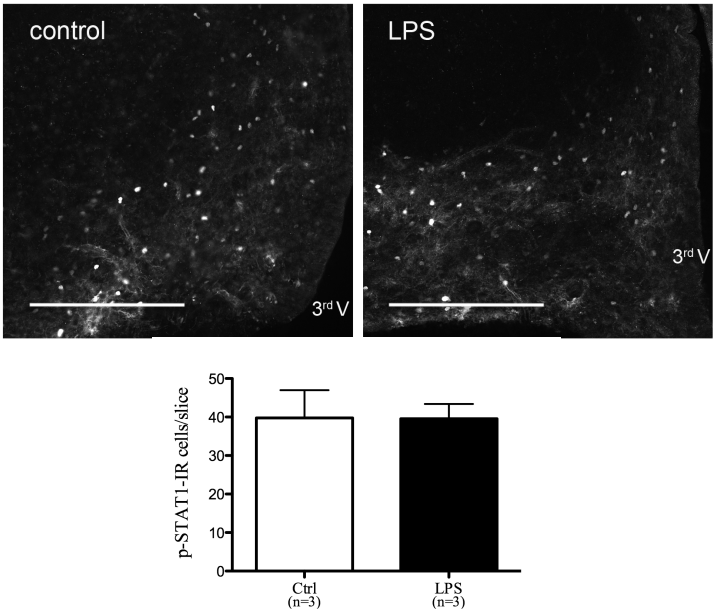

Figure 30: pSTAT1 immunostaining of the Arc after 4 h incubation in aCSF (control) or LPS. (3^{rd}V = third ventricle, scale bar = 50 µm). 4h LPS incubation did not lead to a significant difference in the number of pSTAT1 immunoreactive cells in the Arc (Student´s t-test).

6.5 Co-sensitivity of Arc neurons for HM01 and ghrelin

In the second part of the electrophysiological studies 17 ArcM neurons were recorded. The mean amplitude of the action potentials was 185 μV, which allowed an accurate discrimination from background noises.

To determine the co-sensitivity for ghrelin and HM01 we compared the responses of the recorded neurons (n = 17) to both substances (Table 11). 100% of the tested neurons showed the same response after ghrelin and HM01 superfusion (10^{-6} to10^{-7} M). 76% (13/17) were exited by both ghrelin and HM01, 1 neuron (6%) was inhibited and 18% (3/17) were insensitive to both substances. We tested the ghrelin-agonist HM01 at two different concentrations (10^{-6} and 10^{-7} M).

Table 11: Co-sensitivity between ghrelin (10^{-8} M) and HM01 (10^{-6}/10^{-7} M) (n=17).

		HM01			
		Excited	Inhibited	Insensitive	**Total**
Ghrelin	Excited	13 (76%)	0 (0%)	0 (0%)	**13 (76%)**
	Inhibited	0 (0%)	1 (6%)	0 (0%)	**1 (6%)**
	Insensitive	0 (0%)	0 (0%)	3 (18%)	**3 (18%)**
	Total	**13 (76%)**	**1 (6%)**	**3 (18%)**	

Excitatory responses after ghrelin and HM01 superfusion

76% (13/17) of the recorded ArcM neurons showed an excitatory response after both ghrelin and HM01 (Figure 31 and Figure 32)

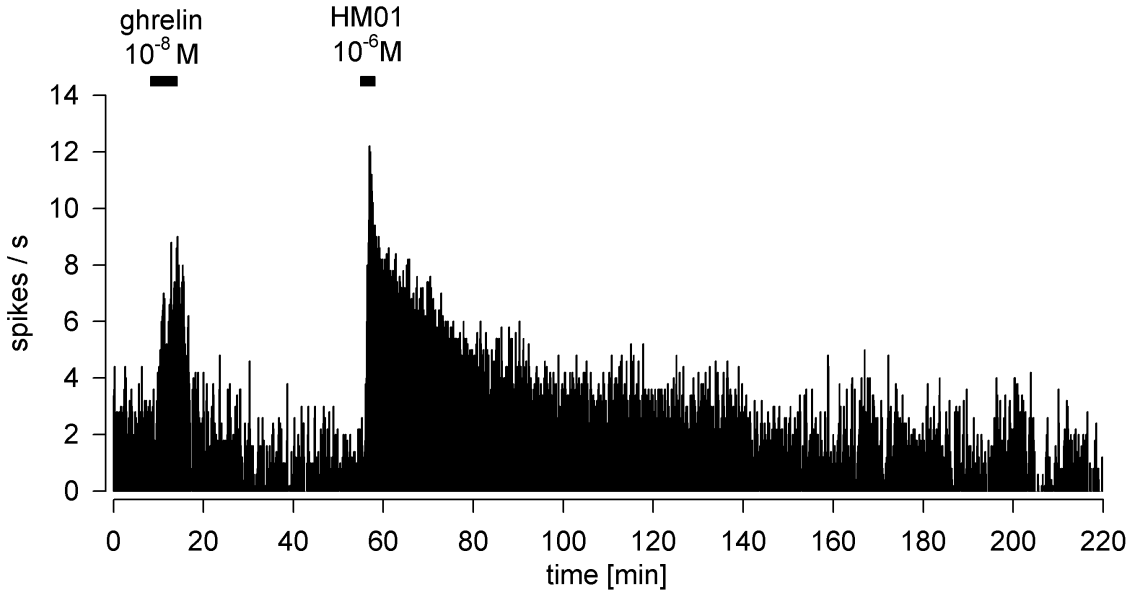

Figure 31: Representative recording of an ArcM neuron, which shows an excitatory response after superfusion of ghrelin (10^{-8} M) and HM01 (10^{-6} M).

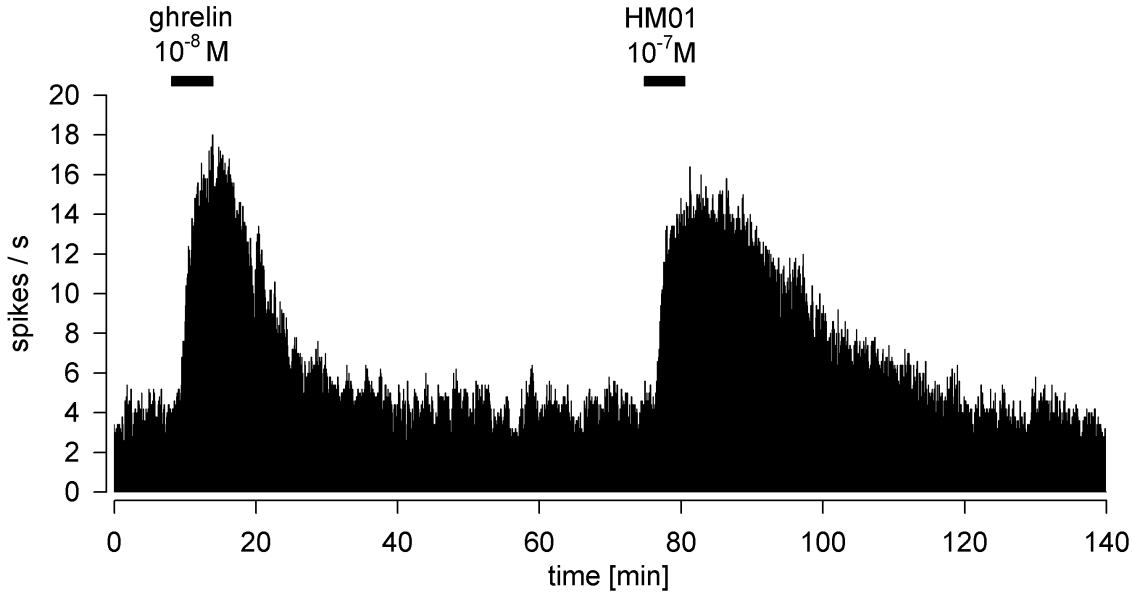

Figure 32: Representative recording of an ArcM neuron, which was exited after superfusion of ghrelin (10^{-8} M) as well as after HM01 (10^{-7} M).

We compared the effect parameters of the excitatory responses (Table 12) after superfusion of ghrelin (10^{-8} M), HM01 (10^{-6} M) and HM01 (10^{-7} M) using a one-way ANOVA or the Kruskal-Wallis test if not normally distributed. The excitatory responses after superfusion of HM01 (10^{-7} M) showed a significant longer latency period compared to the responses induced by ghrelin and HM01 (10^{-6} M) (*p = 0.03*). After superfusion of HM01 (10^{-6} M) the excitatory responses lasted significantly longer in comparison to ghrelin-induced stimulatory effects (*p = 0.03*). The spontaneous activity and the absolute responses did not differ between the three groups (Figure 33)

Table 12: Effects parameters of the excitatory responses after superfusion of ghrelin 10^{-8} M (n=13), HM01 10^{-6} M (n=8) and HM01 10^{-7} M (n=5)

Parameters	**Ghrelin 10^{-8} M (M ± SEM)**	**HM01 10^{-6} M (M ± SEM)**	**HM01 10^{-7} M (M ± SEM)**
Mean spontaneous activity (Hz)	2.7 ± 0.5	2.5 ± 0.7	1.7 ± 0.7
Mean latency (s)	53± 7.9	63 ± 13.7	128 ± 36.3
Absolute response (Hz)	2.5 ± 0.6	2.7 ± 0.6	3.9 ± 1.1
Absolute peak response (Hz)	5.2 ± 1	4.5 ± 1	6.1 ± 1.7
Mean response duration (s)	899 ± 76.2	2103 ± 552	1952 ± 537

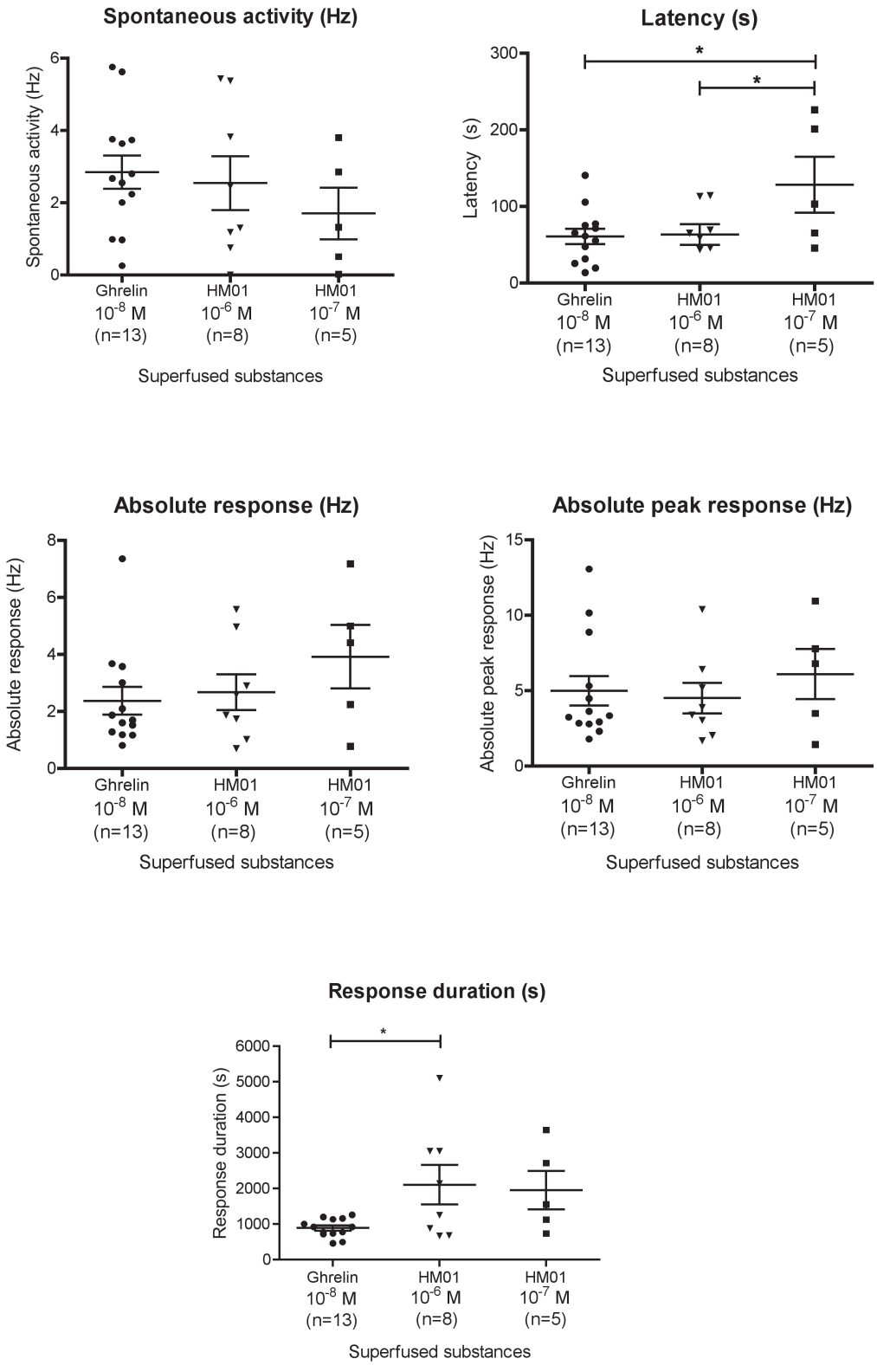

Figure 33: Effect parameters of the excitatory responses induced by ghrelin (10^{-8} M) and HM01 (10^{-6} M and 10^{-7} M) (one-way ANOVA or Kruskal-Wallis test if not normally distributed, the Newmann-Keuls Multiple Comparison Test served as post hoc test; * < *0.05*).

Inhibitory responses after ghrelin and HM01 superfusion

One of the recorded neurons (6%) was inhibited by the application of both ghrelin and HM01 (Figure 34). The inhibitory effect of ghrelin started with a latency of 337 s and lasted for 709 s, whereas the inhibition after superfusion with HM01 started after 115 s and lasted for 4131s.

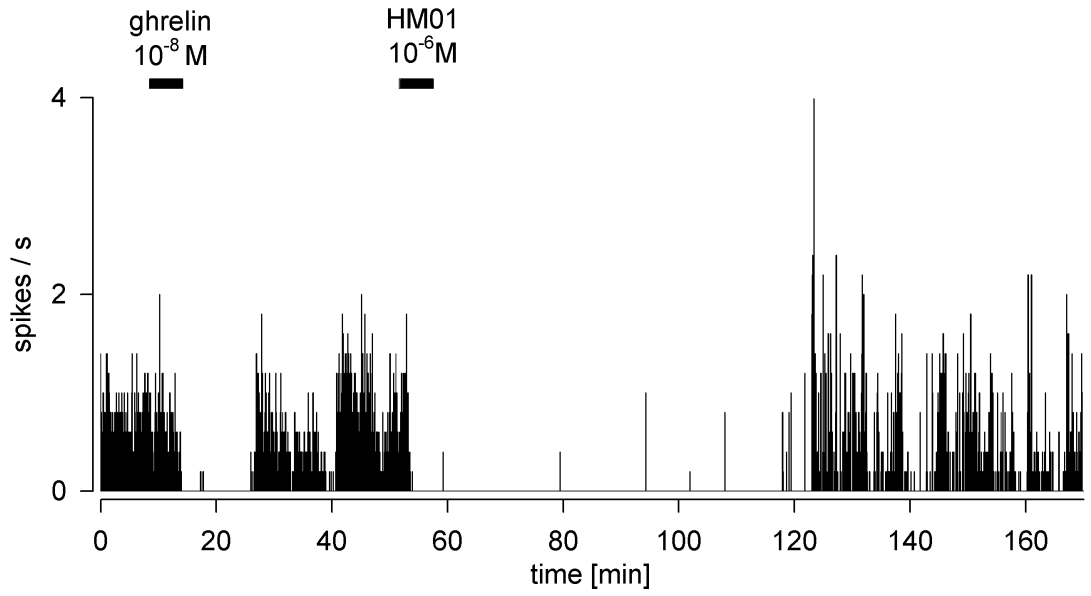

Figure 34: Recording of the ArcM neuron, which was inhibited after the application of ghrelin (10^{-8} M) and HM01 (10^{-6} M).

Repeated stimulation with HM01

In previous studies electrophysiological studies repeated superfusion of ghrelin did not lead to reduced neuronal sensitivity (Traebert et al., 2002). To evaluate whether this is also true for the ghrelin agonist 7 cells were repeatedly stimulated with HM01 at both concentrations. All of these cells were excited after the first application of ghrelin and HM01. In 4 recordings the repeated superfusion of HM01 induced excitatory responses (Figure 35). The absolute mean responses after the second stimulation with HM01 10^{-7} M were significantly reduced ($p = 0.017$) (Figure 36). In 3 of the repeatedly stimulated cells no further response occurred after the subsequent superfusions with HM01 (Figure 37).

To test if the loss of sensitivity was specific for the ghrelin receptor or might reflect a general loss of excitability we superfused glucagone-like-peptide-1 (GLP-1). As shown in Figure 37, GLP-1 elicited an excitatory response despite the loss of HM01 sensitivity before and after superfusion of GLP-1. Hence, the repeated stimulation with HM01 does not seem to exert a generalized loss of responsiveness to hormonal stimuli. Moreover, it is unlikely that the loss of responsiveness was due to the higher dose HM01 (10^{-6} M) since we had repeated responses in one cell tested at this concentration (data not shown).

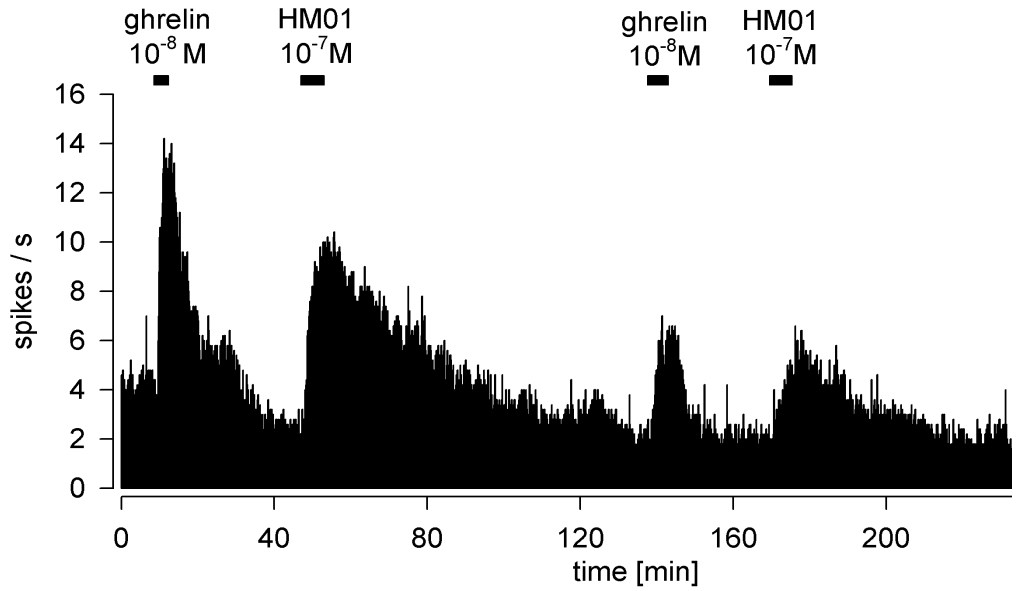

Figure 35: Recording of an ArcM neuron repeatedly stimulated with ghrelin (10^{-8} M) and HM01 (10^{-7} M). Not only the first application of ghrelin (10^{-8} M) and HM01 (10^{-7} M), but also their subsequent superfusions, led to excitatory responses.

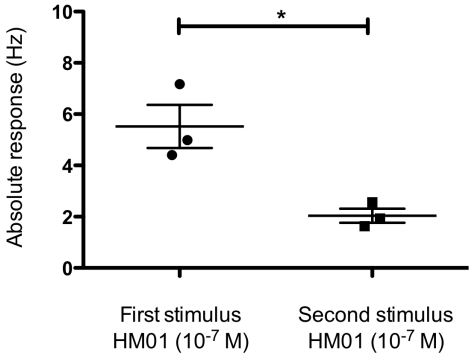

Figure 36: Mean absolute response of the excitatory effects after HM01 superfusion of the cells repeatedly stimulated wit HM01 (10^{-7} M). The mean absolute response after the second stimulus with HM01 was significantly smaller if compared to the mean absolute response of the second one. Data were analyzed with the student's *t*-test, p = 0.017

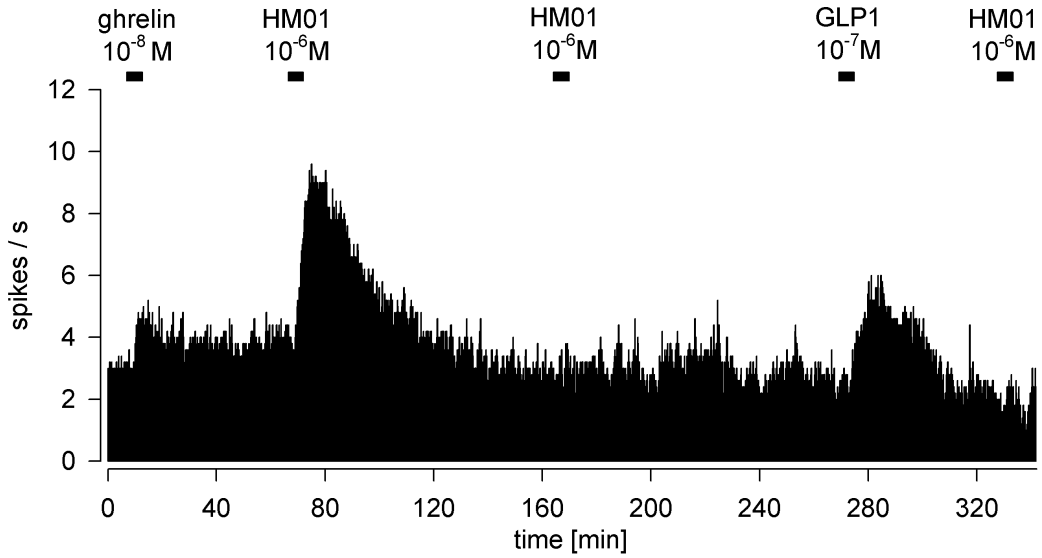

Figure 37: Representative recording of an Arc neuron, which shows excitatory responses after ghrelin (10^{-8} M) and the first HM01 (10^{-6} M) superfusion. No change in neuronal activity was seen after the second and third application of HM01 (10^{-6} M). GLP-1 (10^{-7} M) led to an excitatory response.

6.6 Effect of the ghrelin agonist HM01 on food intake and body weight in rats

In order to investigate the effect of chronic HM01 treatment on food intake and body weight, rats were divided in two groups. Animals of the control group were implanted with an osmotic minipump filled with saline, whereas the treatment group received minipumps filled with the ghrelin agonist HM01 (10 µg/µl, pump rate 50 µg/h). HM01 potently and significantly stimulated food intake starting from the first day after minipump implantation (Figure 38). This effect remained stable during the 12 days of measurements. On average the HM01-treated rats consumed about 6-7 g (20-30 %) more food than the controls. HM01 treatment significantly increased cumulative food intake (12-day cumulative food intake: HM01, 405 ± 6 g; saline, 329 ±7 g. (Figure 39). The HM01-induced increase in food intake was paralleled by an increase in body weight relative to controls, which became significant from day 5 after minipump implantation (Figure 40). At the end of the experiments the difference in body weight was about 35 g (HM01 treated group 369 ± 6 g vs controls 334 g ± 8 g). HM01 treated animals gained 27.6% of their initial body weight, whereas controls gained only 17.6% of the initial body weight ($p = 0.0014$).

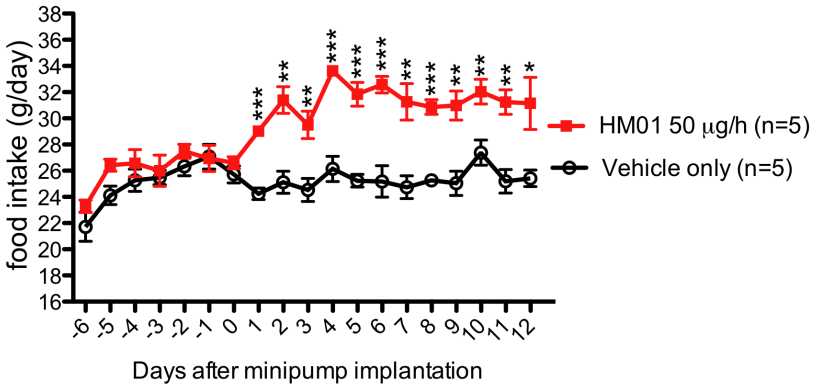

Figure 38: Daily food intake of HM01 (red) and saline (black) treated rats. Data were analyzed using the student's *t-test* (**p < 0.01, *** p < 0.001)

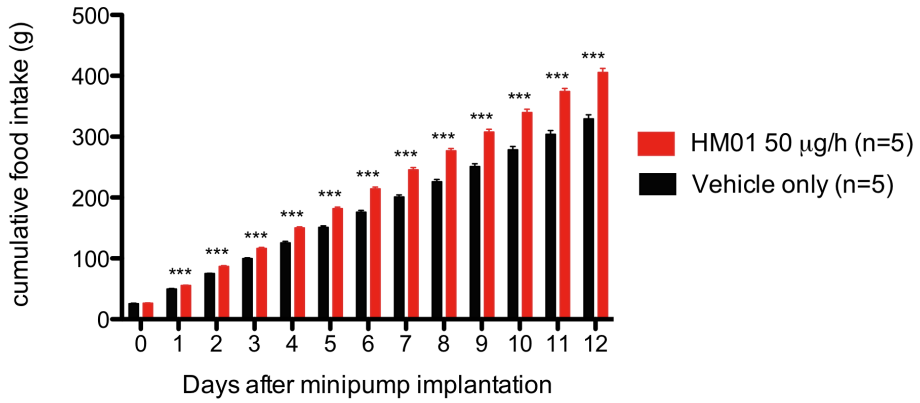

Figure 39: Cumulative food intake of HM01 (red) and saline (black) treated rats. Data were analyzed using the student's *t-test* (*** $p < 0.001$)

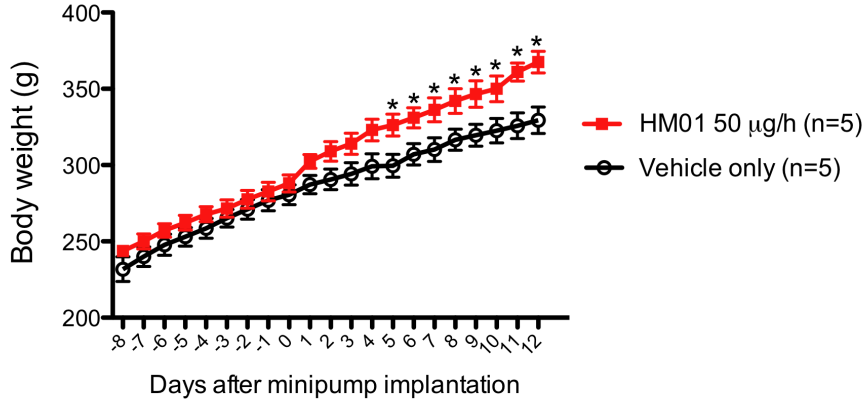

Figure 40: Body weight of HM01 (red) and saline (black) treated animals. Data were analyzed using the student's *t-test* (*$p < 0.05$)

7 Discussion

7.1 Central neuroinflammatory pathways involved in sickness anorexia

7.1.1 Involvement of NF-*κ*B and JAK/STAT pathways in the LPS/NO-dependent inhibition of neurons in the arcuate nucleus

In previous immunohistochemical and electrophysiological studies the inhibitory effects of LPS and the nitric oxide donor SNP on orexigenic Arc neurons have been demonstrated (Becskei et al., 2008; Riediger et al., 2010; Riediger et al., 2006). Subsequent studies have shown that this inhibition is mediated through stimulation of endogenous iNOS-dependent NO production (Borner et al., 2012). However, the signaling pathways involved in the iNOS dependent NO effects in the Arc under inflammatory condition have not been analyzed yet.

The current study provides electrophysiological evidence that the NF-κB signaling pathway is involved in the LPS induced iNOS dependent effects in the Arc. In contrast, JAK2-dependent STAT phosphorylation does not seem to be essential for LPS-induced NO effects in the Arc at least under our experimental in vitro conditions.
The results of the immunohistochemical experiments of this study show a pSTAT3 but not pSTAT1 formation in the Arc after 4 h in vitro LPS stimulation. Although activation of the NF-κB pathways tended to be higher in the Arc 2 hours after LPS in vivo stimulation compared to controls, these differences did not reach statistical significance. Moreover, we characterized the cells with nuclear NF-κB as endothelial cells using the endothelial marker von Willebrand factor.

Electrophysiological studies

The involvement of NF-κB in the transcriptional regulation of iNOS expression has been described in rat (Eberhardt et al., 1998), mouse (Xie et al., 1994) and human (Marks-Konczalik et al., 1998) cell lines. We used an electrophysiological approach to examine the role of the transcription factor NF-κB in the LPS-induced NO effects in the Arc under inflammatory in vitro conditions.

To evaluate the LPS-induced NO-dependent inhibition of orexigenic Arc neurons, we tested 1400W-responsiveness of Arc neurons after LPS incubation. Similar to previous electrophysiological studies (Borner et al., 2012), 1400W induced excitatory responses under these inflammatory conditions. Furthermore, there was a high degree of co-sensitivity for 1400W and ghrelin because 60% of all tested neurons were excited by both stimuli. These findings further substantiate an iNOS/NO-mediated inhibition of orexigenic Arc neurons by LPS.

Our results show a significantly decreased number of 1400W-excited neurons after NF-κB blockade whith Bay 11-7085. This lack of responsiveness was not due to NO insensitivity as confirmed by the sensitivity to the NO donor SNP. Although the number of excited neurons after superfusion of 1400W was clearly higher in the LPS stimulated positive control group (80%), one of the recorded neurons (10%) was sensitive to 1400W after co-incubation with Bay 11-7085. Whether the persistence of 1400W responsiveness might reflect NF-κB-independent NO signaling has not been specifically investigated owing to the low incidence of such responses. An alternative explanation might be an incomplete inhibition of NF-κB. The NF-κB inhibitor Bay 11-7085 was used at a concentration of 1 μM and its reported IC_{50} values are in the range of 5-10 μM (Pierce et al., 1997). However, previous studies demonstrated an effect of Bay 11-7085 on mouse leukemia cell lines already at concentration of 0.14 μM (Cory and Cory, 2005). For this reason the first hypothesis (NF-κB-independent NO signaling) appears more likely. In this context it is also important to note that superfusion of Bay 11-7085 did not affect neuronal activity in any of the 10 tested neurons, indicating the absence of any effects that would interfere with neuronal function.

In conclusion these findings are in line with the pivotal role of NF-κB in iNOS regulation. They provide the first functional evidence for the involvement of NF-κB in the LPS-induced NO dependent inhibition of orexigenic Arc neurons.

Using a similar electrophysiological approach we also examined the involvement of JAK2 in the LPS-induced iNOS-dependent NO production in the Arc during inflammation. After blocking JAK2 phosphorylation with the JAK2 inhibitor WP1066 we still observed excitatory 1400W effects in 25% of all tested neurons. Although this

percentage of sensitive cells was considerably lower than under positive control conditions (63%), this difference did not reach statistical significance. In contrast to Bay 11-7085, superfusion of the JAK2 inhibitor WP1066 induced both excitatory and inhibitory effects in the Arc. The underlying cellular mechanisms of these effects remain unknown. Due to the short onset of these responses any effects that are based on alterations of gene expression are unlikely. We used an effective concentration of WP1066, which was 2-fold higher than the IC_{50} (Iwamaru et al., 2007). There was no indication that the 4 h incubation with WP1066 might have compromised neuronal function, which could for example be reflected by a loss of neuronal excitability in general.

Based on our findings, JAK2 dependent STAT1 and STAT3 phosphorylation does not seem to be essential for the LPS/NO-mediated effects in the Arc at least under the current experimental in vitro conditions. In light of the well-known role of STAT signaling in iNOS gene expression the persistence of LPS/NO signaling after JAK2 blockade might appear surprising. However, these results do not rule out an involvement of STAT signaling in LPS/NO in vivo. In contrast to in vivo LPS treatment, a systemic cytokine response does not occur under in vitro conditions. While a local cytokine production in the Arc has been demonstrated after LPS treatment (Konsman et al., 2004), the Arc intrinsic production of cytokines has not yet been investigated after in vitro stimulation with LPS. Due to the multitude of interacting inflammatory mediators induced by LPS in vivo, the inflammatory impact on the Arc might be higher after in vivo than under in vitro conditions. While LPS is known to directly activate the NF-κB pathway (Aktan, 2004; Gao et al., 1998), the JAK2/STAT is mainly activated by cytokines. Although many different cytokines activate the same JAKs (Imada and Leonard, 2000), there are different JAK/STAT pathways, which are activated through specific cytokines. For example, IFNγ has been shown to lead almost exclusively to STAT1 activation (Aaronson and Horvath, 2002; Meraz et al., 1996; Tedeschi et al., 2003). It is not known if IFNγ is produced in the Arc following in vitro LPS stimulation. A partial inhibitory effect of WP1066 seems unlikely, since we used a 2-fold higher dose of the reported IC_{50} for WP1066 (Iwamaru et al., 2007).

NF-κB and STAT signaling cascades interact to regulate iNOS gene transcription. Interestingly both pathways appear to have specific activators (Gao et al., 1998). In fact, co-stimulation of mouse macrophages with LPS and INFγ leads to increased NO production if compared to stimulation with LPS alone, suggesting that iNOS expression levels are synergistically augmented by the combination of LPS and INFγ (Lorsbach et al., 1993; Lowenstein et al., 1993). Based on the model that LPS/NF-κB and IFNγ/STAT1 pathways seem to act synergistically to regulate iNOS-dependent NO production (Figure 41) our demonstration of NF-κB-mediated iNOS signaling in vitro might only reflect activation of the direct LPS-dependent pathway. Because of the absence of a peripheral cytokine response the IFNγ- or cytokine-dependent pathway is likely to be less activated in vitro, which could explain why the blockade of JAK2/STAT pathway did not significantly affect LPS/NO signaling in our study. This assumption might be supported by future electrophysiological studies using IFNγ or other cytokines activating the STAT1 pathway.

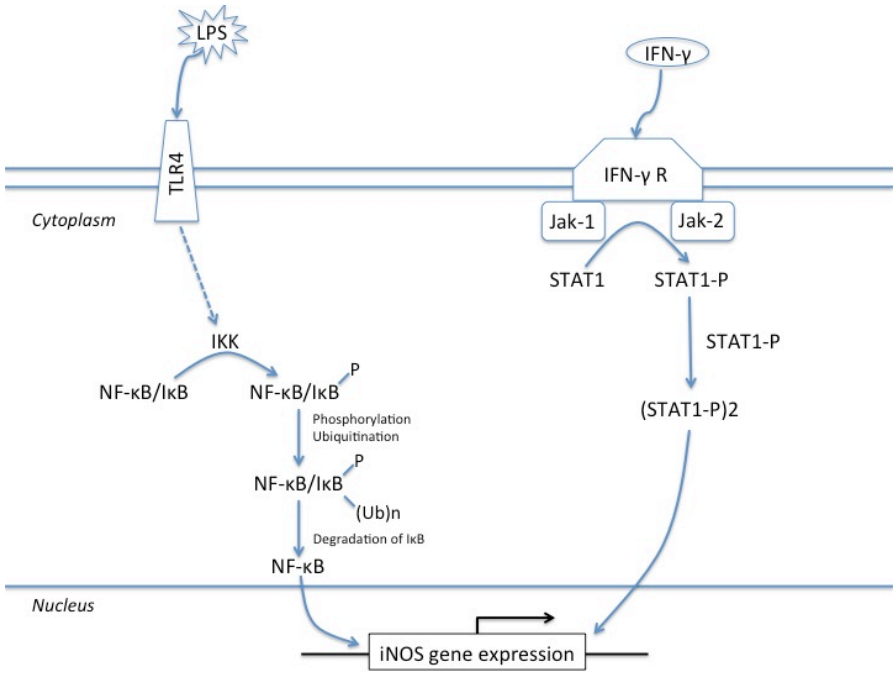

Figure 41: iNOS activation through LPS/NF-κB and IFNγ/STAT1 signaling pathways (From Aktan, 2004 modified by T. Borner)

Immunohistological studies

STAT1 and STAT3 phosphorylation in the Arc in response to LPS injection in vivo have been shown in several immunohistochemical studies (Gautron et al., 2002; Riediger et al., 2010; Rummel et al., 2005). In the present study 4 h after in vitro LPS stimulation a pSTAT3 formation in the Arc of rats was shown. However, no significant difference if compared to the control group was found for STAT1 phosphorylation. The absence of a pSTAT1 response seems to support the electrophysiological observation that the LPS-induced NO responses in vitro are independent of JAK2/STAT signaling. The detection of pSTAT3 is not contradictory to the electrophysiological outcome because pSTAT3 is likely to be involved in iNOS independent signaling cascades that have not been specifically investigated in this study (e.g. expression of neuropeptides, inflammatory mediators) (Bates and Myers, 2004). However, several considerations should be to taken into account for the interpretation of the immunohistological findings, particularly in relation to previous studies reporting LPS-induced pSTAT1 and pSTAT3 responses in vivo.

While the in vitro pSTAT3 response is in line with the reported in vivo STAT3 responses in mice, the LPS-dependent STAT1 phosphorylation in the Arc has only been reported in vivo (Borner et al., 2012) but not in vitro (current study). One possible explanation for the lacking STAT1 phosphorylation in vitro might be the absence of an activating stimulus for STAT1 under these in vitro conditions. Under in vivo conditions circulating cytokines play an important role. As mentioned above, although many different cytokine activate the same JAKs (Imada and Leonard, 2000), there are different JAK/STAT pathways, which are selectively activated through specific cytokines. For example type I interferon (IFNα/β) activates STAT1 and STAT2, while type II interferon (IFNγ) almost exclusively leads to STAT1 phosphorylation. Therefore the absence of a pSTAT1 response in the current study indicates that LPS alone does not seem to be sufficient for an activation of the STAT1 pathway in the Arc. Notably, this finding does not rule out the possible importance of LPS dependent STAT1/iNOS signaling in vivo, because LPS induces an IFN response by interacting with immune cells.

There are also experimental aspects that need to be considered. Under in vitro conditions a phosphorylation of STAT1 might occur at a different time point than after in vivo LPS stimulation. Hence it might be interesting to analyze both earlier and later time points after LPS in vitro stimulation. Furthermore, the lack of a pSTAT1 response in vitro might be due to other stimuli that potentially mask an LPS induced STAT1 phosphorylation. In contrast to our in vitro studies, basal pSTAT1 formation was low in saline treated control mice (Borner et al., 2012) whereas we found considerable basal STAT1 activation under control condition in vitro. Although species differences might also account for differences in basal pSTAT1, the mechanical stimulation of Arc sections during the preparation and subsequent incubation might increase STAT1 phosphorylation via local inflammatory or non-inflammatory mechanisms. It is difficult to control for such influences, which could override a specific LPS effect on STAT1 phosphorylation.

Despite the clear electrophysiological evidence for an involvement of NF-κB in the LPS/NO-dependent modulation of neuronal Arc activity, the immunohistological studies did not provide further evidence for a significant activation of the NF-κB pathway in the Arc under the current testing conditions after in vivo as well as in vitro LPS stimulation. For our immunohistochemical study we used an anti-NF-κB antibody directed against the p65 subunit. This antibody has been evaluated for specificity and reported to be the most reliable antibody to detect NF-κB immunoreactivity in the brain (Herkenham et al., 2011). Inactive NF-κB is located in the cytosol of unstimulated cells as homo- or heterodimers, usually comprising p50 and p65, bound to IκB proteins.
iNOS gene expression in the Arc peaks between 2 and 6 hours after peripheral LPS administration (Wong et al., 1996). This time course parallels the anorectic response to LPS that usually starts between 2 and 6 hours (Langhans et al., 1991; Langhans et al., 1993). Based on these findings, we examined NF-κB activity in the Arc 2 and 4 hours after LPS injection in rats. Furthermore, we included an 1 hour time point after in vitro incubation of Arc slices in order to detect possible direct effects of LPS that might occur early and independent of immune cell responses. To differentiate between nuclear and cytoplasmatic localization of NF-κB immunoreactivity we performed a Nf-κB-DAPI double staining.

4 hours after LPS injection NF-κB immunoreactivity was present in structures that resembled blood vessels, and small-diameter round cells spread through the parenchyma. At the 4 h time point there was no nuclear translocation of NF-κB immunoreactivity in LPS and saline treated groups.

A possible explanation for the lack of NF-κB activation 4 hours after LPS injection is an earlier response that is not detected anymore 4 h after LPS injection. This is supported by other studies characterizing temporal pattern of NF-κB activation. NF-κB controls the expression of IκBα creating a feedback loop in which newly synthesized IκBα binds to the nuclear NF-κB exporting it back to the cytosol (Brown et al., 1993; Nelson et al., 2004a; Sun et al., 1993). Therefore, expression of IκBα has also been postulated to reflect the activity of NF-κB (Quan et al., 1997). *In situ* hybridization studies conducted by Quan et al. in the rat brain after peripheral LPS administration have shown different spatiotemporal patterns of IκBα expression. An increase of IκB-mRNA-positive cells was first seen already 0.5-1 h post injection in cells positioned at the blood side of the BBB. After 1 hour, activation in endothelial cells and some astrocytes occurred throughout the entire brain with the highest IκBα activity observed in the circumventricular organs and the choroid plexus. This response peaked after 2 hours and declined afterwards (Quan et al., 1997). However, in this study a septic dose of LPS (2.5 mg/kg) was used, which was much higher as the one used in the current study (100 μg/kg). In a subsequent study, Quan et al. examined the induction of IkBα-mRNA after peripheral injection of subseptic doses of LPS ranging from 0.01 to 1000 μg/kg. Significant induction of IκBα mRNA expression was seen at 2 hours time point in CVOs (organum vasculosum of the lamina terminalis, subfornical organ) and blood vessels already after injection of small doses of 0.1 μg/kg LPS. The high dose (1 mg/kg) LPS induced a different pattern of IκBα mRNA expression. In fact, only the high dose induced the expression of IκBα in the brain parenchyma, beyond the CVOs and blood vessels (Quan et al., 1999). Hence, in our studies the NF-κB response could have peaked at an earlier time point, or the dose we used could have been to low to observe an NF-κB activation under our experimental conditions and with the used techniques. Based on the findings of the aforementioned studies of Quan et al. we performed a second experiment

at an earlier time point (2 hours) and injected LPS at two different doses (100 and 300 μg/kg). Moreover, an endothelial marker was used to identify blood vessels in the Arc.
2 hours after LPS injection NF-κB immunoreactivity was seen in the Arc in each of the three groups (saline, 100 and 300 μg/kg LPS). At this time point we were able to identify nuclear translocation of NF-κB in some cells, which were identified as endothelial cells due to their vWF immunoreactivity. In non-vascular cells of the brain parenchyma NF-κB immunoreactivity was confined to the cytoplasm and no nuclear translocation was observed. Despite the observed nuclear translocation of NF-κB no significant difference in the number of cells with activated NF-κB was found between the three treatments (saline, 100 and 300 μg/kg LPS). Together with the previously reported studies of Quan et al. these findings might suggest that NF-κB activation peaks at an earlier time point than 4 hours. Obviously, we cannot exclude the possibility that a significant activation of the NF-κB pathway might occur at other time-points than 2 and 4h post stimulation.

We further investigated if NF-κB activation occurs after 1 hour in vitro LPS stimulation of Arc slices. NF-κB immunoreactivity was seen in each group and a high number of cells with nuclear NF-κB staining was observed. However, no significant difference between the LPS-stimulated Arc sections was found in comparison to controls. NF-κB activation was present in cells spread through the parenchyma, as well as in cells in close vicinity to blood vessels. Since this high number of cells that showed NF-κB nuclear translocation was present in both groups, we assume that a possible activation of NF-κB signaling by LPS might have been masked by the high baseline activation observed under these experimental conditions. Irrespective of the reason for this high baseline activation, a detection of a specific LPS-mediated effect on NF-κB nuclear translocation might be masked under the current in vitro conditions.

A general aspect important to consider when studying the NF-κB pathway, is the fact that an oscillatory activation of this transcriptional factor has been demonstrated. Using fluorescence imaging techniques and EMSA nuclear-cytoplasmatic oscillation of NF-κB in different type of cell cultures after stimulation with inflammatory cytokines such as TNF-α was observed (Hoffmann et al., 2002; Nelson et al., 2004a). IκBα is a

transcriptional target of NF-κB, and creates a feedback loop transporting NF-κB back from the nucleus to the cytoplasm. This negative feedback was shown to induce oscillatory nuclear NF-κB activity (Hoffmann et al., 2002; Nelson et al., 2004b). With our experimental design the investigation of different time points within the same animals is not possible. Moreover, it might be difficult to detect oscillatory differences between short time intervals with sufficient temporal resolution in this kind of in vivo experiments, also considering the possible inter-individual variability arising from the necessity to use different experimental animals for each time point. For these reasons the detection of such oscillatory activation is much more difficult to investigate compared to cell culture experiments allowing real-time detection NF-κB immunoreactivity within the same cells. Consequently other techniques might be required to further investigate NF-κB activation under our experimental conditions. A possible approach would be Western blot analysis of hypothalamic tissue analyzing cytoplasmatic and nuclear fractions of the NF-κB protein. Moreover, an approach based on *in-situ* mRNA hybridization to detect IκBα-mRNA might shed more light on NF-κB activation under our experimental conditions.

7.1.2 NF-*κ*B signaling pathway in the area postrema after LPS stimulation in vivo

Several observations suggest an activation of the AP during systemic inflammation. In fact, neuronal activation occurs in the AP after immune-challenge with LPS or IL-1 (Brady et al., 1994; Sagar et al., 1995). Moreover, the AP is involved in sickness anorexia, since it plays a role in TNF-α and tumor anorexia (Bernstein et al., 1991; Bernstein et al., 1985). In a recent study from our group, surgical removal of the AP prevented tumor-anorexia and body weight loss (Borner T., 2012) However, knowledge about the mechanisms involved in activation of the AP during inflammation is lacking. *In situ* hybridization of IκBα mRNA showed that non-septical LPS doses seems to activate NF-κB signaling mainly in structures non protected by the BBB, namely in CVOs and blood vessels (Quan et al., 1999). Unfortunately the AP was not included in this study. The presence of NF-κB signaling in the AP was shown in a subsequent study, in which nuclear translocation of NF-κB was observed in the AP after immune challenge with IL1-

β (Nadjar et al., 2003). However they did not quantify the number of cells with activated NF-κB.

In the current study we demonstrated that LPS significantly increases nuclear translocation of NF-κB in the AP at both tested doses (100 μg/kg and 300 μg/kg). No difference was observed between the group treated with the lower (100 μg/kg) and the higher dose (300 μg/kg) of LPS. Using an antibody against rat RECA-1 as endothelial marker, most of the cells with activated NF-κB were identified as endothelial cells. Not all the cells with nuclear NF-κB co-expressed RECA-1. Interestingly, these non-endothelial cells with activated NF-κB were located in close vicinity to vascular structures. The phenotype of these cells remains to be identified.

iNOS is expressed in the AP under inflammatory conditions (Konsman et al., 1999) and iNOS inhibition reduces neuronal activation in the AP during sepsis (Bruhn et al., 2009). Although NF-κB is known to regulate iNOS expression, it remains to be elucidated if the LPS-induced activation of the NF-κB pathway observed in the current study in the AP leads to iNOS signaling. Whether this pathway is also activated during chronic disease conditions associated with anorexia also remains to be determined. Apart from a possible modulation of ingestive behavior, the AP seems to mediate LPS-induced behavioral depression, such as social withdrawal (Marvel et al., 2004). Hence, the NF-κB pathway might play a role in the transduction of immune-related signals relevant for the induction of such behavioral responses. However, further experiments are needed to better understand these mechanisms.

7.2 Electrophysiological and in vivo studies with the synthetic ghrelin-agonist HM01

In this study we provide the first in vitro electrophysiological characterization of the new synthetic ghrelin agonist HM01. In order to analyze the effects on neuronal activity of this compound, the co-sensitivity of Arc neurons for ghrelin and HM01 was analyzed. In addition, the effects of chronically administered HM01 on food intake and body-weight in healthy rats were investigated during a 12 day period.

In the electrophysiological experiments HM01 and ghrelin showed a completely concordant response profile in all of the 17 tested neurons. These results demonstrate that under in vitro experimental conditions, HM01 mimics the effects of ghrelin on neuronal activity of ArcM neurons. Similar to our previous electrophysiological studies from medial Arc neurons (Borner et al., 2012; Riediger et al., 2003), ghrelin, and in this case also HM01, predominantly induced excitatory responses (76%).

We performed recordings using two concentration of HM01 (10^{-6} M and 10^{-7} M). We observed a significant longer response duration after superfusion of the higher concentration of HM01 (10^{-6} M) in comparison to ghrelin. Additionally, application of the lower concentration of HM01 (10^{-7} M) led to a significant longer latency period of the excitatory effects if compared to ghrelin and HM01 (10^{-6} M). However, no difference was seen in the absolute response and the peak response. The lack of a concentration-dependence of these effects for part of the effect parameters might be related to the fact the used concentrations reside in the upper range of the concentration-response curve of HM01. Although dose-response characteristics may vary between different assays this assumption appears plausible considering the EC50 of 1-2 nM for HM01 (unpublished observations). However, it was not the aim of this study to establish a complete dose-response characteristic for the excitatory effects of HM01. Such measurements are more relevant for endogenous hormones and the related question whether physiological hormone levels might reach the threshold required for neuronal activation.

Although it as been shown in electrophysiological studies that repeated stimulations with ghrelin do not lead to reduced neuronal sensitivity (Riediger et al., 2003), we investigated possible desensitizations by repeated stimulation with HM01 stimulating 7 neurons. In 4 of these cells we observed excitatory responses after the subsequent superfusions of HM01 (10^{-6} M, 10^{-7} M). However, the absolute response of the second excitatory effect of HM01 was significantly reduced after the second superfusion with HM01 10^{-7} M. In the remaining 3 neurons no further response occurred after the second superfusion with HM01. In order to exclude a reduced general responsiveness, an additional stimulus acting on a different receptor than ghrelin receptor was set. In fact, GLP-1 was still effective to induce an excitatory response demonstrating that the general neuronal excitability has not been affected by HM01. A possible explanation for the observed loss

of responsiveness for HM01 after the first stimulation might be a desensitization of the growth hormone secretagogue receptor (GHS-R) itself or of the intracellular signaling cascade coupled to the receptor. However, as discussed below, this desensitization did to translate into desensitization in vivo at least under the current experimental conditions.

Immunhistochemical and electrophysiological studies suggest that the orexigenic effect of ghrelin is mediated via stimulation of NPY/AgRP neurons located in the ArcM of rats (Riediger et al., 2003; Traebert et al., 2002; Willesen et al., 1999). Therefore, the ghrelin-like action of HM01 on neuronal activity in the ArcM is in line with the orexigenic effect of HM01 observed in the current study. HM01 treatment in healthy rats was associated with increased body weight gain. HM01 strongly stimulated food intake already starting from the first day after minipump implantation. In a similar study Strassburg et al. tested the metabolic effects of long-term treatment with ghrelin and the GHS-R agonist BIM-28131. The substances were administered using subcutaneous osmotic minipumps for 4 weeks. Both led to substantially elevated body weight gain compared with control. However, BIM-28131 appeared to be the most potent compound regarding its potency to increase body weight. In fact, body weight of the animals receiving BIM-28131 was significantly higher than that of ghrelin treated animals (Strassburg et al., 2008). The mean increase of body weight after 2 weeks of treatment with BIM-28131 was comparable to what we observed in the current study after 12 days treatment with HM01. After 2 weeks of BIM-28131 administration the mean daily food intake was 31 ± 1 g vs. 26 ± 1 g in controls. Likewise, we show that after 12 days of HM01 administration the mean food intake was 31 ± 2 vs. 25 ± 1 in controls.

Interestingly, although we observed a desensitization of the electrophysiological responses of HM01, we did not observed any attenuation in the feeding stimulating effect of HM01 during the whole testing period. It is not possible to directly compare the concentrations of HM01 between the electrophysiological and in vivo studies. However, the concentration of HM01 in the brain during chronic HM01 administration at the used dosage is presumably lower than the superfused concentration during the electrophysiological recordings. Since receptor desensitization can result from excessive receptor stimulation the lack of such an effect under the current vivo condition might be

due to the lower concentration of HM01 at the receptor. This is indicative of a sufficient therapeutic or pharmacological window, in which an effect on food intake occurs in the absence of undesired desensitizing actions.

Based on the longer half-life time and higher metabolic stability, synthetic ghrelin mimetics (Akamizu et al., 2004; Blum R, 2006; Nass et al., 2008), are effective in a daily single treatment regimen, which is beneficial for their use a anti-anorectic drugs. In a recent study the novel ghrelin agonist Anamorelin was tested in patients with cancer-related cachexia. The half-life of Anamorelin (7 to 12 hours) is much longer compared to ghrelin (Blum R, 2006), allowing for a once-a day oral administration. Currently, Anamorelin is the only ghrelin-based drug that is in clinical phase III studies for the treatment of cancer ACS. This compound was well tolerated and demonstrated significant appetite stimulation in healthy volunteers (Garcia and Polvino, 2007). Oral Anamorelin treatment for 12 weeks in cachectic patient significantly increased mean lean body mass and total body mass when compared to placebo (Garcia JM, 2007).

Apart from their effects on energy homeostasis ghrelin and ghrelin mimetics are supposed to exert further beneficial actions in the context of inflammatory diseases. Ghrelin exerts anti-inflammatory actions because it reduces the production of pro-inflammatory cytokines, which are also elevated during sickness anorexia (Dixit et al., 2004). Furthermore, in vitro studies postulated an anti-inflammatory effect of ghrelin through an inhibition of NF-κB activation (Li et al., 2004). An additional effect of ghrelin is the stimulation of growth hormone secretion, which leads to an increase of IGF-1 levels (Takaya et al., 2000). Since IGF-1 levels are low under cachexia, ghrelin treatment could reverse this response leading to an improvement of anabolic functions (Morley et al., 2006). Whether any of these effects might contribute the possible therapeutic effects of ghrelin-beased approaches will be investigated in follow up studies.

In summary, based on the results of the current study HM01 treatment qualifies as a promising drug candidate for the treatment of ACS.

8 Perspectives

Therapy with ghrelin agonists appears to be a promising approach in the management of chronic sickness anorexia. However, it seems that under cancer ACS ghrelin responsiveness is reduced, which could limit therapeutic approaches with ghrelin or ghrelin receptor agonists. The exact mechanism underlying this reduced ghrelin effects is still unknown. Our previous and current demonstration that NO signaling inhibits the target cells of the orexigenic hormone ghrelin suggest a direct link between inflammatory NO signaling and decreased ghrelin responsiveness. Blockade of iNOS activity appears to be a promising strategy for the treatment of disease-related anorexia either as single drug treatment or in combination with other anti-anorectic agents. The current studies shed more light on the intracellular signaling mechanisms implicated in LPS/NO dependent modulation of hypothalamic arcuate neurons involved in energy homeostasis suggesting that inhibitors of inflammatory transcription pathways might be therapeutic options for the treatment of the anorexia-cachexia syndrome.

The use of synthetic ghrelin mimetics instead of ghrelin appear to be an interesting approach in treatment of human ACS, given the longer half-life and the much more practical possibility of the route of administration. Therefore a combination treatment with GHS-R agonists and inhibition of NO signaling might improve treatment outcome.

9 Acknowledgements

I would like to thank to everyone who supported me during my doctoral theses and helped me conduct the experiments and write my thesis.
In particular,

PD Dr. Thomas Riediger for the supervision, for teaching me the methods and for his support during the entire thesis.

Prof. Dr. Thomas Lutz for giving me the opportunity to perform my doctoral thesis in this group.

Tito Borner for all his help and support and always being there for me.

Many thanks go to all other the members of the lab for all the help and for the great atmosphere.

Finally, I want to thank my parents, my sister and my friends for the support and motivation, not only during the past year, but also during everything it took to get to this point.

10 References

Aaronson, D.S., Horvath, C.M., 2002, A road map for those who don't know JAK-STAT. Science 296, 1653-1655.

Akamizu, T., Kangawa, K., 2010, Ghrelin for cachexia. J Cachexia Sarcopenia Muscle 1, 169-176.

Akamizu, T., Takaya, K., Irako, T., Hosoda, H., Teramukai, S., Matsuyama, A., Tada, H., Miura, K., Shimizu, A., Fukushima, M., Yokode, M., Tanaka, K., Kangawa, K., 2004, Pharmacokinetics, safety, and endocrine and appetite effects of ghrelin administration in young healthy subjects. Eur J Endocrinol 150, 447-455.

Aktan, F., 2004, iNOS-mediated nitric oxide production and its regulation. Life Sci 75, 639-653.

Asakawa, A., Inui, A., Kaga, T., Yuzuriha, H., Nagata, T., Ueno, N., Makino, S., Fujimiya, M., Niijima, A., Fujino, M.A., Kasuga, M., 2001, Ghrelin is an appetite-stimulatory signal from stomach with structural resemblance to motilin. Gastroenterology 120, 337-345.

Banks, W.A., 2001, Anorectic effects of circulating cytokines: role of the vascular blood-brain barrier. Nutrition 17, 434-437.

Bates, S.H., Myers, M.G., 2004, The role of leptin-->STAT3 signaling in neuroendocrine function: an integrative perspective. J Mol Med (Berl) 82, 12-20.

Becskei, C., Riediger, T., Hernadfalvy, N., Arsenijevic, D., Lutz, T.A., Langhans, W., 2008, Inhibitory effects of lipopolysaccharide on hypothalamic nuclei implicated in the control of food intake. Brain Behav Immun 22, 56-64.

Bernstein, I.L., Taylor, E.M., Bentson, K.L., 1991, TNF-induced anorexia and learned food aversions are attenuated by area postrema lesions. Am J Physiol 260, R906-910.

Bernstein, I.L., Treneer, C.M., Kott, J.N., 1985, Area postrema mediates tumor effects on food intake, body weight, and learned aversions. Am J Physiol 249, R296-300.

Blum R, P.W., 2006, Pharmacokinetic (PK) Profile Of RC-1291, A Novel Oral Ghrelin Mimetic For The Treatment Of Cancer Anorexia/Cachexia. Supportive Care in Cancer 14, 593.

Borison, H.L., Brizzee, K.R., 1951, Morphology of emetic chemoreceptor trigger zone in cat medulla oblongata. Proc Soc Exp Biol Med 77, 38-42.

Borner, T., Pinkernell, S., Lutz, T.A., Riediger, T., 2012, Lipopolysaccharide inhibits ghrelin-excited neurons of the arcuate nucleus and reduces food intake via central nitric oxide signaling. Brain Behav Immun 26, 867-879.

Borner T., L.T., Ruud J., Blomqvist A., Riediger T., 2012, Involvement of the area postrema in cancer-induced anorexia and body weight loss. (Abstract).

Brady, L.S., Lynn, A.B., Herkenham, M., Gottesfeld, Z., 1994, Systemic interleukin-1 induces early and late patterns of c-fos mRNA expression in brain. J Neurosci 14, 4951-4964.

Breder, C.D., Hazuka, C., Ghayur, T., Klug, C., Huginin, M., Yasuda, K., Teng, M., Saper, C.B., 1994, Regional induction of tumor necrosis factor alpha expression in the mouse brain after systemic lipopolysaccharide administration. Proc Natl Acad Sci U S A 91, 11393-11397.

Bredt, D.S., Hwang, P.M., Snyder, S.H., 1990, Localization of nitric oxide synthase indicating a neural role for nitric oxide. Nature 347, 768-770.

Broadwell, R.D., Sofroniew, M.V., 1993, Serum proteins bypass the blood-brain fluid barriers for extracellular entry to the central nervous system. Exp Neurol 120, 245-263.

Broberger, C., De Lecea, L., Sutcliffe, J.G., Hokfelt, T., 1998, Hypocretin/orexin- and melanin-concentrating hormone-expressing cells form distinct populations in the rodent lateral hypothalamus: relationship to the neuropeptide Y and agouti gene-related protein systems. J Comp Neurol 402, 460-474.

Broberger, C., Landry, M., Wong, H., Walsh, J.N., Hokfelt, T., 1997, Subtypes Y1 and Y2 of the neuropeptide Y receptor are respectively expressed in pro-opiomelanocortin- and neuropeptide-Y-containing neurons of the rat hypothalamic arcuate nucleus. Neuroendocrinology 66, 393-408.

Bromberg, J.F., 2001, Activation of STAT proteins and growth control. Bioessays 23, 161-169.

Brown, K., Park, S., Kanno, T., Franzoso, G., Siebenlist, U., 1993, Mutual regulation of the transcriptional activator NF-kappa B and its inhibitor, I kappa B-alpha. Proc Natl Acad Sci U S A 90, 2532-2536.

Bruhn, F.H., Correa, P.B., Oliveira-Pelegrin, G.R., Rocha, M.J., 2009, Blocking systemic nitric oxide production alters neuronal activation in brain structures involved in cardiovascular regulation during polymicrobial sepsis. Neurosci Lett 453, 141-146.

Burney B, G.J.M., 2012, Use of ghrelin and ghrelin receptor agonists in cancer- and chemotherapy-induced cachexia, In: Smith, R.G., Thorner MO (Ed.) Ghrelin in healt and disease. Humana Press, New York, pp. 213-230.

Butler, P.C., Chou, J., Carter, W.B., Wang, Y.N., Bu, B.H., Chang, D., Chang, J.K., Rizza, R.A., 1990, Effects of meal ingestion on plasma amylin concentration in NIDDM and nondiabetic humans. Diabetes 39, 752-756.

Chronwall, B.M., 1985, Anatomy and physiology of the neuroendocrine arcuate nucleus. Peptides 6 Suppl 2, 1-11.

Cory, A.H., Cory, J.G., 2005, Induction of apoptosis in p53-deficient L1210 cells by an I-kappa-B-alpha-inhibitor (Bay 11-7085) via a NF-kappa-B-independent mechanism. Adv Enzyme Regul 45, 85-93.

Cowley, M.A., Smart, J.L., Rubinstein, M., Cerdan, M.G., Diano, S., Horvath, T.L., Cone, R.D., Low, M.J., 2001, Leptin activates anorexigenic POMC neurons through a neural network in the arcuate nucleus. Nature 411, 480-484.

Cowley, M.A., Smith, R.G., Diano, S., Tschop, M., Pronchuk, N., Grove, K.L., Strasburger, C.J., Bidlingmaier, M., Esterman, M., Heiman, M.L., Garcia-Segura, L.M., Nillni, E.A., Mendez, P., Low, M.J., Sotonyi, P., Friedman, J.M., Liu, H., Pinto, S., Colmers, W.F., Cone, R.D., Horvath, T.L., 2003, The distribution and mechanism of action of ghrelin in the CNS demonstrates a novel hypothalamic circuit regulating energy homeostasis. Neuron 37, 649-661.

Cummings, D.E., Purnell, J.Q., Frayo, R.S., Schmidova, K., Wisse, B.E., Weigle, D.S., 2001, A preprandial rise in plasma ghrelin levels suggests a role in meal initiation in humans. Diabetes 50, 1714-1719.

Dalton, D.K., Pitts-Meek, S., Keshav, S., Figari, I.S., Bradley, A., Stewart, T.A., 1993, Multiple defects of immune cell function in mice with disrupted interferon-gamma genes. Science 259, 1739-1742.

Damm, J., Harden, L.M., Gerstberger, R., Roth, J., Rummel, C., 2013, The putative JAK-STAT inhibitor AG490 exacerbates LPS-fever, reduces sickness behavior, and alters the expression of pro- and anti-inflammatory genes in the rat brain. Neuropharmacology 71, 98-111.

Date, Y., Kojima, M., Hosoda, H., Sawaguchi, A., Mondal, M.S., Suganuma, T., Matsukura, S., Kangawa, K., Nakazato, M., 2000, Ghrelin, a novel growth hormone-releasing acylated peptide, is synthesized in a distinct endocrine cell type in the gastrointestinal tracts of rats and humans. Endocrinology 141, 4255-4261.

DeBoer, M.D., Zhu, X.X., Levasseur, P., Meguid, M.M., Suzuki, S., Inui, A., Taylor, J.E., Halem, H.A., Dong, J.Z., Datta, R., Culler, M.D., Marks, D.L., 2007, Ghrelin treatment causes increased food intake and retention of lean body mass in a rat model of cancer cachexia. Endocrinology 148, 3004-3012.

Dell'Albani, P., Santangelo, R., Torrisi, L., Nicoletti, V.G., de Vellis, J., Giuffrida Stella, A.M., 2001, JAK/STAT signaling pathway mediates cytokine-induced iNOS expression in primary astroglial cell cultures. J Neurosci Res 65, 417-424.

Dixit, V.D., Schaffer, E.M., Pyle, R.S., Collins, G.D., Sakthivel, S.K., Palaniappan, R., Lillard, J.W., Jr., Taub, D.D., 2004, Ghrelin inhibits leptin- and activation-induced proinflammatory cytokine expression by human monocytes and T cells. J Clin Invest 114, 57-66.

Doi, M., Shichiri, M., Katsuyama, K., Ishimaru, S., Hirata, Y., 2002, Cytokine-activated Jak-2 is involved in inducible nitric oxide synthase expression independent from NF-kappaB activation in vascular smooth muscle cells. Atherosclerosis 160, 123-132.

Eberhardt, W., Pluss, C., Hummel, R., Pfeilschifter, J., 1998, Molecular mechanisms of inducible nitric oxide synthase gene expression by IL-1beta and cAMP in rat mesangial cells. J Immunol 160, 4961-4969.

Elmquist, J.K., Bjorbaek, C., Ahima, R.S., Flier, J.S., Saper, C.B., 1998, Distributions of leptin receptor mRNA isoforms in the rat brain. J Comp Neurol 395, 535-547.

Evans, W.J., Morley, J.E., Argiles, J., Bales, C., Baracos, V., Guttridge, D., Jatoi, A., Kalantar-Zadeh, K., Lochs, H., Mantovani, G., Marks, D., Mitch, W.E., Muscaritoli, M., Najand, A., Ponikowski, P., Rossi Fanelli, F., Schambelan, M., Schols, A., Schuster, M., Thomas, D., Wolfe, R., Anker, S.D., 2008, Cachexia: a new definition. Clin Nutr 27, 793-799.

Fan, W., Boston, B.A., Kesterson, R.A., Hruby, V.J., Cone, R.D., 1997, Role of melanocortinergic neurons in feeding and the agouti obesity syndrome. Nature 385, 165-168.

Feil, R., Kleppisch, T., 2008, NO/cGMP-dependent modulation of synaptic transmission. Handb Exp Pharmacol, 529-560.

Ferrajoli, A., Faderl, S., Van, Q., Koch, P., Harris, D., Liu, Z., Hazan-Halevy, I., Wang, Y., Kantarjian, H.M., Priebe, W., Estrov, Z., 2007, WP1066 disrupts Janus kinase-2 and induces caspase-dependent apoptosis in acute myelogenous leukemia cells. Cancer Res 67, 11291-11299.

Forstermann, U., Boissel, J.P., Kleinert, H., 1998, Expressional control of the 'constitutive' isoforms of nitric oxide synthase (NOS I and NOS III). Faseb J 12, 773-790.

Friedman, J.M., Halaas, J.L., 1998, Leptin and the regulation of body weight in mammals. Nature 395, 763-770.

Gabellec, M.M., Griffais, R., Fillion, G., Haour, F., 1995, Expression of interleukin 1 alpha, interleukin 1 beta and interleukin 1 receptor antagonist mRNA in mouse brain: regulation by bacterial lipopolysaccharide (LPS) treatment. Brain Res Mol Brain Res 31, 122-130.

Gao, J.J., Filla, M.B., Fultz, M.J., Vogel, S.N., Russell, S.W., Murphy, W.J., 1998, Autocrine/paracrine IFN-alphabeta mediates the lipopolysaccharide-induced activation of transcription factor Stat1alpha in mouse macrophages: pivotal role of Stat1alpha in induction of the inducible nitric oxide synthase gene. J Immunol 161, 4803-4810.

Garcia JM, G.C., Kumor KWP, 2007, A Phase II, randomized, placebo-controlled, double blind study of the efficacy and safety of RC-1291 for the treatment of cancer-cachexia (Abstract). J Clin Oncol.

Garcia, J.M., Polvino, W.J., 2007, Effect on body weight and safety of RC-1291, a novel, orally available ghrelin mimetic and growth hormone secretagogue: results of a phase I, randomized, placebo-controlled, multiple-dose study in healthy volunteers. Oncologist 12, 594-600.

Garthwaite, J., Charles, S.L., Chess-Williams, R., 1988, Endothelium-derived relaxing factor release on activation of NMDA receptors suggests role as intercellular messenger in the brain. Nature 336, 385-388.

Garvey, E.P., Oplinger, J.A., Furfine, E.S., Kiff, R.J., Laszlo, F., Whittle, B.J., Knowles, R.G., 1997, 1400W is a slow, tight binding, and highly selective inhibitor of inducible nitric-oxide synthase in vitro and in vivo. J Biol Chem 272, 4959-4963.

Gautron, L., Lafon, P., Chaigniau, M., Tramu, G., Laye, S., 2002, Spatiotemporal analysis of signal transducer and activator of transcription 3 activation in rat brain astrocytes and pituitary following peripheral immune challenge. Neuroscience 112, 717-729.

Ghosh, S., May, M.J., Kopp, E.B., 1998, NF-kappa B and Rel proteins: evolutionarily conserved mediators of immune responses. Annu Rev Immunol 16, 225-260.

Goehler, L.E., Erisir, A., Gaykema, R.P., 2006, Neural-immune interface in the rat area postrema. Neuroscience 140, 1415-1434.

Gordon, J.N., Green, S.R., Goggin, P.M., 2005, Cancer cachexia. Qjm 98, 779-788.

Hanada, T., Toshinai, K., Kajimura, N., Nara-Ashizawa, N., Tsukada, T., Hayashi, Y., Osuye, K., Kangawa, K., Matsukura, S., Nakazato, M., 2003, Anti-cachectic effect of ghrelin in nude mice bearing human melanoma cells. Biochem Biophys Res Commun 301, 275-279.

Hart, B.L., 1988, Biological basis of the behavior of sick animals. Neurosci Biobehav Rev 12, 123-137.

Hataya, Y., Akamizu, T., Hosoda, H., Kanamoto, N., Moriyama, K., Kangawa, K., Takaya, K., Nakao, K., 2003, Alterations of plasma ghrelin levels in rats with lipopolysaccharide-induced wasting syndrome and effects of ghrelin treatment on the syndrome. Endocrinology 144, 5365-5371.

Hayden, M.S., Ghosh, S., 2004, Signaling to NF-kappaB. Genes Dev 18, 2195-2224.
Heimberger, A.B., Priebe, W., 2008, Small molecular inhibitors of p-STAT3: novel agents for treatment of primary and metastatic CNS cancers. Recent Pat CNS Drug Discov 3, 179-188.
Herkenham, M., Rathore, P., Brown, P., Listwak, S.J., 2011, Cautionary notes on the use of NF-kappaB p65 and p50 antibodies for CNS studies. J Neuroinflammation 8, 141.
Hevel, J.M., White, K.A., Marletta, M.A., 1991, Purification of the inducible murine macrophage nitric oxide synthase. Identification as a flavoprotein. J Biol Chem 266, 22789-22791.
Hoffmann, A., Levchenko, A., Scott, M.L., Baltimore, D., 2002, The IkappaB-NF-kappaB signaling module: temporal control and selective gene activation. Science 298, 1241-1245.
Horiguchi, A., Asano, T., Kuroda, K., Sato, A., Asakuma, J., Ito, K., Hayakawa, M., Sumitomo, M., 2010, STAT3 inhibitor WP1066 as a novel therapeutic agent for renal cell carcinoma. Br J Cancer 102, 1592-1599.
Imada, K., Leonard, W.J., 2000, The Jak-STAT pathway. Mol Immunol 37, 1-11.
Inui, A., Asakawa, A., Bowers, C.Y., Mantovani, G., Laviano, A., Meguid, M.M., Fujimiya, M., 2004, Ghrelin, appetite, and gastric motility: the emerging role of the stomach as an endocrine organ. Faseb J 18, 439-456.
Iwamaru, A., Szymanski, S., Iwado, E., Aoki, H., Yokoyama, T., Fokt, I., Hess, K., Conrad, C., Madden, T., Sawaya, R., Kondo, S., Priebe, W., Kondo, Y., 2007, A novel inhibitor of the STAT3 pathway induces apoptosis in malignant glioma cells both in vitro and in vivo. Oncogene 26, 2435-2444.
Jang, P.G., Namkoong, C., Kang, G.M., Hur, M.W., Kim, S.W., Kim, G.H., Kang, Y., Jeon, M.J., Kim, E.H., Lee, M.S., Karin, M., Baik, J.H., Park, J.Y., Lee, K.U., Kim, Y.B., Kim, M.S., 2010, NF-kappaB activation in hypothalamic pro-opiomelanocortin neurons is essential in illness- and leptin-induced anorexia. J Biol Chem 285, 9706-9715.
Jansky, L., Vybiral, S., Pospisilova, D., Roth, J., Dornand, J., Zeisberger, E., Kaminkova, J., 1995, Production of systemic and hypothalamic cytokines during the early phase of endotoxin fever. Neuroendocrinology 62, 55-61.
Johnson, A.K., Gross, P.M., 1993, Sensory circumventricular organs and brain homeostatic pathways. FASEB journal : official publication of the Federation of American Societies for Experimental Biology 7, 678-686.
Kamijo, R., Shapiro, D., Le, J., Huang, S., Aguet, M., Vilcek, J., 1993, Generation of nitric oxide and induction of major histocompatibility complex class II antigen in macrophages from mice lacking the interferon gamma receptor. Proc Natl Acad Sci U S A 90, 6626-6630.
Katafuchi, T., Motomura, K., Baba, S., Ota, K., Hori, T., 1997, Differential effects of tumor necrosis factor-alpha and -beta on rat ventromedial hypothalamic neurons in vitro. Am J Physiol 272, R1966-1971.
Kim, O.S., Park, E.J., Joe, E.H., Jou, I., 2002, JAK-STAT signaling mediates gangliosides-induced inflammatory responses in brain microglial cells. J Biol Chem 277, 40594-40601.

Kleinert, H., Schwarz, P.M., Forstermann, U., 2003, Regulation of the expression of inducible nitric oxide synthase. Biol Chem 384, 1343-1364.
Koedel, U., Bayerlein, I., Paul, R., Sporer, B., Pfister, H.W., 2000, Pharmacologic interference with NF-kappaB activation attenuates central nervous system complications in experimental Pneumococcal meningitis. J Infect Dis 182, 1437-1445.
Kojima, M., Hosoda, H., Date, Y., Nakazato, M., Matsuo, H., Kangawa, K., 1999, Ghrelin is a growth-hormone-releasing acylated peptide from stomach. Nature 402, 656-660.
Kojima, M., Hosoda, H., Matsuo, H., Kangawa, K., 2001, Ghrelin: discovery of the natural endogenous ligand for the growth hormone secretagogue receptor. Trends Endocrinol Metab 12, 118-122.
Konsman, J.P., Kelley, K., Dantzer, R., 1999, Temporal and spatial relationships between lipopolysaccharide-induced expression of Fos, interleukin-1beta and inducible nitric oxide synthase in rat brain. Neuroscience 89, 535-548.
Konsman, J.P., Vigues, S., Mackerlova, L., Bristow, A., Blomqvist, A., 2004, Rat brain vascular distribution of interleukin-1 type-1 receptor immunoreactivity: relationship to patterns of inducible cyclooxygenase expression by peripheral inflammatory stimuli. J Comp Neurol 472, 113-129.
Kumar, N.B., Kazi, A., Smith, T., Crocker, T., Yu, D., Reich, R.R., Reddy, K., Hastings, S., Exterman, M., Balducci, L., Dalton, K., Bepler, G., 2010, Cancer cachexia: traditional therapies and novel molecular mechanism-based approaches to treatment. Curr Treat Options Oncol 11, 107-117.
Kuo, P.C., Schroeder, R.A., 1995, The emerging multifaceted roles of nitric oxide. Ann Surg 221, 220-235.
Laflamme, N., Rivest, S., 2001, Toll-like receptor 4: the missing link of the cerebral innate immune response triggered by circulating gram-negative bacterial cell wall components. FASEB journal : official publication of the Federation of American Societies for Experimental Biology 15, 155-163.
Langhans, W., 2000, Anorexia of infection: current prospects. Nutrition 16, 996-1005.
Langhans, W., 2007, Signals generating anorexia during acute illness. Proc Nutr Soc 66, 321-330.
Langhans, W., Balkowski, G., Savoldelli, D., 1991, Differential feeding responses to bacterial lipopolysaccharide and muramyl dipeptide. Am J Physiol 261, R659-664.
Langhans, W., Savoldelli, D., Weingarten, S., 1993, Comparison of the feeding responses to bacterial lipopolysaccharide and interleukin-1 beta. Physiol Behav 53, 643-649.
Laye, S., Parnet, P., Goujon, E., Dantzer, R., 1994, Peripheral administration of lipopolysaccharide induces the expression of cytokine transcripts in the brain and pituitary of mice. Brain Res Mol Brain Res 27, 157-162.
Levinson, B., Gertner, J., 2012, Randomized study of the efficacy and safety of SUN11031 (synthetic human ghrelin) in cachexia associated with chronic obstructive pulmonary disease. e-SPEN Journal.
Li, W.G., Gavrila, D., Liu, X., Wang, L., Gunnlaugsson, S., Stoll, L.L., McCormick, M.L., Sigmund, C.D., Tang, C., Weintraub, N.L., 2004, Ghrelin inhibits proinflammatory responses and nuclear factor-kappaB activation in human endothelial cells. Circulation 109, 2221-2226.

Licinio, J., Wong, M.L., 1997, Pathways and mechanisms for cytokine signaling of the central nervous system. J Clin Invest 100, 2941-2947.
Lim, C.P., Cao, X., 2006, Structure, function, and regulation of STAT proteins. Mol Biosyst 2, 536-550.
Lorsbach, R.B., Murphy, W.J., Lowenstein, C.J., Snyder, S.H., Russell, S.W., 1993, Expression of the nitric oxide synthase gene in mouse macrophages activated for tumor cell killing. Molecular basis for the synergy between interferon-gamma and lipopolysaccharide. J Biol Chem 268, 1908-1913.
Lowenstein, C.J., Alley, E.W., Raval, P., Snowman, A.M., Snyder, S.H., Russell, S.W., Murphy, W.J., 1993, Macrophage nitric oxide synthase gene: two upstream regions mediate induction by interferon gamma and lipopolysaccharide. Proc Natl Acad Sci U S A 90, 9730-9734.
Lundholm, K., Gunnebo, L., Korner, U., Iresjo, B.M., Engstrom, C., Hyltander, A., Smedh, U., Bosaeus, I., 2010, Effects by daily long term provision of ghrelin to unselected weight-losing cancer patients: a randomized double-blind study. Cancer 116, 2044-2052.
Luquet, S., Magnan, C., 2009, The central nervous system at the core of the regulation of energy homeostasis. Front Biosci (Schol Ed) 1, 448-465.
Lutz, T.A., Del Prete, E., Scharrer, E., 1994, Reduction of food intake in rats by intraperitoneal injection of low doses of amylin. Physiol Behav 55, 891-895.
Lutz, T.A., Geary, N., Szabady, M.M., Del Prete, E., Scharrer, E., 1995, Amylin decreases meal size in rats. Physiol Behav 58, 1197-1202.
Lutz, T.A., Mollet, A., Rushing, P.A., Riediger, T., Scharrer, E., 2001, The anorectic effect of a chronic peripheral infusion of amylin is abolished in area postrema/nucleus of the solitary tract (AP/NTS) lesioned rats. Int J Obes Relat Metab Disord 25, 1005-1011.
Lutz, T.A., Senn, M., Althaus, J., Del Prete, E., Ehrensperger, F., Scharrer, E., 1998, Lesion of the area postrema/nucleus of the solitary tract (AP/NTS) attenuates the anorectic effects of amylin and calcitonin gene-related peptide (CGRP) in rats. Peptides 19, 309-317.
Margetic, S., Gazzola, C., Pegg, G.G., Hill, R.A., 2002, Leptin: a review of its peripheral actions and interactions. Int J Obes Relat Metab Disord 26, 1407-1433.
Marks-Konczalik, J., Chu, S.C., Moss, J., 1998, Cytokine-mediated transcriptional induction of the human inducible nitric oxide synthase gene requires both activator protein 1 and nuclear factor kappaB-binding sites. J Biol Chem 273, 22201-22208.
Marvel, F.A., Chen, C.C., Badr, N., Gaykema, R.P., Goehler, L.E., 2004, Reversible inactivation of the dorsal vagal complex blocks lipopolysaccharide-induced social withdrawal and c-Fos expression in central autonomic nuclei. Brain Behav Immun 18, 123-134.
McKinley, M.J., McAllen, R.M., Davern, P., Giles, M.E., Penschow, J., Sunn, N., Uschakov, A., Oldfield, B.J., 2003, The sensory circumventricular organs of the mammalian brain. Adv Anat Embryol Cell Biol 172, III-XII, 1-122, back cover.
Meraz, M.A., White, J.M., Sheehan, K.C., Bach, E.A., Rodig, S.J., Dighe, A.S., Kaplan, D.H., Riley, J.K., Greenlund, A.C., Campbell, D., Carver-Moore, K., DuBois, R.N., Clark, R., Aguet, M., Schreiber, R.D., 1996, Targeted disruption of the

Stat1 gene in mice reveals unexpected physiologic specificity in the JAK-STAT signaling pathway. Cell 84, 431-442.
Miller, A.D., Leslie, R.A., 1994, The area postrema and vomiting. Front Neuroendocrinol 15, 301-320.
Mizuno, T.M., Mobbs, C.V., 1999, Hypothalamic agouti-related protein messenger ribonucleic acid is inhibited by leptin and stimulated by fasting. Endocrinology 140, 814-817.
Moncada, S., Palmer, R.M., Higgs, E.A., 1991, Nitric oxide: physiology, pathophysiology, and pharmacology. Pharmacol Rev 43, 109-142.
Montague, C.T., Farooqi, I.S., Whitehead, J.P., Soos, M.A., Rau, H., Wareham, N.J., Sewter, C.P., Digby, J.E., Mohammed, S.N., Hurst, J.A., Cheetham, C.H., Earley, A.R., Barnett, A.H., Prins, J.B., O'Rahilly, S., 1997, Congenital leptin deficiency is associated with severe early-onset obesity in humans. Nature 387, 903-908.
Moore, C.X., Cooper, G.J., 1991, Co-secretion of amylin and insulin from cultured islet beta-cells: modulation by nutrient secretagogues, islet hormones and hypoglycemic agents. Biochem Biophys Res Commun 179, 1-9.
Morley, J.E., Thomas, D.R., Wilson, M.M., 2006, Cachexia: pathophysiology and clinical relevance. Am J Clin Nutr 83, 735-743.
Nadjar, A., Bluthe, R.M., May, M.J., Dantzer, R., Parnet, P., 2005, Inactivation of the cerebral NFkappaB pathway inhibits interleukin-1beta-induced sickness behavior and c-Fos expression in various brain nuclei. Neuropsychopharmacology 30, 1492-1499.
Nadjar, A., Combe, C., Laye, S., Tridon, V., Dantzer, R., Amedee, T., Parnet, P., 2003, Nuclear factor kappaB nuclear translocation as a crucial marker of brain response to interleukin-1. A study in rat and interleukin-1 type I deficient mouse. J Neurochem 87, 1024-1036.
Nagaya, N., Itoh, T., Murakami, S., Oya, H., Uematsu, M., Miyatake, K., Kangawa, K., 2005, Treatment of cachexia with ghrelin in patients with COPD. Chest 128, 1187-1193.
Nass, R., Pezzoli, S.S., Oliveri, M.C., Patrie, J.T., Harrell, F.E., Jr., Clasey, J.L., Heymsfield, S.B., Bach, M.A., Vance, M.L., Thorner, M.O., 2008, Effects of an oral ghrelin mimetic on body composition and clinical outcomes in healthy older adults: a randomized trial. Ann Intern Med 149, 601-611.
Neary, N.M., Small, C.J., Wren, A.M., Lee, J.L., Druce, M.R., Palmieri, C., Frost, G.S., Ghatei, M.A., Coombes, R.C., Bloom, S.R., 2004, Ghrelin increases energy intake in cancer patients with impaired appetite: acute, randomized, placebo-controlled trial. J Clin Endocrinol Metab 89, 2832-2836.
Nelson, D.E., Ihekwaba, A.E., Elliott, M., Johnson, J.R., Gibney, C.A., Foreman, B.E., Nelson, G., See, V., Horton, C.A., Spiller, D.G., Edwards, S.W., McDowell, H.P., Unitt, J.F., Sullivan, E., Grimley, R., Benson, N., Broomhead, D., Kell, D.B., White, M.R., 2004a, Oscillations in NF-kappaB signaling control the dynamics of gene expression. Science 306, 704-708.
Nelson, D.E., See, V., Nelson, G., White, M.R., 2004b, Oscillations in transcription factor dynamics: a new way to control gene expression. Biochem Soc Trans 32, 1090-1092.

Nguyen, M.D., Julien, J.P., Rivest, S., 2002, Innate immunity: the missing link in neuroprotection and neurodegeneration? Nat Rev Neurosci 3, 216-227.
Ollmann, M.M., Wilson, B.D., Yang, Y.K., Kerns, J.A., Chen, Y., Gantz, I., Barsh, G.S., 1997, Antagonism of central melanocortin receptors in vitro and in vivo by agouti-related protein. Science 278, 135-138.
Palmer, R.M., Rees, D.D., Ashton, D.S., Moncada, S., 1988, L-arginine is the physiological precursor for the formation of nitric oxide in endothelium-dependent relaxation. Biochem Biophys Res Commun 153, 1251-1256.
Pautz, A., Art, J., Hahn, S., Nowag, S., Voss, C., Kleinert, H., 2010, Regulation of the expression of inducible nitric oxide synthase. Nitric Oxide 23, 75-93.
Paxinos, G., Watson, C., 2007, The rat brain in stereotaxic coordinates. Academic Press/Elsevier, Amsterdam; Boston.
Perkins, N.D., 2007, Integrating cell-signalling pathways with NF-kappaB and IKK function. Nat Rev Mol Cell Biol 8, 49-62.
Pierce, J.W., Schoenleber, R., Jesmok, G., Best, J., Moore, S.A., Collins, T., Gerritsen, M.E., 1997, Novel inhibitors of cytokine-induced IkappaBalpha phosphorylation and endothelial cell adhesion molecule expression show anti-inflammatory effects in vivo. J Biol Chem 272, 21096-21103.
Plata-Salaman, C.R., 1996, Anorexia during acute and chronic disease. Nutrition 12, 69-78.
Plata-Salaman, C.R., ffrench-Mullen, J.M., 1994, Interleukin-1 beta inhibits Ca2+ channel currents in hippocampal neurons through protein kinase C. Eur J Pharmacol 266, 1-10.
Pollock, J.S., Forstermann, U., Mitchell, J.A., Warner, T.D., Schmidt, H.H., Nakane, M., Murad, F., 1991, Purification and characterization of particulate endothelium-derived relaxing factor synthase from cultured and native bovine aortic endothelial cells. Proc Natl Acad Sci U S A 88, 10480-10484.
Prast, H., Philippu, A., 2001, Nitric oxide as modulator of neuronal function. Prog Neurobiol 64, 51-68.
Price, C.J., Hoyda, T.D., Ferguson, A.V., 2008, The area postrema: a brain monitor and integrator of systemic autonomic state. Neuroscientist 14, 182-194.
Quan, N., Stern, E.L., Whiteside, M.B., Herkenham, M., 1999, Induction of pro-inflammatory cytokine mRNAs in the brain after peripheral injection of subseptic doses of lipopolysaccharide in the rat. J Neuroimmunol 93, 72-80.
Quan, N., Whiteside, M., Kim, L., Herkenham, M., 1997, Induction of inhibitory factor kappaBalpha mRNA in the central nervous system after peripheral lipopolysaccharide administration: an in situ hybridization histochemistry study in the rat. Proc Natl Acad Sci U S A 94, 10985-10990.
Rao, K.M., 2000, Molecular mechanisms regulating iNOS expression in various cell types. J Toxicol Environ Health B Crit Rev 3, 27-58.
Riediger, T., Bothe, C., Becskei, C., Lutz, T.A., 2004, Peptide YY directly inhibits ghrelin-activated neurons of the arcuate nucleus and reverses fasting-induced c-Fos expression. Neuroendocrinology 79, 317-326.
Riediger, T., Cordani, C., Potes, C.S., Lutz, T.A., 2010, Involvement of nitric oxide in lipopolysaccharide induced anorexia. Pharmacol Biochem Behav 97, 112-120.

Riediger, T., Giannini, P., Erguven, E., Lutz, T., 2006, Nitric oxide directly inhibits ghrelin-activated neurons of the arcuate nucleus. Brain Res 1125, 37-45.
Riediger, T., Schmid, H.A., Lutz, T., Simon, E., 2001, Amylin potently activates AP neurons possibly via formation of the excitatory second messenger cGMP. Am J Physiol Regul Integr Comp Physiol 281, R1833-1843.
Riediger, T., Traebert, M., Schmid, H.A., Scheel, C., Lutz, T.A., Scharrer, E., 2003, Site-specific effects of ghrelin on the neuronal activity in the hypothalamic arcuate nucleus. Neurosci Lett 341, 151-155.
Rietschel, E.T., Schletter, J., Weidemann, B., El-Samalouti, V., Mattern, T., Zahringer, U., Seydel, U., Brade, H., Flad, H.D., Kusumoto, S., Gupta, D., Dziarski, R., Ulmer, A.J., 1998, Lipopolysaccharide and peptidoglycan: CD14-dependent bacterial inducers of inflammation. Microb Drug Resist 4, 37-44.
Roseberry, A.G., Liu, H., Jackson, A.C., Cai, X., Friedman, J.M., 2004, Neuropeptide Y-mediated inhibition of proopiomelanocortin neurons in the arcuate nucleus shows enhanced desensitization in ob/ob mice. Neuron 41, 711-722.
Rowland, N.E., Crews, E.C., Gentry, R.M., 1997, Comparison of Fos induced in rat brain by GLP-1 and amylin. Regul Pept 71, 171-174.
Rummel, C., Voss, T., Matsumura, K., Korte, S., Gerstberger, R., Roth, J., Hubschle, T., 2005, Nuclear STAT3 translocation in guinea pig and rat brain endothelium during systemic challenge with lipopolysaccharide and interleukin-6. J Comp Neurol 491, 1-14.
Sagar, S.M., Price, K.J., Kasting, N.W., Sharp, F.R., 1995, Anatomic patterns of Fos immunostaining in rat brain following systemic endotoxin administration. Brain Res Bull 36, 381-392.
Schindler, C.W., 2002, Series introduction. JAK-STAT signaling in human disease. J Clin Invest 109, 1133-1137.
Schmidt, H.H., Lohmann, S.M., Walter, U., 1993, The nitric oxide and cGMP signal transduction system: regulation and mechanism of action. Biochim Biophys Acta 1178, 153-175.
Schwartz, M.W., Seeley, R.J., Campfield, L.A., Burn, P., Baskin, D.G., 1996, Identification of targets of leptin action in rat hypothalamus. J Clin Invest 98, 1101-1106.
Schwartz, M.W., Woods, S.C., Porte, D., Jr., Seeley, R.J., Baskin, D.G., 2000, Central nervous system control of food intake. Nature 404, 661-671.
Sergeyev, V., Broberger, C., Hokfelt, T., 2001, Effect of LPS administration on the expression of POMC, NPY, galanin, CART and MCH mRNAs in the rat hypothalamus. Brain Res Mol Brain Res 90, 93-100.
Stanley, B.G., Kyrkouli, S.E., Lampert, S., Leibowitz, S.F., 1986, Neuropeptide Y chronically injected into the hypothalamus: a powerful neurochemical inducer of hyperphagia and obesity. Peptides 7, 1189-1192.
Stephens, T.W., Basinski, M., Bristow, P.K., Bue-Valleskey, J.M., Burgett, S.G., Craft, L., Hale, J., Hoffmann, J., Hsiung, H.M., Kriauciunas, A., et al., 1995, The role of neuropeptide Y in the antiobesity action of the obese gene product. Nature 377, 530-532.
Strassburg, S., Anker, S.D., Castaneda, T.R., Burget, L., Perez-Tilve, D., Pfluger, P.T., Nogueiras, R., Halem, H., Dong, J.Z., Culler, M.D., Datta, R., Tschop, M.H.,

2008, Long-term effects of ghrelin and ghrelin receptor agonists on energy balance in rats. Am J Physiol Endocrinol Metab 295, E78-84.

Strasser, F., Lutz, T.A., Maeder, M.T., Thuerlimann, B., Bueche, D., Tschop, M., Kaufmann, K., Holst, B., Brandle, M., von Moos, R., Demmer, R., Cerny, T., 2008, Safety, tolerability and pharmacokinetics of intravenous ghrelin for cancer-related anorexia/cachexia: a randomised, placebo-controlled, double-blind, double-crossover study. Br J Cancer 98, 300-308.

Sun, S.C., Ganchi, P.A., Ballard, D.W., Greene, W.C., 1993, NF-kappa B controls expression of inhibitor I kappa B alpha: evidence for an inducible autoregulatory pathway. Science 259, 1912-1915.

Suzuki, K., Simpson, K.A., Minnion, J.S., Shillito, J.C., Bloom, S.R., 2010, The role of gut hormones and the hypothalamus in appetite regulation. Endocr J 57, 359-372.

Takaya, K., Ariyasu, H., Kanamoto, N., Iwakura, H., Yoshimoto, A., Harada, M., Mori, K., Komatsu, Y., Usui, T., Shimatsu, A., Ogawa, Y., Hosoda, K., Akamizu, T., Kojima, M., Kangawa, K., Nakao, K., 2000, Ghrelin strongly stimulates growth hormone release in humans. J Clin Endocrinol Metab 85, 4908-4911.

Takeda, K., Kaisho, T., Akira, S., 2003, Toll-like receptors. Annu Rev Immunol 21, 335-376.

Tedeschi, E., Menegazzi, M., Margotto, D., Suzuki, H., Forstermann, U., Kleinert, H., 2003, Anti-inflammatory actions of St. John's wort: inhibition of human inducible nitric-oxide synthase expression by down-regulating signal transducer and activator of transcription-1alpha (STAT-1alpha) activation. J Pharmacol Exp Ther 307, 254-261.

Tisdale, M.J., 2002, Cachexia in cancer patients. Nat Rev Cancer 2, 862-871.

Traebert, M., Riediger, T., Whitebread, S., Scharrer, E., Schmid, H.A., 2002, Ghrelin acts on leptin-responsive neurones in the rat arcuate nucleus. J Neuroendocrinol 14, 580-586.

Tsoyi, K., Kim, H.J., Shin, J.S., Kim, D.H., Cho, H.J., Lee, S.S., Ahn, S.K., Yun-Choi, H.S., Lee, J.H., Seo, H.G., Chang, K.C., 2008, HO-1 and JAK-2/STAT-1 signals are involved in preferential inhibition of iNOS over COX-2 gene expression by newly synthesized tetrahydroisoquinoline alkaloid, CKD712, in cells activated with lipopolysacchride. Cell Signal 20, 1839-1847.

Turrin, N.P., Gayle, D., Ilyin, S.E., Flynn, M.C., Langhans, W., Schwartz, G.J., Plata-Salaman, C.R., 2001, Pro-inflammatory and anti-inflammatory cytokine mRNA induction in the periphery and brain following intraperitoneal administration of bacterial lipopolysaccharide. Brain Res Bull 54, 443-453.

Verma, I.M., Stevenson, J.K., Schwarz, E.M., Van Antwerp, D., Miyamoto, S., 1995, Rel/NF-kappa B/I kappa B family: intimate tales of association and dissociation. Genes Dev 9, 2723-2735.

Wang, L., Saint-Pierre, D.H., Tache, Y., 2002, Peripheral ghrelin selectively increases Fos expression in neuropeptide Y - synthesizing neurons in mouse hypothalamic arcuate nucleus. Neurosci Lett 325, 47-51.

Wang, W., Andersson, M., Iresjo, B.M., Lonnroth, C., Lundholm, K., 2006, Effects of ghrelin on anorexia in tumor-bearing mice with eicosanoid-related cachexia. Int J Oncol 28, 1393-1400.

Wang, W., Svanberg, E., Delbro, D., Lundholm, K., 2005, NOS isoenzyme content in brain nuclei as related to food intake in experimental cancer cachexia. Brain Res Mol Brain Res 134, 205-214.

Weingarten, S., Senn, M., Langhans, W., 1993, Does a learned taste aversion contribute to the anorectic effect of bacterial lipopolysaccharide? Physiol Behav 54, 961-966.

Willesen, M.G., Kristensen, P., Romer, J., 1999, Co-localization of growth hormone secretagogue receptor and NPY mRNA in the arcuate nucleus of the rat. Neuroendocrinology 70, 306-316.

Wisse, B.E., Frayo, R.S., Schwartz, M.W., Cummings, D.E., 2001, Reversal of cancer anorexia by blockade of central melanocortin receptors in rats. Endocrinology 142, 3292-3301.

Wong, M.L., Rettori, V., al-Shekhlee, A., Bongiorno, P.B., Canteros, G., McCann, S.M., Gold, P.W., Licinio, J., 1996, Inducible nitric oxide synthase gene expression in the brain during systemic inflammation. Nat Med 2, 581-584.

Woods, S.C., 2009, The control of food intake: behavioral versus molecular perspectives. Cell Metab 9, 489-498.

Woods, S.C., D'Alessio, D.A., 2008, Central control of body weight and appetite. J Clin Endocrinol Metab 93, S37-50.

Wren, A.M., Small, C.J., Abbott, C.R., Dhillo, W.S., Seal, L.J., Cohen, M.A., Batterham, R.L., Taheri, S., Stanley, S.A., Ghatei, M.A., Bloom, S.R., 2001, Ghrelin causes hyperphagia and obesity in rats. Diabetes 50, 2540-2547.

Wuchert, F., Ott, D., Rafalzik, S., Roth, J., Gerstberger, R., 2009, Tumor necrosis factor-alpha, interleukin-1beta and nitric oxide induce calcium transients in distinct populations of cells cultured from the rat area postrema. J Neuroimmunol 206, 44-51.

Xie, Q.W., Kashiwabara, Y., Nathan, C., 1994, Role of transcription factor NF-kappa B/Rel in induction of nitric oxide synthase. J Biol Chem 269, 4705-4708.

Zhang, Y., Proenca, R., Maffei, M., Barone, M., Leopold, L., Friedman, J.M., 1994, Positional cloning of the mouse obese gene and its human homologue. Nature 372, 425-432.

Curriculum Vitae

Persönliches

Name	Laura Loi
Geburtsdatum	30.12.1987
Geburtsort	Singen (DE)
Nationalität	Deutschland

Ausbildung

2013	Dissertation am Institut für Veterinärphysiologie, Vetsuisse-Fakultät Universität Zürich
2013	Eidgenössiche Prüfung der Veterinärmedizin
2007 – 2013	Studium der Veterinärmedizin an der Vetsuisse Fakultät Universität Zürich
2003 – 2007	Liceo cantonale di Mendrisio (TI). Schwerpunkt: Biologie und Chemie
1999 – 2003	Scuole medie di Stabio (TI)
1994 – 2003	Scuole elementari di Stabio (TI)

Zürich, 14.01.14